

ABSTRACT

Title of Document: LIVE-ATTENUATED VACCINES AGAINST INFLUENZA VIRUSES AND ROLE OF NS1 IN HOST RESPONSE

Yibin Cai, Doctor of Philosophy, 2013

Directed By: Professor, Daniel R. Perez, Department of Veterinary Medicine

(1). In this study, we improved the hatchability ($\geq 90\%$) of egg embryos after vaccination with live attenuate influenza vaccines using modified H7 and H9 hemagglutinin (HA) proteins with amino acid substitutions at the cleavage site for those found in the H6 HA subtype. A single dose *in ovo* vaccination of 19-day old eggs provided complete protection against homologous challenge with low pathogenic H7 and H9 virus in $\geq 70\%$ of chickens at 2 or 6 weeks post-hatching.

(2). The HA titer of a recombinant live-attenuated influenza vaccine (2 mouse-adapted(ma) Ca/04 H1N1:6WF10*att*) against pandemic H1N1 was improved through egg adaptation. By whole viral genome sequencing and with viral kinetics study of reverse genetics viruses, I found an amino acid substitution in PA polymerase subunit, at position 59, from glutamic acid to valine, which is responsible for the enhancement of HA and viral titer. This mutation did not impair the

temperature sensitive phenotype of prototypic live attenuated backbone, WF10*att*.

The PA E59V mutation moderately enhanced the HA and viral titer of wt WF10 and ty/04*att* backbones. However, it had no effect on two commercially licensed influenza vaccine internal backbones PR/8- or *ca* Ann Arbor/60. Interestingly, although the E59V had no significant effect on increasing HA/NP ratio of the wt WF10 or WF10*att* system; both backbones resulted in higher antigenic content on viral particles than PR/8- or *ca* Ann Arbor/60-based virus particles.

(3). Our laboratory previously generated an adapted virus from wildtype duck H9N2, A/duck/Hong Kong/702/79 virus, through 23 serial passages in lung of quail (QA23). QA23 gained the new phenotype of replicating and transmitting efficiently in chickens and quail. NS1 protein localization studies demonstrated that QA23 NS1 was mainly distributed in the cytoplasm; while WT702 NS1 predominantly accumulated in the nucleus; and nuclear localization sequence 2 is important for the nuclear import of NS1. QA23 NS1 up-regulated the viral protein synthesis in DF1 cells; did not affect the inhibition of IFN- β ; and greatly reduced the apoptotic activity level during infection. However, there is no evidence showing that QA23 NS1 is associated with the enhanced replication and transmission of the virus in quail.

LIVE-ATTENUATED VACCINES AGAINST INFLUENZA VIRUSES AND
ROLE OF NS1 IN HOST RESPONSE

By

Yibin Cai

Dissertation submitted to the Faculty of the Graduate School of the
University of Maryland, College Park, in partial fulfillment
of the requirements for the degree of
Doctor of Philosophy
2013

Advisory Committee:
Professor Daniel R. Perez, Chair
Professor Xiaoping Zhu
Associate Professor Yanjing Zhang
Assistant Professor Georgiy Belov
Professor Jeffrey DeStefano

© Copyright by
Yibin Cai
2013

Dedication

This body of work is dedicated to the memory of my maternal grandmother, Genbao Xu.

I wish you could see all this, and I know you are happy for me.

Acknowledgements

The process of pursuing the PhD was a special journey in my life. The experiences I had during my degree research will always be a great treasure to me. It was a wonderful time that I spent in the Department of Veterinary Medicine, University of Maryland, College Park. My colleagues were all kind and warm. The department has a very good scientific environment with lots of support for research work; the communications among researchers are great. All these made my studies much easier than I thought they would be. This dissertation is an achievement and reward for all these years of my hard work. I could not have accomplished it all by myself without other's help. Hence, I would like to acknowledge number of people who help me "make my dream come true."

First and most, I would like to thank my wonderful research mentor, Dr. Daniel R. Perez, who is a great scientist I will always admire. I have been extremely fortunate to work under his direction. Without his guide and help, I will never make it this far. I hope some day I can be a scientist like him. He taught me not only how to learn, but also how to train myself to think scientifically and work independently. He always be emphasized on every details of my research. Looking back, without him, I could not really "grow up".

I also feel fortunate to have had faculty members on my dissertation committee who contributed their precious time to provide comments and evaluate the progress of my dissertation process. Dr. Samal, Dr. Zhang, Dr. DeStefano and Dr.

Georgiy Belov are all great scientists. They are always there to help me out whenever I had questions that were really outside the box, and continuously gave me advice and encouraged me; Dr. Zhu, an outstanding immunologist, always shared his knowledge with me and gave advices to me during the process. Their insights broaden my knowledge and thinking and improved the quality of my dissertation. I am very thankful they were on my dissertation committee.

I would like to give my thanks to all of the former and current members in my lab. They are fantastic individuals: smart, thoughtful, friendly and working as a team. They are willing to help me whenever I need. They encouraged me whenever I was frustrated with my work. I would like to give my special thanks to my former colleagues Dr. Haichen Song, Dr. Jianqiang Ye, Dr. Hongxia Shao, and Dr. Danielle Hickman. I extended the part of projects in my dissertation based on the significant results they obtained previously. I would like to thank Dr. Hongjun Chen, Dr. Weizhong Li and Dr. Troy Sutton, for their suggestions and helps on my research work.

I would also like to thank everyone in the department and to all past and present office staff in the department office. Their friendship and generous help make my doctoral study a pleasant journey.

Finally, but most importantly, I would like to thank my parents, Mr. Cai, Shanyu and Mrs. Hu, Fen as well as my elder sister Cai, Yiyi, for their strongest support. Their love drives everything I have accomplished in the University of Maryland.

Table of Contents

Dedication.....	ii
Acknowledgements.....	iii
Table of Contents.....	v
List of Tables.....	ix
List of Figures.....	x
Chapter 1: Influenza A virus.....	1
Introduction.....	1
Viral proteins.....	1
HA.....	7
NA.....	10
M1.....	13
M2.....	14
NP.....	15
RNA-depedent RNA polymeras.....	16
NS1.....	20
NEP.....	25
Influenza A life cycle.....	25
Entry into the host cell and uncoating.....	26
mRNA transcription and viral genome replication.....	27
Export of vRNP.....	29
Assembly and budding.....	30
Chapter 2: Influenza vaccines.....	39
Introduction.....	39
Inactivated vaccines.....	41
Live-attenuated vaccines.....	44
Vaccine expressed by viral vectors.....	46
Virus-like particle vaccines.....	47
Universal vaccines.....	48
Recombinant M2 vaccine.....	48
H2 stalk vaccine.....	48
DNA-based vaccines.....	49
Chapter 3: Host immune responses and evasion strategies of influenza virus.....	50
Innate immune response.....	50
The TLR pathway.....	50
RIG-I.....	51
Type I IFN signaling.....	51

The interaction of innate and adaptive immune responses	52
Adaptive immune response	53
Humoral response	53
Cell-mediated immune response	54
Evasion of immune response by influenza virus	55
Escaping of adaptive immune response by influenza virus	57
Chapter 4: Improved hatchability and efficient protection after in ovo vaccination with live-attenuated H7N2 and H9N2 avian influenza viruses	59
Abstract	59
Introduction	60
Materials and methods	63
Virus, cells and Animals	63
Generation of recombinant virus by reverse genetics	63
Hatchability in embryonated chicken eggs	65
Plaque assay in chicken embryonic kidney (CEK) cells and immunostaining	66
Viral replication in MDCK cells	66
Virus replication and transmission in quail	67
Challenge studies	67
Results	68
Chicken hatchability is impaired after in ovo vaccination with H7N2 and H9N2 WF10att viruses	68
Chicken hatchability after modification of the HA cleavage site in H7N2 and H9N2 WF10att viruses	69
Stability of new recombinant viruses	70
Modification of the HA cleavage site reduces replication of 2mH7N2:6WF10att virus in quail	70
Single dose in ovo vaccination provides protection in chickens from homologous challenge with H7 and H9 LPAI viruses at 2 and 6 weeks post-hatching	72
Discussion	73
Chapter 5: Glutamic Acid to Valine Substitution at Position 59 in PA Enhances Growth of Live-Attenuated Influenza Vaccines in Eggs and Mammalian Cells	85
Abstract	85
Introduction	86
Materials and methods	89
Virus, plasmid and cells	89
Generation of recombinant virus by reverse genetics	90
Sequence analysis	90
Viral replication study in eggs and mammalian cells	91
Western blot	92
Reverse transcription and real-time PCR	93
The comparison of HA/NP ratio of the purified viruses using ELISA	94
Statistical analysis	95
Results	96

Preparation of an alternative pH1N1 live attenuated influenza virus (LAIV) based on the WF10att background (pH1N1 WF10att)	96
The enhanced HA and viral titer of live-attenuated virus was confirmed in egg embryos and MDCK cells using reverse genetics	97
The substitution of PA E59V increased mRNA, cRNA and vRNA level during early phase of infection in MDCK cells using strand-specific real-time RT-PCR	98
The substitution of PA E59V did not impair the temperature sensitive phenotype of the live-attenuated backbone	99
The substitution of PA E59A had no effect on the viral replication of live-attenuated virus in egg embryos and MDCK cells	99
The substitution of PA E59V moderate enhanced the HA titer of vaccines with WF10 and Ty/04att backbones; but had no effect in PR/8 and Ann Arbor backbones.....	100
WF10att and wild-type WF10 backbones have higher HA/NP ratio than that of PR8 and Ann Arbor/60	100
Discussion.....	101
Chapter 6: Cytoplasmic accumulation of NS1 enhances the viral replication and anti-apoptotic activity of an avian influenza virus (H9N2).....	119
Abstract.....	119
Introduction.....	120
Materials and methods.....	122
Virus, plasmid and cells.....	122
Generation of recombinant virus by reverse genetics.....	123
Sequence analysis	123
Immunofluorescence assay.....	124
Dissociation of nuclear and cytoplasmic fractions	125
Minigenome assay	126
IFN- β ELISA	127
Apoptosis Assay	128
Quail study.....	129
Statistical analysis.....	130
Results.....	130
The mutation K219E enhanced cytoplasmic accumulation of NS1 in mammalian and avian cell lines.....	130
NLS2 is the major functional signal for importing NS1 into the nucleus	132
QA23 NS1 up-regulated the viral protein synthesis in DF1 cells.....	132
The predominant cytoplasmic distribution of NS1 did not affect on inhibition the induction of host IFN- β	134
The predominant cytoplasmic distribution of NS1 enhanced the anti-apoptotic activity level.....	134
QA23 NS1 has no significant effect on the viral replication and transmission in Japanese quail	136
Discussion.....	137

Chapter 7: Perspective	154
Appendices.....	159
Bibliography	160

List of Tables

Table 1.1. Influenza A virus genome segments and genes.....	33
Table 1.2. The strain-specific functions of NS1.....	34
Table 4.1. The gene constellations of the recombinant viruses	77
Table 4.2. Comparison of the hatchability of new recombinant viruses in embryonated chicken eggs vs. the viruses with wild type HAs and the optimization of the dose and timing for <i>in ovo</i> vaccination.....	78
Table 4.3. Replication and transmission study of recombinant virus 2H7N2:6WF10att and 2mH7N2:6WF10att in quails.	79
Table 4.4. Single-dose 2mH7N2:6WF10att <i>in ovo</i> vaccination study in chickens challenged with low-pathogenic H7N2 (Ck/04) at 2 and 6-week post-hatching.	80
Table 4.5. Single-dose 2mH9N2:6WF10att <i>in ovo</i> vaccination study in chickens challenged with low-pathogenic H9N2 (WF10) at 2 and 6-week post-hatching.	81
Table 5.1. Gene constellations of recombinant viruses	107
Table 5.2. Enhanced HA titers after serially propagated recombinant influenza virus ma-CA/04 H1N1:6WF10att in egg embryos.....	108
Table 5.3. The nucleotide changes in the genes of P8 virus.....	109
Table 5.4. The primer sets for strand-specific real-time RT-PCR using tagged primers for quantification of the vRNA, cRNA, and mRNA of HA and NP of 2 mouse-adapted (ma) Ca/04 H1N1:6WF10att	110
Table 5.5. The comparison of HA to NP ratios of the pH1N1 vaccines with different internal backbones.....	111
Table 6.1. Replication and transmission of H9N2 viruses in Japanese quail.....	143

List of Figures

Figure 1.1. The structure of Influenza A virus.....	35
Figure 1.2. The structure domains of influenza A virus polymerase complex.....	36
Figure 1.3. The interaction of NS1 with host factors.....	37
Figure 1.4. The life cycle of Influenza A virus.....	38
Figure 4.1. Strategy of modifying the HA cleavage site.....	82
Figure 4.2. Viral replication kinetics of the live-attenuated viruses in MDCK cells at (A) 35°C and (B) 39°C using MOI of 0.001.....	83
Figure 4.3. Plaque morphology of the live-attenuated viruses in CEK cell at different temperatures.....	84
Figure 5.1. Comparison of the HA and viral titers of 2 ma-Ca/04 H1N1:mPA (E59V):5WF10att and 2 ma-Ca/04 H1N1:6WF10att in 10-day-old embryonated eggs and MDCK cells.....	112
Figure 5.2. Comparison of the viral protein: HA and NS1 synthesis level in MDCK cells during infection.....	113
Figure 5.3. Evaluation of HA and NP viral mRNA, cRNA and vRNA level at early phase of infection in MDCK cells at different time points using RT real-time PCR.....	115
Figure 5.4. Viral replication kinetics of the live-attenuated viruses in MDCK cells at 35°C and 39°C using MOI of 0.001.....	116
Figure 5.5. The comparison of live-attenuated virus of PA 59A with 59E and 59V in egg embryos and MDCK cells.....	117
Figure 5.6. Evaluation of the effect of PA amino acid 59 substitution on WF10, Ty/04att, PR8 and ca Ann Arbor/60 internal backbone.....	118
Figure 6.1. Immunofluorescence of NS1 protein localization and cytoplasmic and nuclear and fractions of NS1.....	144

Figure 6.2. Immunofluorescence of NS1 mutants localization.....	148
Figure 6.3. Minigenome assay.....	149
Figure 6.4. INF- β level induced by Recombinant viruses.	150
Figure 6.5. Apoptosis detection using TUNEL assay.....	151
Figure 6.6. Viral shedding from the trachea of quails.....	152
Figure 6.7. Influenza virus infection activates Akt phosphorylation.....	153

Chapter 1: Influenza A virus

Introduction

Influenza viruses are enveloped single-stranded negative-sense RNA viruses, belonging to the family *Orthomyxoviridae*. There are 6 genera in this family, including Influenza A, B, C, Isavirus, Thogotovirus and an unnamed, novel and uncharacterized genus [1]. Influenza A, B and C viruses are classified according to the differences in matrix protein (M1) and nucleoprotein (NP). Influenza A viruses can infect humans and a broad range of animal species, including birds, pigs, horses, dogs and sea mammals; whereas Influenza B viruses infect only humans [2], seals [3] and ferrets [4]; and Influenza C viruses infect only humans, dogs and pigs [5]. Amongst them, Influenza A is the major pathogen causing the seasonal flu and sporadic pandemics. Pandemic flu in the 20th century (1918 H1N1 Spanish flu, 1957 H2N2 Asian flu and 1968 H3N2 Hong Kong flu) caused millions of deaths [6]. The 2009 swine-origin pandemic H1N1 (pH1N1) influenza virus (“swine flu”) rapidly spread around the world. By July 2010, this pandemic resulted in more than 18,000 deaths worldwide [7]. Currently, highly pathogenic avian influenza (HPAI) H5N1 virus (“bird flu”) is circulating in many countries, occasionally infecting humans with mortality as high as 60% [8].

Influenza A virus contains a genome with 8 RNA segments, which encode at least 12 identified proteins. RNA segments 1, 2 and 3 encode polymerase basic proteins PB2 and PB1 and polymerase acid protein PA, respectively. Segments 4, 5, and 6 encode hemagglutinin (HA), nucleoprotein (NP), neuraminidase (NA), respectively. Segment 7 encodes the matrix protein 1 (M1) and M2 protein. Segment 8 encodes non-structural

protein 1 (NS1) and the nuclear export protein (NEP; also known as NS2). In addition, PB1-F2 and N40 are translated from PB1 mRNA by leaky scanning [9,10], and PA-X is translated by ribosomal frameshifting of the PA gene [11]. PB1, PB2 and PA are subunits of RNA-dependent RNA polymerase (RdRP). NP packages the segmented viral RNA and binds to RdRP to form the ribonucleoprotein (RNP) in the viral particles (Table 1.1 and Figure 1.1).

Influenza A virus possesses a lipid bilayer envelope derived from the host membrane. HA and NA are surface glycoproteins on the viral envelope, and both proteins recognize sialic acid (SA) [12,13]. Influenza A viruses can be classified into 17 HA subtypes (H1–H17) and 10 NA subtypes (N1–N10) based on the antigenic differences of the proteins [14,15]. The virus strains from all HA and NA subtypes except H17 and N10 were isolated from birds, and the novel strain H17N10 has only been found in bats.

The influenza A virus RdRP lacks of proofreading activity, which leads to the sequence variations in the different strains and within the same strain. The accumulation of the mutations on the proteins possessing the neutralizing antibody-binding sites may result in the generation of escape-mutants, a process called antigenic drift [16,17]. Two subtypes of the influenza A viruses are currently co-circulating in humans: pH1N1 and H3N2. The influenza vaccine against seasonal flu needs to be designed according to the antigenic drift of the current year and updated annually.

The most deadly pandemic in last century occurred in 1918-1920 and was caused by the H1N1 influenza virus (“Spanish flu”) of unknown origin. The disease was first observed in January 1918 in the US, and then the outbreaks began in several places of the US in March 1918 [18]. The transportation of the soldiers in World War I caused the

rapid spread of the virus to Europe and Africa, and later, to Asia and Oceania by June 1918. The second wave of the infection occurred in August 1918 from Europe across the world with much higher virulence than the first wave [19]. It is estimated that half of the population of the world at that time was infected with the pandemic 1918 influenza virus, which caused at least 20 million deaths [18]. Unlike other influenza pandemics, with a mortality rate less than 0.1%, the 1918 pandemic had an unusually high mortality rate among infected humans at 2.5% [20].

The infection of one single cell with two or more different influenza virus strains simultaneously can lead to gene mixing, or reassortment. The reassortment of the viral genomes may result in the generation of new subtype, which causes the generation of new influenza virus strains associated with the occurrence of human pandemics. This process is called antigenic shift. Pandemic 1957 Asian H2N2, 1968 Hong Kong H3N2 and 2009 swine-origin H1N1 influenza are all reassorted viruses [21,22].

The pandemic H2N2 (“Asian flu”) was first discovered in Guizhou province of China in February 1957 [23]. It rapidly spread to Hong Kong, Singapore and Japan, and then to the Southern Hemisphere, Europe and North America by August 1957. It is calculated that one fourth of the world’s population was infected with the virus, and the total deaths included more than one million people [19]. The 1957 pandemic H2N2 influenza is an avian/human reassortant virus carrying the surface glycoproteins H2 HA and N2 NA and PB1 originated from avian [21].

Another avian/human reassortant H3N2 virus caused the pandemic “Hong Kong” flu in 1968. The outbreak first appeared in Hong Kong in July 1968; and then spread to South Asia, Australia, Europe, North America, Africa and South America by 1969 [24].

This reassortant virus was generated from the pandemic 1957 H2N2 virus by replacing the HA and PB1 segments from an avian-origin virus [21]. It is estimated that this H3N2 pandemic virus killed approximately one million people worldwide [25].

A novel swine-origin H1N1 emerged from Mexico in March-April 2009, and caused the first influenza pandemic of the 21st century. By June 2009, more than 29,000 cases were confirmed from 74 countries. Up until July 2010, confirmed cases of the 2009 pandemic H1N1 were reported from 214 countries, causing more than 18,000 deaths worldwide [26]. This pandemic influenza formed by a swine triple-reassortant virus (originated from classical swine H1N1, North American avian and human H3N2 viruses) reassorted with a Eurasian avian-like swine virus. The HA, NP and NS segments are from the classical swine virus; the PB2 and PA segments are from the North American avian virus; and PB1 is from the human H3N2 virus. The NA and M segments originated from Eurasian avian-like swine H1N1 virus [27,28]. After 2010, this pandemic H1N1 has moved into the post-pandemic period, but continues to circulate as a seasonal flu by replacing the former H1N1 strain.

Aquatic birds are believed to be the natural reservoir of influenza A viruses, and the HA subtypes H1-H16 and NA subtypes N1-N9 have been isolated from them. Some of the avian viruses have sporadically crossed the species barrier and caused severe diseases in land-based birds and mammals, including humans.

In May 1997, the first HPAI H5N1 virus infecting humans was found in Hong Kong, leading to 6 deaths in 18 infected patients [29,30]. This H5N1 virus disappeared after the poultry depopulation in Hong Kong [31]. The precursor of the H5N1 influenza virus causing the human illness and death in 1997 was first isolated from geese in

Guangdong Province of China in 1996 [31]. The internal gene segments of the virus originated from a quail H9N2 virus, and the NA segment was from a duck H6N1 virus [29]. In February 2003, two people from Hong Kong who had travelled to southern China were confirmed to be infected with HPAI H5N1 [32]. Since 2003, at least 633 human cases of H5N1 infection were reported from 15 countries, including Vietnam, Indonesia, Japan, China and Egypt, and 377 of them died [33]. Meanwhile, the HPAI H5N1 virus spread throughout the countries in East and Southeast Asia, the Middle East, Africa and Europe since 1997, and caused the outbreaks in poultry farms. It is estimated that more than 400 million of the domestic birds were killed by the virus or depopulated to prevent the spread of the virus [34].

From the 1996 precursor strain, the HPAI H5N1 virus has evolved into at least 10 clades based on the genetic and antigenic differences in the strains infecting wild birds and domestic poultry species. Amongst them, clade 0, 1, 2 and 7 have infected humans, and clade 2 can be further divided into 3 subclades. For example, the virus strain that caused severe poultry loss and human illness in Indonesia belongs to subclade 2.1 [8]. Fortunately, no sustained human-to-human transmission of HPAI H5N1 has been observed since 1997 [35]. The potential of HPAI H5N1 acquiring the capability to transmit between humans and resulting in a human pandemic either by antigenic drift or antigenic shift, has been a hot spot for research during recent years. Adaptation studies with whole or reassortment of HPAI H5N1 virus were independently carried out in a ferret model by two different research groups, and the results emphasized the potential of this virus to acquire transmissibility in mammals and cause pandemic. Five amino acid substitutions (N224K, Q226L, T318I, N158D and T160A (H3 numbering)), or four

amino acid substitutions (N224K, Q226L, T318I and N158D (H3numbering) with reassortment, might be sufficient to confer a virus with H5 HA (from HPAI H5N1) aerosol transmission capability in ferrets [36,37]. Amongst them, N224K and Q226L are receptor-binding substitutions, N158D and T160A are HA glycosylation sequon substitutions, and T318I is located at the stalk region.

In March 2013, a novel reassortant avian-origin influenza A (H7N9) virus was identified to infect humans in eastern China [38]. Up to July 4, 2013, a total of 133 people were infected, including 43 cases ending in death [39]. The phylogenetic analysis revealed that the genome of the novel H7N9 resulted from reassortment: the H7 gene most likely originated from the HA of the H7N3 virus isolated from Zhejiang Province of China; the N9 gene may come from the NA of the H7N9 virus of wild birds or ducks from Korea; and all six internal genes most likely originated from the avian influenza virus H9N2 circulating in chickens [40,41]. The virus strains isolated from human cases displayed several molecular virulence makers and pathogenic determinants related to human adaptation [38,42,43,44]. Although a recent epidemiological investigation report showed that the novel H7N9 may be capable of limited human to human transmission [45], no evidence has shown that this novel H7N9 virus sustained the transmission between humans by respiratory droplets.

Low pathogenic avian influenza (LPAI) H9N2 virus has adapted to land-based poultry since the middle of 1990s, and mainly infected chickens. From then on, this virus has overcome the barrier of the host range and caused infections in different hosts, such as quail, turkeys, pheasants, ostriches, mallards and pigs, in many countries across Asia, the Middle East, Europe and Africa [46,47,48]. LPAI H9N2 was also reported to be

sporadically isolated from humans with mild symptoms [49]. Despite the efforts to control the disease, the virus continued to cause the economic loss and public health concern in some of those countries.

Viral proteins

HA

The influenza HA protein is the most important protein in influenza viruses, as it is a critical determinant of host range and virulence [50,51], and the main antigenic determinant of the virus [52]. Based on the sequences and antigenic properties, 17 HA subtypes can be classified into two groups: group 1(H1, H2, H5, H6, H8, H9, H11, H12, H13, H16 and H17) and group 2 (H3, H4, H7, H10, H14 and H15) [53,54].

HA is a homotrimer of three identical subunits [17]. The two main functions of HA during viral entry are receptor binding and viral-host membrane fusion. The precursor HA0 must be post-translationally cleaved into HA1 and HA2 by host extracellular proteases, and thus, the potential of the membrane fusion function of HA2 is activated [55]. HA1 (328 amino acids) and HA2 (221 amino acids) are connected by a disulfide bond linker [56]. The extracellular trypsin-like proteases are responsible for the cleavage of the HAs in LPAI viruses and mammalian influenza viruses [57]. These proteases recognize the HA cleavage sites with a single arginine, such as Q/E-X-R in the amino acid sequence [58]. Whereas, the HA of HPAI viruses (H5 and H7 subtypes) contain the polybasic amino acid cleavage sites, such as R-X-R/K-R, can be recognized by the intracellular ubiquitous proteases, such as furin-like protease [22,57]. The spread of LPAI viruses and mammalian influenza viruses are limited as their HAs are cleaved

extracellularly on the host intestinal and respiratory mucus surfaces where the trypsin-like proteases are found. Whereas the HPAI viruses cause systemic and virulent infections, because their HAs are cleaved intracellularly by the furin-like proteases which are distributed in multiple organs of the host [22].

The terminal sialic acids (SA) of the glycoproteins and glycolipids on the cell surface are the receptors of influenza A viruses [52]. The receptor-binding site (RBS) of HA1 is located on the global head region, including four conserved secondary structures: the 130-, 150- and 220-loops, and the 190-helix [17,59,60,61], which contain several residues highly conserved in most subtypes of influenza [17,62]. Ser-136 and Tyr-98 form hydrogen bonds with the carboxylate and the 8-hydroxyl group of the sialic acid, respectively. His-183 and Glu-190 form a hydrogen bond with the 9-hydroxyl group, and Trp-153 contacts with the methyl group of sialic acid through van der Waals force. Leu-194 and Tyr-195 are also important residues for receptor binding [62,63,64].

Avian-like influenza viruses preferentially bind to α -2,3-linked sialic acid (α -2,3-SA), which are distributed on the epithelial cells of the intestine of birds and lower respiratory tract (LRT) of humans [65]. Human-like viruses preferentially bind to α -2,6-linked sialic acids (α -2,6-SA), which are distributed on the bronchial epithelial cells of the human upper respiratory tract (URT) [65,66]. Interestingly, swine viruses may bind to both α -2,3-SA and α -2,6-SA receptors [67,68,69]; however, the 2009 H1N1 swine-origin pandemic influenza virus is reported to bind to α -2,6-SA, as well as limited α -2,3-SA [70,71]. Six residues in HA RBS, Ala-138, Glu-190, Leu-194, Gly-225, Gln-226 and Gly-228, are important determinants for the host range. They are highly conserved among avian-like influenza viruses, and generally require the mutations in HA RBS to increase

the binding affinity to α -2,6-SA when adapted to humans [72]. The newly identified influenza A virus H17N10 has only been found in bats. The crystal structure and glycan microarray studies of H17 HA revealed that although the H17 has a protein folding similar to other HA subtypes, it does not bind to either human α -2,6-SA or avian α -2,3-SA receptors; and no H17 binding was detected either using a glycan microarray with more than 600 known glycans [73,74]. The analysis of the H17 putative RBS showed that some key residues, such as Trp-153, His-183, Leu-194 and Tyr-195 are conserved as the typical influenza A HA, but substitutions Y98F, T136D, and G228D and the truncated 150-loop due to a 157 and 158 aa deletion may account for the failure of H17 binding to canonical human or avian receptors [73]. The results suggested that H17N10 may utilize different receptor-binding and cell-entry mechanisms from other subtypes of the influenza A virus.

Asp-190 and Asp-225 in the HA of 1918 pandemic and 2009 pandemic H1N1 are critical for the α -2,6-SA affinity in humans [66,75]. The studies have shown that HPAIV H5N1 HA preferentially binds to terminal α -2,3-SA moieties, but the H5N1 mutants discovered in recent years contained the substitutions G143R and N186K, or Q226L and G228S, or T160A, or Q196R in HA, which changed the receptor-binding specificity of the virus from α -2,3-SA to α -2,6-SA [76]. The amino acid substitution Q226L on the HA RBS of avian H9N2 viruses has been showed to increase α -2,6-SA binding affinity and enhance virus replication in human respiratory epithelial cells and in ferrets [77,78]. Q226L has also been found in the HA of two strains (A/Anhui/1/2013/and A/Shanghai/2/2013) from the novel avian-origin H7N9 virus, which indicate that the virus acquired the increased affinity for the α -2,6-SA receptor of UTR in humans

[38,42]. However, one of the latest structural analysis and glycan studies has shown that the binding of H7N9 HA to human receptors was limited; and further introduction of a single substitution G228S in HA would greatly increase the receptor binding affinity of H7N9, and result in a better fitness of the virus in humans [79].

HA is the main antigenic determinant of the influenza A virus. The antibodies against HA can be classified into two groups: the first group recognizes and binds the epitopes on HA1, blocking the attachment of HA on the receptors; whereas the second group prevents membrane fusion by binding to the stalk region of HA [80,81]. The antigenic sites of the first group, termed Sa, Sb, Ca, and Cb, are located on the globular head of HA surrounding the RBS [17]. In contrast, the antigenic binding sites of stalk antibodies are generally distant from the RBS [80]. Influenza viruses overcome the host antibodies through antigenic drift and antigenic shift.

NA

The influenza NA protein, an exosialidase (EC 3.2.1.18), catalyzes the cleavage between the terminal sialic acid and the adjacent sugar of the viral receptor. This receptor-destroying activity facilitates the release of the progeny virions from the surface of the infected cells [82], and it can be directly inhibited by the NA antibodies [83]. NA also plays important role in the early stages of viral infection by the removal of the glycan structure of mucus and promoting the binding of HA to the receptors in the respiratory tract [84]. The functional balance between HA receptor-binding and the receptor-destroying activity of NA is important for the efficient replication of the influenza virus. For example, the 1957 pandemic H2N2 virus strain possessed an HA preferentially binding to α -2,6-SA and an NA preferentially binding to α -2,3-SA. Since

1957, N2 gradually adapted with the HA sialic acid binding affinity and evolved to cleave both α -2,3 and α -2,6-SA receptors [85]. By now, ten subtypes of NAs have been identified in influenza A viruses. Influenza A NA can be phylogenetically classified into 2 groups: the N1, N4, N5 and N8 subtypes belong to group 1, and the second group is composed of the N2, N3, N6 N7 and N9 subtypes [86]. Recent studies have demonstrated that the crystal structure of newly identified N10 (from influenza A virus H17N10, discovered in little yellow-shouldered bats) is similar to that of the other NA subtypes, but N10 exhibits extremely low NA activity [87,88].

NA forms a tetramer on the surface of influenza virus, and is also a glycoprotein (with a 60 kDa molecular mass for the monomer, and 240 kDa for the tetramer) [82]. The 3D structures of N1, N2, N4, N8 and N9 have been resolved, showing that the protein contains cytoplasmic, transmembrane, “head” and “stem” domains [89]. The catalytic site and metal-ion binding domain are located in the head of the NA [90], and the amino acid residues 74-390 (N2 numbering) are highly conserved in this region in all subtypes of NA. The residues Arg-118, Asp-151, Arg-152, Arg-224, Glu-276, Arg-292, Arg-371, and Tyr-406 are critical to the function of the active site; and the residues Glu-119, Arg-156, Trp-178, Ser-179, Asp (or Asn in N7 and N9) -198, Ile-222, Glu-227, Glu-277, Asp-293 and Glu-425 stabilize the structure of the domain [89].

N-Acetylneuraminic acid (Neu5Ac) is the predominant sialic acid existing on the surface of mammalian cells, and the binding of Neu5Ac to the active site of NA triggers a conformational change. Neu5Ac interacts with the residues Arg-118, Arg-292 and Arg-371 of NA, and subsequently drives the cleavage of the sialic acid [91]. The NA inhibitors oseltamivir (Tamiflu®) (containing the Neu5Ac group) and zanamivir

(Relenza®) (containing the Neu5Ac2en group) are both sialic acid-mimicking drugs, which block the sialidase activity of NA by binding to the active sites [92,93].

In the recent years, H274Y in group 1 NAs and R292K in group 2 NAs have been identified as the oseltamivir-resistant mutations [94]. The NA R292K mutation has also been found in two patients with novel H7N9 in China who received corticosteroid treatments [95]. Both the H274Y and R292K mutations in NA reposition the side chain of Glu-276, which developed oseltamivir resistance by distinguishing the L-ethylpropoxy group from the glycerol part of the sialic acid. Therefore, the mutant NA with H274Y or R292K lost the function of binding to the L-ethylpropoxy group of oseltamivir, but still retained the interactions with the glycerol part of the sialic acid receptors [93].

Deletions on the NA stalk region occur in the interspecies transmission of influenza viruses from aquatic birds to gallinaceous poultry (chickens or turkeys) [96,97,98,99], and during the transmission of influenza viruses in poultry [100,101]. In 2000, the HPAI H5N1 strain with a 20-amino acid deletion (49-68 aa) in the NA stalk has been first discovered from human isolates. From 2000 to 2007, the percentage of human H5N1 isolates possessing this deletion dramatically increased from 15.8% to 100%. The NA with different stalk deletions has been demonstrated to be associated with the high virulence of HPAI H5N1 in chickens and mice [99]. The interspecies transmission studies of H2N2 and H9N2 avian influenza viruses from wild aquatic birds to quail and chickens led to a 27- and 21- amino acid deletions in the NA stalk, respectively, and enhanced virus replication in chickens and mice [96,98]. A 5-amino acid deletion (69-73 aa) has also been detected from the NA stalk region of the 2013 novel avian-origin H7N9 virus insulates, which may be associated with the adaptation in poultry and increased

virulence in humans [102]. The mechanism of the deletion in the NA stalk region is still unclear, but the deletion generally appears following the increased glycosylation sites in HA, which may result in the immune escape from the neutralizing antibody recognition [103,104].

M1

M1, the most abundant protein in the virion, is under the lipid bilayer membrane, and binds to the viral RNPs. M1 plays important roles in the life cycle of influenza virus, including uncoating, viral mRNA transcription, vRNA export, assembly and budding. The interactions among M1, vRNP and NEP trigger the export of vRNPs from the nucleus and the budding of the progeny virions from the cell surface [105,106].

The crystal structural study revealed that M1 is composed of an N-terminal domain and a C-terminal domain, which are connected by a linker. Both domains have a α -helical structure, and the N-terminal domain contains two subdomains. A binding domain is located on residues 89–164, which are responsible for the NEP binding [107]. This domain also consists of a well-characterized basic amino acid-rich nuclear localization signal (NLS) (101-RKLKR-105), which is critical for the transport of M1 into the nucleus [108,109]. The newly synthesized M1 protein is imported into the nucleus by importin- α 1 via the NLS [110]. In the nucleus, M1 interacts with the histones and involves in the release of vRNPs from the nuclear matrix [111]. The binding of M1 to vRNP subsequently inhibits the viral mRNA transcription. M1 also binds to NEP to form the NEP–M1–vRNP complex, which is exported from the nucleus by a nuclear export signal (NES) on the NEP (amino acid residues 12 to 21) [112]. Recently a leucine-

rich NES was also identified in the M1, and Leu-66 and Val-68 are critical residues for the export of the M1 into the cytoplasm [113]. In the cytoplasm, the binding of M1 to vRNP prevents the reentry of vRNP into the nucleus [114].

Three consecutive arginine residues 76 to 78 (76-RRR-78) in the M1 gene are highly conserved among the influenza A viruses. This basic amino acid stretch affects the M1 transportation, virus assembly and budding, and plays a critical role in the viral replication [115].

Phosphorylated tyrosine is important to the nuclear import of M1 by binding the protein to the nuclear import factor importin- α 1. The amino acid residue Tyrosine 132 in the M1 of the influenza virus A/WSN/1933(H1N1) has been identified as a phosphorylation site which is crucial to the nuclear import of M1 and virus replication [110].

M2

M2 monomer is a polypeptide with 97 amino acids. The homotetramer of the M2 protein forms a proton ion channel, which is regulated by pH. The N-terminal transmembrane (TM) domain of M2 extends outside the viral membrane, and the C-terminal connects the viral interior [116]. The highly conserved residue His-37 is a “pH sensor” of the channel to enhance the H⁺ flow at low pH; and Trp-41 forms a “gate” to block the ion channel at high pH [117,118]. During viral entry, M2 pumps protons from the endosome and reduces the pH of the viral interior, subsequently dissociating M1 protein from vRNP, and initiating the uncoating process [56]. In the trans-Golgi network

(TGN), M2 prevent HA from premature conformational rearrangement by connecting the TGN with the cytoplasm and equilibrating the pH [119].

The anti-influenza drugs amantadine and rimantadine bind to the channel pore of the M2 as targets, and block the ion channel, so that they stop the acidification of the viral interior [120,121,122,123]. The X-ray and NMR structural studies of the M2 TM domain revealed that amantadine has two different binding sites on M2: at pH 5.3, it binds to M2 near Ser-31 and directly stops the proton flow [124]; and at pH 7.5, it binds to the TM helix near Trp-41 and allosterically blocks proton conductance [119].

However, the use of M2 inhibitor drugs amantadine and rimantadine has caused the occurrence of resistant mutation strains in nature under selection stress [125,126]. In recent years, a typically resistant mutation N31S has also been discovered in numerous of virus strains from the M2 of different subtypes, such as the seasonal H3N2, 2009 swine-origin pandemic H1N1, HPAI H5N1 infecting humans as well as the novel avian-origin reassortant H7N9 viruses [22,44,127]. The structural study demonstrated that the substitution N31S does not change the ion channel pore structure, but greatly reduces the affinity of anti-influenza drug binding to the allosteric site [128]. Therefore, N31S does not impair the M2 function on protons pumping, but blocks the binding of the M2 inhibitors to the ion channel.

NP

NP encapsidates the segmented RNA and binds to the RdRP to form ribonucleoprotein particles (RNPs) [112]. The NP protein monomer contains a head and a

body domain, and folds into a crescent-shape. The exterior surface of the head and body domain has a single strand RNA binding groove. The tail loop (residue 408-419) of the NP protein inserts into the loop-binding cavity of a neighboring NP monomer, and self-associates into the oligomeric structure. The loop-binding cavity is considered to be a potential target for anti-influenza drugs [93,129]. A salt bridge between Arg-416 in the tail loop and Glu-339 in the neighboring NP monomer plays an important role in the NP-NP interaction and viral replication [130].

The nuclear localization sequence (NLS) on the NP mediates the import of the vRNP complex into the nucleus in the influenza life cycle. The NP monomer contains three NLS: NLS1 is located at residues 3-13 at the N-terminus, NLS2 is located at residues 90-121, and NLS3 is located at residues 198-216 [131,132,133].

NP is a major component of the influenza vRNP, which is responsible for the transcription and replication of viral RNA. A recent report revealed that NP is not necessary for the initiation or termination of viral transcription and replication, but a cofactor of RdRP for elongation during the replication of the full-length viral genome. The recruitment of NP to newly produced vRNA is mediated unidirectionally through NP oligomerization, and this processing is independent of RNA binding [129].

RNA-dependent RNA polymerase

The influenza virus RNA-dependent RNA polymerase (RdRP), a heterotrimer of three subunits (PB1, PB2 and PA), with a combined mass of around 250 kDa, is responsible for viral RNA transcription and replication. The PA subunit, a 80 kDa subunit, contains an N-terminal endonuclease and protease activities domain and a C-terminal

domain interacts with the PB1 subunit. The crystal structure of both the N-terminal endonuclease activity domain (PA_N: residual 1-197 aa) and C-terminal PB1 binding domain (PA_C residual 237-716 aa) have been solved [134,135,136,137]. Recent structural studies of PA have indicated that the N-terminal 209 amino acids are responsible for an endonuclease activity of the virus polymerase [134]. Manganese (Mn) ions play important roles in stabilizing the active site [134]. The crystal structure study demonstrated PA is a type II restriction endonuclease [134]. The active sites of PA bind to two manganese ions, following two-metal-dependent endonuclease pattern. Two active sites involved in Mn⁺⁺ binding were identified: Glu-80 and Asp-108 are critical for Mn₁ binding and His 40, Asp 108 and Glu 109 important for Mn₂ binding [134,136] (Figure 1.2).

The synthesis of viral mRNA utilizes the short capped primers derived from the host cells using a ‘cap-snatching’ mechanism: PB2 binds to the cap of the cellular pre-mRNA, the endonuclease activity of PA cleaves onto the 10-13 nt downstream the cap and then PB1 takes the short capped mRNA as the primer to synthesize the viral mRNA. The “cap” prevents the viral mRNA from degradation by exonuclease and promotes the viral mRNA translation [134,138,139,140]. The negative-sense vRNA is the template for both mRNA and cRNA, but cRNA does not consist of 5’-cap or 3’- poly(A) tail. Meanwhile, unlike mRNA transcription, the replications of cRNA and vRNA are primer-independent [141].

C-terminal PA binds to the N-terminal PB1 (PB1_N) in the RdRP complex. The structure of PA_C-PB1_N demonstrated that the PA residues 257-716 contain a motif to interact with the first 14 amino acid residues of PB1 [135,137]. An earlier report even

showed that the first 12 amino acids of the N-terminal PB1 form the interaction interface, and could be enough for PA binding [142].

Some important residues on the PA have been identified for their biological functions. The mutation T157E dramatically decreases the RNP replication activity [143]. Ser-186 of the N-terminal PA plays an important role in the polymerase activity of the 2009 swine-origin pandemic H1N1. While residual G186 is more common for most of the influenza virus PAs, PAs possessing S186 is more fit for PB1 and PB2 in the 2009 swine-origin pandemic H1N1 strain, resulting in a high RdRP activity [144]. The PA subunit is also involved in the regulation of the RdRP activity in some temperature sensitive strains, and residue 114 is critical for stability under the thermal stress [145].

PB1 is another subunit of RdRP, which is responsible for the polymerase activities of viral mRNA transcription and cRNA and vRNA replication. Four conserved motifs have been identified in PB1, which are responsible for the RNA-dependent RNA polymerase activity and RNA-dependent DNA polymerase activity: A (residues 298-311), B (residues 399-412), C (residues 438-453) and D (residues 474-484) [146,147]. In addition, motifs pre-A and E are also responsible for the RNA-dependent RNA polymerase activity [148]. However, the structure of the catalytic sites have not yet been resolved yet, and detailed information about the motifs is unclear [56]. The C-terminal region (residues 678-757) of PB1 binds to the N-terminal region (residue 1-37) of PB2 (Figure 1.2).

A small helix containing the residues P_{TLLFLK} of PB1_N interacts with a cleft flanked by four α -helices and a β -hairpin of the PA_C. This interaction stabilizes the

complex between the domains of PB1 and PA. The amino acid residues on the PA_C and PB1_N interface are highly conserved among all subtypes of influenza A viruses [135,137].

PB2 has been featured in binding the “cap” of host pre-mature mRNA to its binding domain (residue 318-483), and facilitating the cleavage of the downstream mRNA by PA following the “cap-snatching” mechanism [134,138,139,140]. A RNA-binding domain is located at residues 535-684. The PB2 contains at least one NLS at C-terminus, which binds to the cargo adaptor importin- α and mediates the import of the vRNP into the nucleus [149]. The crystal structure of the PB2-human importin- α 5 complex displayed the presence of NSL: 736-KRKR (X)₁₂K-752 [150,151]. Another putative binding domain of PB2 is located on residues 535-684, which is next to the NLS-containing domain, and has been identified as an RNA binding domain [152,153] (Figure 1.2).

Position 627 in PB2 has been recognized as a key host range determinant: glutamic acid is generally found at residue 627 in the avian virus isolates, whereas almost all human isolates present a lysine at this position. The PB2 627K has been identified from most human H1N1 and H3N2 virus strains. HPAI H5N1 carrying 627K showed enhanced virulence in humans, and caused a systemic and lethal infection in mice [154,155]. The virus bearing the PB2 K627 residue can replicate efficiently in the URT of humans at 33°C. In contrast, the avian-like viruses containing E627 in the PB2 preferentially replicate in the intestinal tract at the temperature of 41°C [155]. Therefore, position 627 in the PB2 is a temperature sensitive determinant for viral replication in avian and mammal hosts [21].

Another important mutation D701N in the PB2, has been identified from HPAI H5N1 isolates from infected humans, and is believed to be associated with the enhanced virulence when the avian viruses adapted in mammal hosts [156]. D701N modulates the transmissibility of the influenza virus in mammal hosts for the lack of E627K. D701N may enhance the viral replication by facilitating the import of PB2 into the nucleus of human cells, but not avian cells [157]. Interestingly, both E627K and D701D mutations have been discovered from the PB2 protein of the novel avian-origin H7N9 isolates, which suggest that these two mutations are critical for the adaptation of the avian virus to replicate in human cells [38]. The 2009 pandemic H1N1 strain does not contain K627 or N701 in the PB2 gene, but is replicated and transmitted efficiently in humans. It has recently been reported that the residue R591 in the PB2 protein is responsible for the enhanced replication of pandemic 2009 H1N1 in mammals in the absence of K627 and N701 [158].

NS1

The non-structural protein 1 (NS1) of the influenza A virus has been identified to be the protein with multiple accessory functions during viral infection, and virulence determinant. Phylogenetic analysis of the influenza A virus NS1 amino acid sequences showed that they can be divided into two groups: allele A and allele B [97,159]. The NS1 in all human, swine, equine, and most of the avian influenza viruses are allele A, while the NS1 in other avian influenza virus belongs to allele B [159].

NS1 protein contains 230-237 amino acids, depending on the strains, and has a molecular weight around 26 kDa. According to the biological function, NS1 can be divided into the N-terminal (residues 1-73) RNA-binding domain (RBD) and C-terminal

(residues 84-207) effector domain (ED), which are connected by a linker. The structure of the 20 amino acids on the C-terminal domain may be naturally disordered [160]. The RBD domain is reported to be a homo-dimer made up of two monomers with three α -helices [161]. Dimerization is critical for dsRNA binding, and several residuals contribute to this RNA-protein interaction [162], amongst them, two basic residues Arg-38 and Lys-41 are critical to the RNA-binding activity [160]. Structural studies indicated that the ED domain may homodimerize independently, and that the monomer contains three α -helices and seven β -stands [163]. However, the latest NS1 protein x-ray structural study of HPAI H5N1 virus suggested that the NS1 formed multimers instead of separated homodimers, and that three NS1 chains can interact together to form a “tubular organization” [164]. It seems that this model may explain why NS1 can interact with dsRNA and importin- α by its RNA-binding domain, simultaneously [164].

There are generally two nuclear localization sequences (NLS1 and NLS2) and one nuclear export sequence (NES) on NS1: 35-41 are highly conserved amino acids for nuclear export sequence (NES) on NS1: 35-41 are highly conserved amino acids for NLS1 (R38 and K41 are critical amino acids for importin- α binding and translocation), and NLS2 (with basic amino acids at position 219, 220, 224, 229, 231 and 232) is deficient in some of the strains [165]. A newly identified nucleolar localization signal (NoLS) overlaps with NLS2, and residue Lys-221 was identified as the critical residue for NoLS [166]. Newly synthesized NS1 is imported into the nucleus by binding to cellular importin- α [165], while it has been reported that NS1 also has a potential nuclear export signal (NES) responsible for the nucleo-cytoplasmic transportation. Leu-144 and Leu-146 are critical for the function of NES [167].

NS1 interacts with multiple host factors through its binding sites on the protein during viral infection [160] (Figure 1.3). One of the major functions of NS1 is to antagonize the innate immune response of the host during influenza infection, especially to limit the production of interferon beta (IFN- β) induction by both pre-transcription and post-transcription. In the pre-transcription process, NS1 can inhibit the activation of transcription factors on the IFN- β signaling pathway, such as IRF-3, c-Jun/ATF-2 and NF- κ B, by binding to dsRNA [168,169]. In the post-transcription process, NS1 can block cellular mRNA maturation by binding to the 30 KD cleavage and polyadenylation specific factor (CPSF30) and poly(A)-binding protein II (PABPII) [170,171].

The study of the mechanism found that NS1 also directly binds to the cytosolic sensor RIG-I, forming a complex, and inhibiting its functions of inducing the expression of IFN- β [172,173,174]. The mechanism revealed that TRIM25 activates RIG-I by ubiquitinating RIG-I N-terminal CARD domain; while NS1 inhibits the ubiquitination of the CARD domain and blocks type I IFN production [175]. Residues 200 and 205 of the NS1 have been identified as being critical for the antagonistic activity of type I IFN in the ferret model [176].

A recent study has shown that avian H5N1 NS1 disrupts the IFN- β signaling by decreasing STAT1, STAT2 and STAT3 and limiting the phospho-STAT2 nuclear translocation [177]. Additionally, ISG15, a type I IFN induced, ubiquitin-like molecule, has been demonstrated to target influenza NS1 and protect the cells from viral infection; and the ISGylation of NS1 can prevent the nuclear import of the NS1 protein. Lys-41 has been identified to be an important residue on NS1, responsible for the acceptor site of

ISG15 [178]. Herc5, an ISG15 E3 ligase, could catalyze the conjugation of ISG15 onto the NS1 protein [179].

NS1 can also regulate some other important host cell signaling pathways during influenza virus infection, such as the phosphatidylinositol 3-kinase (PI3K)/Akt pathway, which plays the central role in a number of functions in the host cells, such as anti-apoptosis, cell proliferation and cytokine production [180,181,182,183]. PI3K is a dimeric lipid kinase consisting of a regulatory subunit p85 β and a catalytic subunit p110 [184]. Akt, a serine/threonine protein kinase, is a downstream PIP₃-binding effector of PI3K. In the early phase, the attachment of the virus to the cell surface transiently induces PI3K signaling [185]. In the later phase, PI3K is activated by NS1 and the influenza viral RNA through the stimulation of the cytosolic receptor, RIG-I, promoting the production of type I IFN [186,187]. NS1 activates PI3K signaling by directly binding to inter-HS2 (iSH2) domain of the regulatory subunit p85 of PI3K, and prevents the premature apoptosis of the infected cells, facilitating the viral replication [188,189]. It has been reported that NS1 can preferentially interact with phosphorylated Akt in the nucleus, altering Akt anti-apoptotic activity [190].

NS1 can also interact with a number of host proteins to overcome the innate protection of the host, and facilitates viral replication during infection. NS1 enhances the viral protein synthesis by binding the eukaryotic translation initiation factor eIF4GI to the viral mRNA 5' untranslated region [191]; meanwhile, it limits the expression of the host antiviral gene [137]. It has been also reported that NS1 can suppress the host antiviral function by blocking 2'-5'-oligoadenylate synthetase (OAS) [192] and serine/ threonine protein kinase R (PKR) [193].

Some species-specific and strain-specific studies were carried out to understand the different effects of NS1 on multiple viral and host functions. NS1 from the human influenza virus has the typical C-terminal RSKV motif, while the motif of avian influenza virus is ESEV at the C-terminus. This four-amino acid domain is a species-specific virulence domain [194]. The typical avian influenza NS1 ESEV is also a PDZ-binding motif (PBM), which has an anti-apoptosis function during viral infection through NS1-PDZ interaction to inhibit the proapoptotic function of Scribble [195]. However, the NS1 ESEV motif doesn't have a significant effect on the virulence of the highly pathogenic avian influenza virus A/Vietnam/1203/04 (H5N1) in the host [196]. Glycine 184 in the NS1 of A/PR/8/34 is reported to dramatically affect the virulence through an unclear mechanism other than through IFN signaling [197]. Different HP H5 and H7 NS segments were placed into the background of HP H7N1 (A/FPV/Rostock/34) to generate reassortant influenza viruses, which showed that the host range, viral replication, host type I IFN response and apoptosis were affected by the origin of the NS segment [198]. Comparing NS1 of the highly pathogenic H7N1 (A/ostrich/Italy/984/00) to its low pathogenic precursor H7N1 (A/chicken/Italy/1082/99) showed that the difference is only two mutations in NES, and a 6-amino acid truncation at the C-terminus resulted from the third mutation by introducing a new stop codon. The cytoplasmic accumulation of NS1 is responsible for the enhanced pathogenicity of HP H7N1 [199]. The 2009 pandemic H1N1 NS1 encodes only 219 amino acids with 11 amino acids truncation at the C-terminal domain, resulting in the loss of the NoLS and PABP II binding domain. The restoration of those 11-amino acid did not enhance the viral replication, but did increase the virulence in mice [200]. Those strain-specific functions of NS1 are listed in Table 1.2.

NEP

NEP, a 121 amino acid polypeptide, is produced from a spliced form of segment 8 mRNA [201]. NEP was considered to be non-structural protein, and named as NS2. However, NEP was later found to interact with the M1 protein and exists in the viral particles, and thus, NS2 was renamed nuclear export protein (NEP) [202,203]. NEP consists of an N-terminal domain (residues 1-53) that is sensitive to protease, and a C-terminal domain (residues 54-121) that is resistant to protease [204]. The C-terminal domain contains two α -helices, C1 (residues 64-85) and C2 (residues 94-115) [205].

The functional study of NEP revealed that it is an adaptor protein, binding to both RNPs and the cellular protein Crm1, and mediates the nuclear export of newly produced RNP. NEP interacts with Crm1 via the nuclear export signal (NES), which is located at the N-terminal domain at residues 12-21 [204,205]. W78 was demonstrated to be critical for the binding of the M1 protein [206]. The recent studies demonstrated that NEP is important in modulating the accumulation of viral vRNA, cRNA and mRNA during infection. The function of NEP on the regulation of viral RNA transcription and replication plays an important role in the adaptation of the HPAI H5N1 influenza virus to mammals [207]. In addition, NEP contains the motifs for phosphorylation and SUMOylation, but the functional importance is still unclear [202,208,209].

Influenza A life cycle

Entry into the host cell and uncoating

In the first stage of viral entry, influenza A virus surface glycoprotein HA recognizes and binds to the sialic acid (SA) receptors on the cell surface with its receptor-binding sites (RBS). Another surface glycoprotein NA facilitates HA in accessing the receptors in the respiratory tract, by cleavage of the glycans of the mucus [84]. The HA-receptor binding, in turn, initiates receptor-mediated endocytosis, and the virus enters the endosome of the host. Influenza viruses utilize clathrin-mediated endocytosis and other mechanisms, such as caveolae, nonclathrin/noncaveolae pathway and macropinocytosis, in this step [210]. The low pH of the endosome triggers a conformational change in the HA, and the HA2 fusion peptide is exposed. This fusion peptide inserts itself into the endosomal membrane, bringing the viral lipid-bilayer membrane and endosomal membrane close to each other, and fusing the membranes [141]. However, the details about this membrane fusion process are unclear.

In the endosome, the protons flow into the interior of the virions through the M2 ion channel, creating a low pH environment, and dissociating the vRNPs from the M1 protein [141]. This process is called uncoating [211]. In the cytoplasm, the vRNPs are imported into the nucleus through the host importins, which recognize and bind the NLS of the NP protein. A recent study revealed that the interactions between the unconventional NLS1 (residues 3-13) in the NP, and the cellular import cofactors importin- α 1, α 3 and α 5, are critical to the nuclear localization of vRNP. NLS1 may further regulate viral RNA transcription and replication through the interaction with importin- α 3 [212].

mRNA transcription and genome RNA replication

Host RNA polymerase II activity is important to viral mRNA synthesis. The cellular mRNAs acquire the 3' end poly(A) tails by cleavage at the polyadenylation signal (AAUAAA). However, influenza viral genomic RNA does not have this sequence, but viral mRNA generates a poly(A) tail following a “stuttering” mechanism: RdRP polyadenylates the viral mRNAs by moving back and forth at a stretch of five to seven uridine residues on the 5' ends of the viral RNA templates [213]. The viral mRNAs are exported into the cytoplasm and translated into viral proteins by ribosomes.

The polymerase activity of PB1 is responsible for both transcription and replication. vRNA replicates with steps of (-)vRNA → (+)cRNA → (-)vRNA in a primer-independent manner [141]. However, the mechanism of vRNA replication is still unclear. An internal initiation model has been proposed for vRNA replication recently [214]. In the (-)vRNA → (+)cRNA step, the host RNA-specific ribonucleotidyltransferases add one nucleotide to the 3'-end of cRNA and initiate the full-length copy of (-)vRNA. In the (+)cRNA → (-)vRNA step, the nucleotides AG were synthesized using the nucleotides UC on the 3'-end of cRNA by RdRP, and AG is taken as the primer for the full-length copy of (+)cRNA. The RdRP cannot form the stable initiation complex until it reads through the UUU of cRNA and UUUU of vRNA at their 3'-ends [214].

In the vRNP complex, NP directly binds to the PB1 and PB2 subunits; NP also binds to the RNA in a sequence-independent manner; and NP is essential for the full-length genome replication of the influenza A virus. However, the role of NP in transcription and replication has long remained unclear. One latest study has revealed that NP is a cofactor of RdRP for the elongation during the replication of the full-length viral

genome, but has no effect on the initiation or termination of transcription and replication. The recruitment of NP to newly produced vRNA is mediated through NP oligomerization in a “tail loop first” direction in an RNA binding independent manner [129].

The recent study demonstrated that the differences in the importin- α isoform specificity affect the efficiency of viral RNA transcription and replication in different hosts: PB2 and NP of the human-like viruses prefer importin- $\alpha 7$, whereas PB2 and NP of the avian-like viruses prefer importin- $\alpha 3$. Interestingly, the 2009 pandemic H1N1 showed both importin- $\alpha 7$ and importin- $\alpha 3$ specificities [215]. Another study showed that the substitutions D701N in PB2 and N319K in NP increased the binding affinity of these two proteins to importin- $\alpha 1$ in the mammalian cells, but had no effect in avian cells [157].

The negative-sense small viral RNAs (svRNAs) have been identified as an important regulatory enhancer of viral polymerase activity. svRNAs are produced from the viral positive-sense genomic RNA, and bind to the PA subunit. In the nucleus, svRNAs promote the viral genome replication and maintain the RNA segment balance [216].

The M2 and NEP proteins are produced from the spliced forms of segment 7 and 8 mRNA, respectively; and utilize the host splicing machinery in the nucleus. NS1 is translated and transported into the nucleus, and facilitates the splicing of viral mRNA by binding to and re-localizing the splicing components [217]. NS1 also blocks the export of cellular mRNAs by binding to CPSF 30 and PABP II, and preventing the maturation of cellular mRNAs [170].

Recent studies have shown that NEP plays a critical role in regulating the accumulation of the viral mRNA, cRNA and vRNA produced by RdRP [218].

Furthermore, M16I and other mutations in the NEP of human H5N1 isolates can enhance the polymerase activity of the avian H5N1 virus carrying 627E in PB2. The result suggest that adaptive mutations on NEP can compensate for the lack of 627K in PB2, and increase the viral replication of avian viruses in human cells [219].

The export of vRNP

Newly produced vRNP, M1 and NEP proteins are transported to the nucleus. The C-terminus of M1 binds to the vRNP through NP, and the N-terminus of M1 binds to the C-terminus of NEP with its NLS. The N-terminus of NEP binds to Crm1 through its NES, along with GTP-bound Ran (RanGTP), a cofactor of Crm1 [220]. (Crm1–RanGTP)–NEP–M1–vRNP (also been called the “daisy-chain” complex) mediates the export of vRNP to the cytoplasm [204]. However, a study has shown that without M1 and NEP, NP can directly interact with Crm1 and mediate the export vRNP from the nucleus [221].

The M1 protein plays important roles in the export of vRNP, in addition to forming the complex with vRNP and NEP. In the nucleus, the binding of M1 to the histones may be associated with releasing vRNP from the nuclear matrix [111]. After transportation into the cytoplasm, the binding of M1 to vRNP prevents the reentry of vRNP into the nucleus [114].

Recent studies identified several other host factors that aid or inhibit the export of the vRNP complex from the nucleus. Serum- and glucocorticoid-regulated kinase 1 (SGK1) has been identified as a host factor playing an important role on the nuclear export of vRNP. However, the mechanism of SGK1 interacting with vRNP remains to be

elucidated [222]. The SUMOylation of M1 at K242 by the SUMO-conjugating enzyme Ubc9 is critical to the interaction between M1 and vRNP to form the M1-vRNA complex. Without SUMOylated M1, vRNP export is inhibited, and the viral protein and vRNP are accumulated in the cells [223]. The heat shock protein 70 (HSP70) has been identified as a host factor inhibiting the nuclear export of vRNP at both 37°C and 41°C. HSP70 interacts with the vRNP complex, and disassociates M1, but not NEP from vRNP, so that it blocks the export of vRNP [224].

Multiple approaches have been used to search for the host factors associated with influenza A virus life cycles. Several novel host factors that may be involved in the transport of vRNP from the nucleus to the cytoplasm, such as AKT1, mouse double minute 2 homolog (MDM2) and I-kappa- B kinase epsilon (IKBKE), have been identified by an RNAi-based genome-wide screen. However, the functions of those factors in the influenza life cycle need to be further elucidated [225].

Assembly and budding

The surface proteins HA, NA and M2 are translated by ribosomes associated with the rough endoplasmic reticulum (ER), and processed by post-translational modifications, such as glycosylation at the Golgi apparatus, and then transported to the plasma membrane via the cellular secretory pathway [141]. The study of mutated and truncated M2 suggests that the location of M2 in this process is crucial to the formation of viral particles in that M2 may control the budding process [226]. The NEP-M1-vRNP complex exports into the cytoplasm, mediated by host Crm1 [160]. The M1 protein alone may direct the complex to the plasma membrane [141]. A recent study demonstrated that

the HA and NA concentrate on the plasma membrane with higher cholesterol components, and form a lipid raft microdomain, or bud [226]. A bud neck emerges at the boundary of the lipid raft and the plasma membrane by a line tension. M1 recruits small quantities of the proton ion channel M2 molecule for “membrane scission”, where transmembrane M2 molecules accumulate at the bud neck, and cleave the viral particles from the cell membrane [226]. Therefore, unlike some other enveloped viruses, the influenza A virus evolved the strategy to utilize its own molecule M2 ion channel for budding, instead of the classic endosomal sorting complex required for the transport (ESCRT) pathway [226].

Packing all 8 genomic segments with each into the virions is important for producing an infectious particle [226]. However, the packaging mechanism is still in being debate, though there are two main models: the incorporation of a full genomic complement; and a model which the segments are randomly selected but packaged in sufficient numbers to ensure the newly produced virions are properly formed [227]. In a recent study, the copy number of each RNA segment within a single virus particle was counted using the method based on multicolor single-molecule fluorescent in situ hybridization (FISH) [228]. The result demonstrated that, for the majority of these detected wild type viruses, one virus particle only possessed one copy of each RNA segment, which supports the first RNA packaging model [228]. The packaging signals of the influenza virus located in the coding and non-coding regions have been well mapped [229,230,231]. The sorting of the influenza virus RNA segment occurs, more likely, after the nuclear export of vRNP [228].

After the NEP–M1–vRNP complex associates with the plasma membrane, the membrane fuses and releases the progeny virions [227]. However, the mechanism of this step is not fully understood. In the budding process, the cleavage of the sialic acid and the adjacent sugar by NA is critical, as HA and NA are both glycoproteins binding to the sialic acid of the host surface membrane. The lipid bilayer envelope of the influenza virus is derived from the host plasma membrane in the budding process [141]. A recent study showed, after the vRNP export, that the binding of NEP to the cellular ATPase F₁F_o localizes in the cytoplasm, and is crucial to the efficient budding of the influenza virus [232]. NEP recruits ATPase to the cell membrane and facilitates the release of the new virions [232].

Table 1.1. Influenza A virus genome segments and genes.

Segment	Gene	Size (nt)	Protein and major function
1	PB2	2341	PB2: cellular pre-mRNA cap binding
2	PB1	2341	PB1: viral RNA transcription and replication PB1-F2: mitochondrial targeting and apoptosis
3	PA	2231	PA: cellular pre-mRNA cleavage PA-X: inhibiting host cell gene expression
4	HA	1765	Haemagglutinin: surface glycoprotein, receptor-binding, membrane fusion, antigenic determinant
5	NP	1565	Nucleoprotein: RNA coating, nuclear targeting
6	NA	1465	Neuraminidase: surface glycoprotein, receptor-destroying, new progeny release
7	M	1027	Matrix protein 1 (M1): nuclear export of vRNPs M2: ion-channel
8	NS	890	Nonstructural protein 1 (NS1): inhibition of interferon-beta, inhibition of host cellular mRNA processing NEP: nuclear export of vRNPs

Table 1.2. The strain-specific functions of NS1.

Host factors	The motif or critical residues on NS1	The details about the strain-specific
PDZ domain	PDZ domain-binding motif (residues 227-230)	PDZ domain-NS1 interaction is associated with the virulence. Human-like viruses generally carry a “RSKV/KSEV” motif, whereas avian-like viruses carry a “ESEV” motif, the 2009 pandemic H1N1 virus has a truncation of the motif on NS1 [22,195,233].
CPSF30	Residues 103, 106, and 144-188	NS1 blocks CPSF30-mediated cellular pre-mRNA processing. However, the 2009 pandemic H1N1 NS1 cannot bind to CPSF30 [160,234]. An HPAI H5N1 and a LPAI H5N2 NS1 have different effect on pre-mRNA processing and mRNA translation [235].
PABP II	Residues 223-230	NS1 blocks PABP II-mediated cellular pre-mRNA processing. The 2009 pandemic H1N1 NS1 is lack of this function as it has an 11-amino acid truncation at the C-terminus [160,236].
Host factors involved in IFN- β induction	RNA-binding domain and other residues	NS1 from different H1N1 and H3N2 strains inhibit IFN response with different efficiencies and mechanisms [237].
PI3K (p85 β)	Residues 89,164 and 167	The NS1 of a mouse-adapted rPR8 strain stimulated the activation of PI3K, but the NS1 of a mouse-adapted rWSN strain could not [238].
Cytokine related factors	Residue 92	Residue 92 has been identified as a virulence marker in HPAI H5N1. The presence of glutamic acid at this position is associated with the resistance of the virus to anti-viral cytokines [160,239].

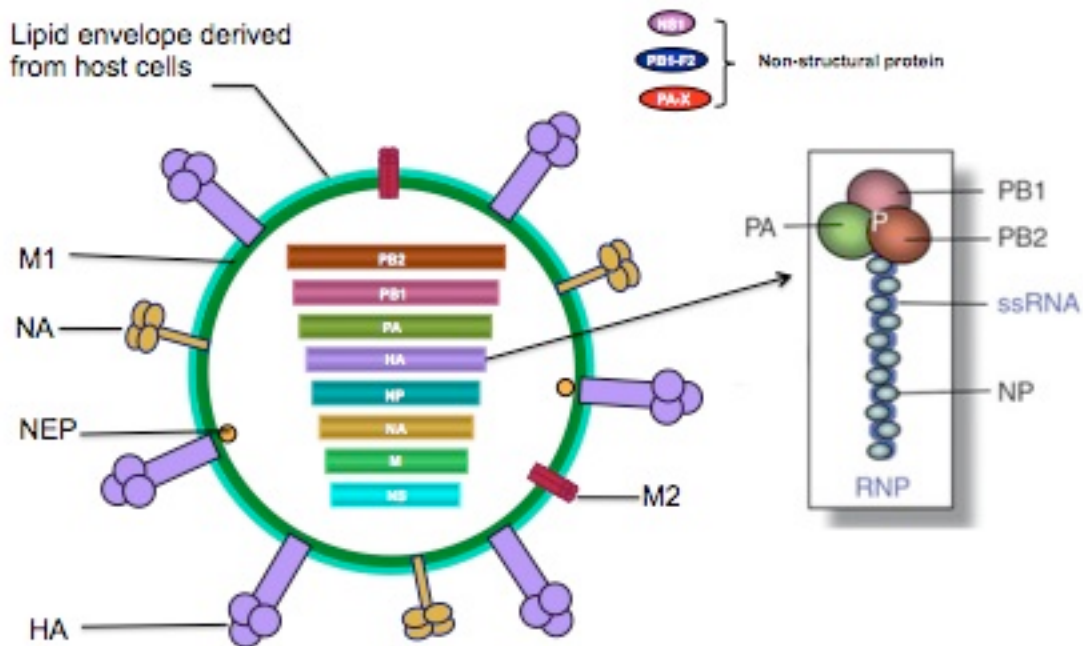


Figure 1.1. The structure of the influenza A virus. The influenza A virus is an enveloped single-stranded negative-sense RNA virus, belonging to the family *Orthomyxoviridae*. The influenza A virus contains a genome with 8 RNA segments, which encode at least 12 identified proteins. RNA segment 1, 2 and 3 encode three RNA-dependent RNA polymerase (RdRP) subunits: polymerase basic proteins PB2 and PB1 and polymerase acid protein PA, respectively. Segment 4, 5, and 6 encode hemagglutinin (HA), nucleoprotein (NP) and neuraminidase (NA), respectively. Segment 7 encodes matrix protein 1 (M1) and M2 protein. Segment 8 encodes the non-structural protein 1 (NS1) and nuclear export protein (NEP; also known as NS2). In addition, PB1-F2 and N40 are translated from PB1 mRNA by leaky scanning, and PA-X is translated by the ribosomal frameshift of the PA gene. PB1, PB2 and PA are subunits of RdRP. NP packages the segmented viral RNA and binds to RdRP to form the ribonucleoprotein (RNP) in the viral particles.

Adapted from (Medina, Garcia-Sastre, 2011).

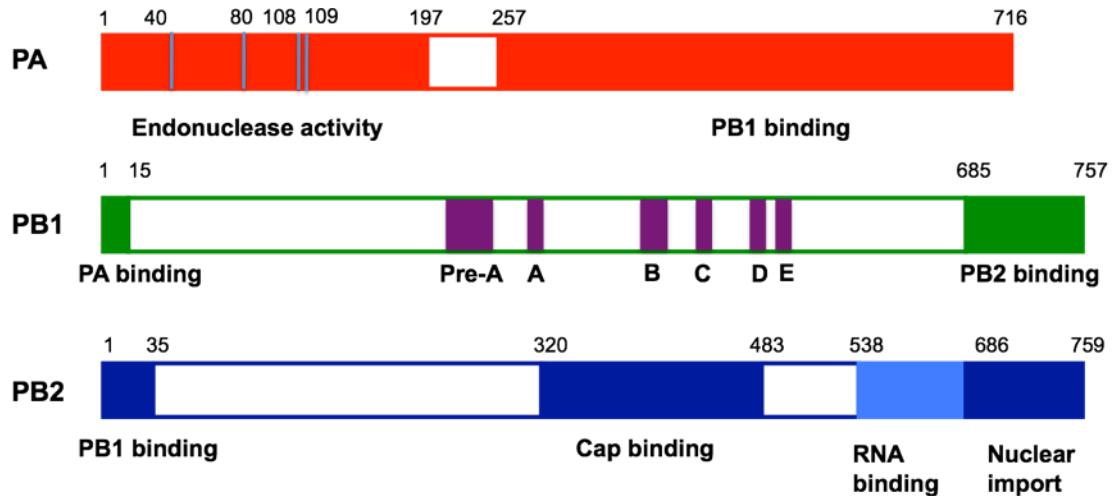


Figure 1.2. The structure of the domains of influenza A virus polymerase complex. The heterotrimeric polymerase complex consists of PA, PB1 and PB2 subunits. The PA subunit contains an endonuclease activity domain (residues 1-197) at the N-terminus, which is responsible for the cleavage of the “cap” from the cellular pre-mRNA and a PB1 binding domain (residues 257-716). PA binds to two manganese ions to its active sites, following a two-metal-dependent endonuclease pattern. Two active sites involved in Mn⁺⁺ binding were identified: Glu-80 and Asp-108 are critical for Mn¹ binding, and His 40, Asp 108 and Glu 109 are important for Mn² binding. The PB1 subunit binds with PA subunit via the first 15 N-terminal amino acids, and interacts with the PB1 N-terminal binding domain (residues 1-35) through its PB2 binding domain (residues 685-757). Four conserved motifs have been identified in PB1, which are responsible for the RNA-dependent RNA polymerase activity and the RNA-dependent DNA polymerase activity: A (residues 298-311), B (residues 399-412), C (residues 438-453) and D (residues 474-484). In addition, motifs pre-A and E are also responsible for the RNA-dependent RNA polymerase activity. The PB2 subunit contains a cap-binding domain (residues 318-483) and an RNA-binding domain (residues 535-684). Two nuclear localization sequences (NLS) are located on the nuclear import domain at the C-terminus of the PB2.

Adapted from (Ruigrok, Hart et al., 2010 and Das, Mramini et al., 2010).

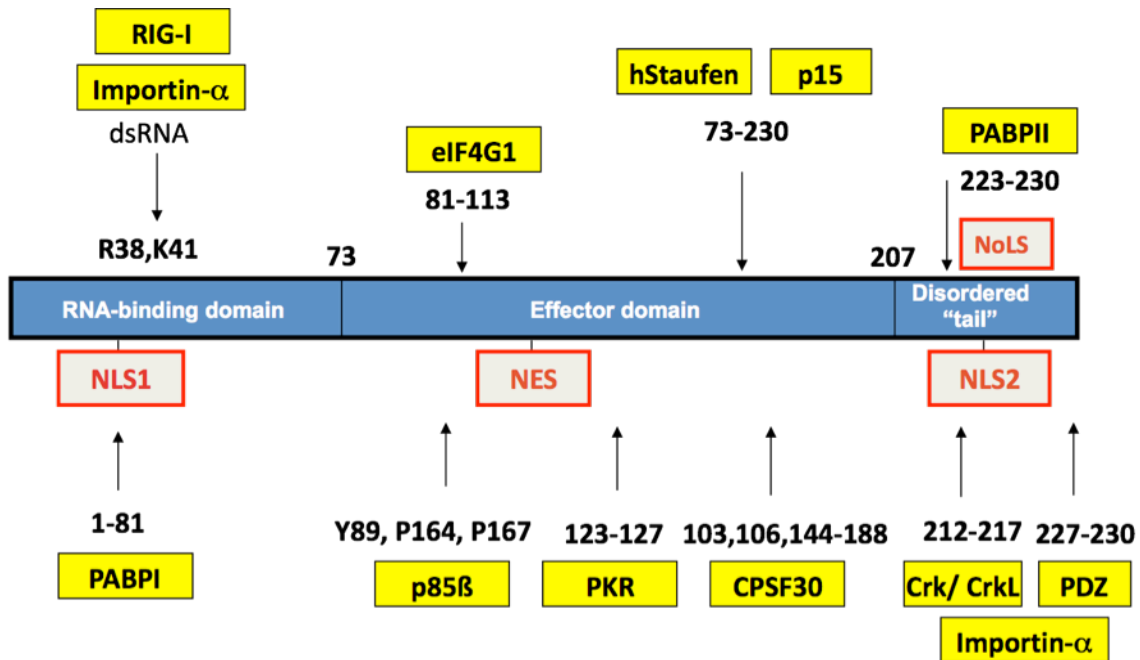


Figure 1.3. The interactions of NS1 with host factors. NS1 (blue) is a nonstructural protein possessing 230-237 amino acids depending upon the strain. NS1 can be divided into an N-terminal RNA-binding domain (RBD), effector domain and C-terminal disordered “tail”. NS1 consists of two nuclear localization sequences (NLS1 and NLS2) which are located at RBD and C-terminus, and a nuclear export sequence (NES). A nucleolar localization sequence (NoLS), which overlaps with NLS2 at the C-terminus, has been found in some strains. Arg-38 and Lys-41 are important residues for RNA-binding, as well as inhibiting the RIG-I-mediated induction of IFN- β by directly binding to it. NS1 is a multifunctional protein which contains several motifs to interact with host factors, including the poly(A)-binding protein I (PABPI), p85 β , CPSF30, eIF4GI, hStaufen, PKR, poly(A)-binding protein II (PABPII), p15, Crk/CrkL and PDZ domain-containing proteins.

Adapted from (Hale, Randall et al., 2008).

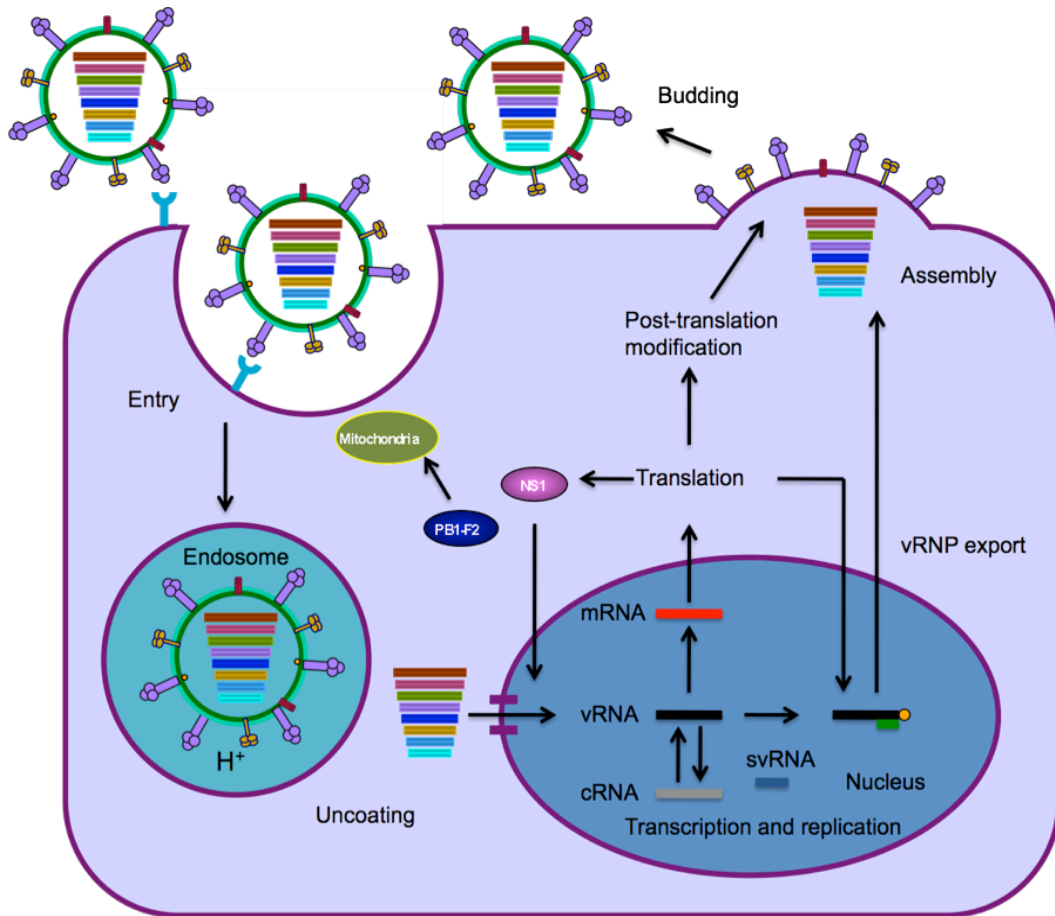


Figure 1.4. The life cycle of the influenza A virus. The surface glycoprotein HA binds to the sialic acid receptors on the cell surface, which initiates the receptor-mediated endocytosis, and then the virus enters the endosome. The low pH of the endosome triggers a conformational change in HA2, and exposes the fusion peptide, which triggers the viral envelope and endosomal membrane fusion. The proton flows into the virus through the M2 ion channel, resulting in the dissociation of vRNP from M1. In the nucleus, the synthesized viral mRNA utilizes the short capped primers derived from the host cells following a ‘cap-snatching’ mechanism, and the vRNA replicates with steps (-) vRNA → (+) cRNA → (-) vRNA. Newly synthesized viral proteins needed for replication and transcription are imported into the nucleus. The vRNPs are exported to the cytoplasm for packaging by binding with M1 and NEP. HA, NA and M2 are post-translationally modified and transported to the plasma membrane by the trans-Golgi secretory pathway. Budding occurs by the cleavage of the M2 on the lipid raft neck, and then the receptor-destroying activity of the NA releases the new virions from the host cells.

Adapted from (Medina, Garcia-Sastre, 2011).

Chapter 2: Influenza Vaccines

Introduction

Vaccination is the main strategy for prevention and control of influenza in humans. The human influenza virus was first isolated in 1933, which led to the characterization of the virus and development of vaccines against influenza [240]. In 1945, the first whole-inactivated influenza virus vaccine was licensed in the US [241].

The amino acid mutations occur at relatively high frequencies in influenza viruses due to the error-prone property of the viral RdRP. The accumulation of small changes in the HA and NA antigenic sites, known as antigenic drift, may result in a new strain that circumvents the pre-existing immunity in humans, and causes seasonal influenza epidemics [16,17,242]. Current trivalent influenza vaccines consist of influenza A (pH1N1), influenza A (H3N2), and influenza B viruses. The World Health Organization (WHO) and the US Public Health Service (PHS) are responsible for the reference strains recommendations. The reference strains for vaccines are determined according to the surveillance data from epidemics around the world, and those with the highest likelihood of circulating in the coming winter season [243].

The egg-based inactivated trivalent vaccines against seasonal flu have long been used for seasonal flu from 1945 in the US. The egg-based live-attenuated trivalent vaccines were licensed in 2003 in the US, although the development started in the 1960s [243]. In November 2012, the first cell-culture based vaccine against seasonal flu was licensed by the US Food and Drug Administration (FDA) [244]. The latest vaccine, FluBlok, is a trivalent recombinant vaccine produced from insect cells using the baculovirus expression system, and it was approved at the beginning of 2013 [245]. The

effectiveness of the vaccines depends on the age and immune competence of the person being vaccinated, and the antigenic relatedness of the vaccine strains to the circulating ones. The effectiveness may reach 70-90%, if the relatedness is high. However, the vaccine is generally poorly effective among aged and immunocompromised persons [243].

For the seasonal epidemics, a predicted vaccine strain may occasionally not match with the circulating strain, leading to suboptimal protection [246]. However, seasonal vaccines cannot induce protection against a pandemic influenza outbreak. Therefore, developing a strategy for the quick generation and distribution of pandemic vaccines is a huge challenge for pandemic outbreaks [246,247]. Compared with antigenic drift, antigenic shift may cause the dramatic changes in HA, and generate the new influenza virus strains. If the new strain infects humans with completely new antigens, and no one has the pre-existing immunity against it, the strain may cause a new human pandemic [248].

The outbreaks of HPAI and LPAI have resulted in the depopulation of flocks and major economic losses in the poultry industry worldwide. The increasing number of reports on the direct transmission of the avian influenza viruses (such as H5N1 [249,250] and H7N9 [251,252]) to human highlights the threat of HPAI and LPAI to public health. In recent years, vaccination has become a key strategy to provide protection to high-risk birds and reduce the possibility of transmission among birds and/or to mammals [253,254]. Currently, there are three types of avian influenza vaccines (AIVs) licensed worldwide: inactivated whole AIV vaccine, recombinant fowlpox virus-vectored vaccine expressing the H5 HA gene, and recombinant Newcastle disease virus (NDV)-vector with

an H5 HA gene insert [255].

However, the limitations of the currently licensed vaccines call for the more effective and efficient vaccines. Several novel vaccines, or called “next generation vaccines”, have been developed on the basis of new technology, and some of them are being tested in clinical trials [256].

Inactivated vaccines

The licensed inactivated trivalent influenza vaccines have been applied in the US since 1945 [243]. These vaccines are amplified in eggs and purified, and then chemically inactivated with formalin. Generally, detergent, such as Triton X-100 is further added to make the viral surface antigens soluble. Furthermore, the detergent mediated disruption (‘splitting’) of influenza viruses reduces the reactogenicity, while retaining the immunogenicity of the viral proteins. Since the 1970s, the detergent has been applied to ‘split’ the vaccines in most of the manufacturing, although the whole-virus vaccines are highly effective [257,258].

In adults, a single dose of 15 µg of HA of the egg-based inactivated trivalent vaccines is sufficient to elicit an acceptable level of antibodies. Whereas children generally need two doses of the inactivated vaccine to produce a protective level of antibody as they are naïve to the viral antigen [257]. In April 2007, the first vaccine against the H5N1 avian influenza in humans was licensed in the US by FDA [259]. Two doses of 90 µg of HA of this vaccine with intramuscular injections provided the patients enough protection against H5N1 in the clinical trial [260]. However, it is difficult to produce such high dose level of the influenza vaccines in the manufacturing plants [261].

A/Puerto Rico/8/34 (PR8) (H1N1) virus is the “master” donor of inactivated influenza vaccines. The vaccine generated is typically a “6+2” reassortant virus, in which 6 internal genes (PB1, PB2, PA, NP, M and NS) are from PR8, and two glycoprotein genes are from the circulating strains. Co-infecting the eggs with the wild type strain and the high yielding virus strain PR8 is a classical approach to generating the reassortant virus. The viruses are collected and propagated in eggs with the addition of anti-PR8 antiserum that can eliminate the virus with PR8 HA or NA [262].

The reverse genetics technology is well developed to realize the fast generation of the recombinant virus without co-infection and screening. Transfection of the cells with plasmids containing RNA polymerase I/II transcription cassettes and influenza genome cDNA fragments, leads to the viral RNA synthesis by cellular RNA polymerase I, and viral mRNA synthesis by cellular RNA polymerase II. In this way, the reassortant influenza virus can be generated completely from cloned cDNA [263].

The trivalent inactivated influenza vaccine (TIV) is administered intramuscularly or intradermally by injection. It is approved for use among persons 6 months and older. The administration of TIV, although inducing serum antibodies IgG, does not elicit the nasal mucosal neutralizing antibody IgA, which is critical to the protecting of the upper respiratory tract in humans [264,265].

Flucelvax[®] is the first cell-culture based influenza vaccine licensed in the US. Flucelvax[®] is produced from the MDCK cell-culture, and then purified, chemically inactivated and disrupted by detergent. The trivalent vaccine contains three influenza strains for seasonal flu as an egg based TIV, and is administered intramuscularly or intradermally by injection for adults 18 years of age or older [266]. Flucelvax[®] utilizes

mammalian cell lines for large-scale vaccine production, and may greatly decrease the requirement for the embryonated eggs in TIV manufacturing [267]. The human influenza virus strains generally produce mutations when adapting in eggs, which may affect the antigenicity of the egg based vaccine; whereas Flucelvax[®] remains the amino acids unchanged in the cell culture. Furthermore, Flucelvax[®] is egg-free, and can be safely used by the people allergic to egg proteins [259,266].

Inactivated whole-virus vaccines are also made up the majority of currently licensed influenza vaccines in poultry farms. The seed strains for inactivated vaccines are generally LPAI isolates from outbreaks in poultry, or from the surveillance of wild birds [268,269]. Similar to human vaccines, the wild-type donor avian vaccine is used to co-infect the egg embryos with an egg-adapted stain, and serially propagated in eggs to generate a reassorted seed strain with the appropriate antigens and high virus yield [268,269].

In the US, inactivated vaccines were mainly applied to protect turkey breeders against different subtypes of the swine influenza viruses. For example, approximately 2.6 million doses of inactivated vaccine were used to immunize turkeys against swine H1 influenza during 2006 in the US [270].

Although inactivated vaccines (“killed virus”) are safe to the host, and stimulate immune responses in different species of poultry, the usage of inactivated vaccines in poultry still has several limitations. Differentiating infected from vaccinated animals (DIVA) is difficult with inactivated whole-virus vaccines, as the strategy requires a vaccine lack of one or more antigens present in the circulating avian influenza strain.

Furthermore, the vaccination of poultry is heavily time-consuming, requiring each bird to be vaccinated individually with a high labor cost for parenteral inoculation [271,272].

Live attenuated vaccines

Currently, FluMist® is the only licensed LAIV in humans in the US. Different from TIV, FluMist® is administered by using a nasal spray. LAIV stimulates the production of both mucosal IgA and serum IgG antibodies [273], therefore it could protect both the upper and lower respiratory tracts from invasion by the influenza virus. Meanwhile, LAIV may elicit cell-mediated immunity with limited replication in the upper respiratory tract [274].

The LAIV strain is featured with cold-adapted (*ca*), temperature-sensitive (*ts*) and attenuated (*att*) characteristics. These characteristics lead the LAIV to replicate efficiently at low temperatures, restrict at 37°C and 39°C, and cause no disease (attenuated). The master donor virus of LAIV, A/Ann Arbor/6/60 (H2N2) and B/Ann Arbor/1/66 were developed by Maassab and his collaborators following the strategy of serially propagating the virus in primary chicken kidney cells at low temperature (25°C) [275].

The sequence analysis demonstrated that the multiple mutations on the internal genes are responsible for the *ca*, *ts* and *att* phenotypes of the cold-adapted virus. Eleven amino acid mutations were found in the attenuated AA/60 (A/A/60 *att*) strain, and the study demonstrated that introducing five *ts* loci, including K391E, E581G, and A661T on the PB1 gene, N265S on PB2 gene, and D34G on the NP gene, is necessary to confer the wt-PR8 strain *ts* and *att* phenotypes [276].

LAIV generates “6+2” reassortant vaccines against the circulating influenza with 6 internal genes (PB1, PB2, PA, NP, M and NS) from a “master donor” A/A/60 *att*, and two glycoprotein genes from the circulating strain [275]. FluMist[®] is approved for use in the population in ages from 2 to 49, except in the pregnant women. LAIV achieved a higher protection efficiency than TIV in children, but is less effective in adults [277,278,279].

To generate attenuate influenza against avian viruses in poultry, several different strategies have been developed [280,281,282,283,284]. An avian influenza (A/FPV/Rostock/34 (H7N1)) was genetically attenuated by replacing the M2 cleavage site with that of the NP's. Vaccination with a single dose of this attenuated virus was sufficient to completely protect the chickens from lethal FPV infections [281]. A live-attenuated recombinant H5N1 influenza virus was generated by removing the polybasic cleavage site from the HA, substituting residue 627 from lysine to glutamic acid in the PB2, and generating a C-terminal truncation of the NS1. This live-attenuated vaccine provided chickens with full protection against the homologous virus and a high level of protection against the heterologous HPAI H5N1 challenge [284].

In our previous reports we demonstrated the potential of a genetically modified LAIV with the internal gene backbone of A/guinea fowl/Hong Kong/WF10/99 (H9N2) (WF10*att*) as a vaccine backbone for H5N1 influenza viruses [254]. The WF10*att* backbone carries mutations in the PB1 (K391E, E581G and A661T) and PB2 (N265S) genes. In addition an HA tag was cloned in the frame at the C-terminus of PB1, and enhanced the *att* phenotype. We also showed that an H5N1 virus carrying the backbone Δ H5N1WF10*att* was amenable for *in ovo* vaccination and provided optimal protection

against H5 HPAI virus in chickens [254,285].

However, field application of these vaccines is difficult due to the inherent segmented nature of the influenza genome and the fear that LAIVs could expand the plethora of influenza viruses through reassortment. Despite recent reports of the potential genomic manipulation of influenza to prevent undesired reassortments, it is unclear how these viruses will behave under more natural conditions; either by providing adequate protection or reverting to wild type-like viruses.

Vaccines expressed by viral vectors

The genetically modified viruses causing no disease have been used as the viral vectors for foreign antigen delivery. Multiple viral vectors, such as Newcastle disease virus, adenoviruses, and vesicular stomatitis virus were used to carry the influenza HA gene from seasonal or H5N1 viruses, or both, and expressed the antigen in animals. The results showed the viral vector-based vaccine elicited protective humoral and CTL responses [286,287,288]. In the early phase of the clinical trial, adenovirus-based HA vaccines yielded encouraging results [289].

For poultry, several viral vectors, such as fowl poxvirus [290], Newcastle disease virus (NDV) [280,291], vaccinia virus[292], and adenoviruses [293] have been used for vaccine development against avian influenza. Currently, the recombinant fowl poxvirus-AI-H5 (rFP-AIV-H5, or Trovac AI-H5) and recombinant NDV-AI expressing H5 HA gene are licensed against avian influenza virus infection. Both of the vaccines are safe, and elicit host humoral and cellular immune responses. DIVA strategies are easy to develop because the viral vector-based vaccines only express HA (or HA and NA).

However, pre-existing maternal and neutralizing antibodies against fowl poxvirus or NDV may limit the replication of the vaccine, and reduce the host immune responses [271,294].

Virus-like particle vaccines

In the assembly step of influenza virus life cycle, the structural proteins HA, NA, and M1 are transported into the plasma membrane and embed onto it, and bud out of the host cells after the vRNP complex interacts with the M1 protein. The baculovirus expression vector (BEVS)/insect cell (IC) system mimics this self-assembly process and produces non-infectious virus-like particles (VLP) via the recombinant baculovirus vector containing the HA, NA and M1 proteins. VLP influenza vaccines are highly safe, as the particles do not contain the genome of the virus [295]. Other influenza or non-influenza proteins can be introduced into the VLP to enhance the immune responses to vaccines [256]. A VLP containing the HA and M1 proteins from the canine influenza virus H3N2 subtype provided the dogs protection against the wild type virus challenge [296]. Interestingly, the triple-subtype VLPs co-expressing influenza HAs were derived from H5N1, H7N2 and H9N2, respectively, and the NA and M1 genes were from PR8 that were produced in the insect cells. The intranasal vaccination with the triple-subtype VLPs induced efficient protection against wild-type H5N1, H7N2 and H9N2 infections in ferrets by neutralizing antibody responses [297].

FluBlok[®] is the first LVP vaccine licensed in the US that is produced from insect cells using the baculovirus expression system [245]. FluBlok[®] contains recombinant trivalent HA derived from the same seasonal influenza strains as TIV, but its HA content is three times higher than that of TIV. FluBlok[®] is administered intramuscularly by

injection, and it is approved to use in persons 18 through 49 years of age. In the clinical development, vaccination with FluBlok[®] resulted in a long-term immune response and a cross-protection against viral mutants [298,299].

Universal vaccines

Recombinant M2 vaccine

M2 is a membrane protein with proton channel activity [119]. During infection, M2 triggers the uncoating of vRNP by introducing H⁺ from the low pH endosome. The extracellular domain of M2 (M2e) is highly conserved in the different subtypes of influenza virus, which renders M2e a good candidate for universal vaccine development. Recombinant vaccines based on the full length or M2e with different carrier, such as VLP and GST, have been evaluated in animal models. It was reported that the M2 vaccine induced cross-protection [300]; however, the protection efficiency of M2 universal vaccines is lower than that of inactivated vaccines. This may be because the M2 antibody is involved in the opsonophagocytosis of macrophages, and cannot neutralize the virus. A clinical trial is needed to further evaluate whether M2 universal vaccine candidates can elicit efficient protection in humans [257].

HA stalk vaccine

The fusion peptide region of the HA2 is highly conserved among all HA proteins [301], and is responsible for the viral and host endosome membrane fusion of influenza virus in the uncoating process. The HA2 subunit is also relatively conserved with a higher than 85% sequence homology in different subtypes. Universal vaccines based on the conserved fusion peptide or HA2 stalk has been developed. A broadly cross-reactive

neutralizing antibody was produced in the HA2 stalk study in mice [302,303]. The antibodies are likely to block the virus-cell membrane fusion in the endosome [81,304], and inhibit virus uncoating.

DNA-based vaccines

DNA-based influenza vaccines have been studied for more than 2 decades. The plasmids containing the HA or NA genes were intramuscularly injected into different animals, inducing protective responses [305,306]. However, recent clinical trials did not show promising results in humans [307,308]. Thus, the potential of DNA-based vaccines becoming commercial products is uncertain.

DNA vaccines against avian influenza virus have been reported in recent years. An influenza gene (generally HA) is cloned and inserted into to the eukaryotic expression vectors, and delivered to the host by intramuscular or intradermal injection. Subsequently, the viral proteins are synthesized via the host transcription or translation mechanism, then taken and processed by antigen-presenting cells (APCs) or myocytes. The viral antigens are presented on the MHC class I and II molecules, eliciting both humoral and cell-mediate immune responses [309]. However, more efforts are needed to improve these promoters for poultry [310]. The prohibitive costs of the vaccine preparation may limit the commercialization of DNA vaccines in poultry [309,311].

Chapter 3: Host immune responses and evasion strategies of influenza A virus

Innate immune response

The innate immune response is the first line of defense against the attack of influenza virus. The innate immune system recognizes pathogen-associated molecular patterns (PAMPs) by endogenous pattern recognition receptors (PRRs), and broadly establishes an antiviral state to the infected tissues. The following responses include the induction of type I and type III interferons (IFNs), recruitment of antigen-presenting cells (APCs), and programmed cell death of the infected cells [312].

The TLR pathway

Toll-like receptors (TLRs) are one of the main families of PRRs. They play a critical role in the innate immune system. Amongst them, TLR3 recognizes double-stranded RNA (dsRNA) and TLR7/8 recognizes single stranded RNA (ssRNA), and both of them may be involved in the immune responses to influenza virus [313]. The binding of dsRNA with TLR3 triggers the activation of transcription factors, such as IFN regulatory factor (IRF) 3, p50/p65 (NF κ B) and activator protein 1 (AP1) [314]. IRF3, NF κ B and AP1 are all the components of IFN- β enhanceosome (a protein complex which binds to the “enhancer” region of a gene [315]), which may relocate into the nucleus and activate the transcription of IFN- β [316].

The plasmacytoid dendritic cells (pDC), which mainly circulate in the blood, are the major source of type I IFN production during the influenza infection. pDCs recognize influenza virus through TLR7 [317]. The mechanism of influenza virus antagonizing TLR signaling during infection remains unknown [312].

RIG-I

Retinoic acid-inducible gene I (RIG-I) is a well-featured member of this PRR family, along with the melanoma differentiation-associated protein (MDA) 5. RIG-I, a cytosolic sensor, contains a repressor domain (RD) and two caspase-recruitment domains (CARD). The binding of RD to 5'-triphosphate dsRNA of influenza virus can cause conformational changes of RD, and activate RIG-I [318]. Activated RIG-I interacts with mitochondrial antiviral-signaling protein (MAVS), which is located on the mitochondria, through its CARD, and MAVS, in turn, activates the components of IFN- β enhanceosome including IRF3, IRF7 and NF κ B, relocating them into the nucleus to activate the transcription of IFN- β and inflammatory cytokines [312].

Type I IFN signaling

The cytoplasmic sensors, such as TLR-3 and RIG-I, recognize influenza virus by binding to the dsRNA or 5'-triphosphate dsRNA, and triggering the cascade of the signaling pathway. The re-location of the enhanceosome into the nucleus subsequently activates the transcription of type I IFN (IFN- α and β). INF- α and β express and bind to the type I IFN receptor IFN- α/β R on the same infected cell (autocrine signaling) or the neighboring cells (paracrine signaling) [318]. The IFN- α/β R is a heterodimer containing IFN- α/β R1 and IFN- α/β R2 subunits. IFN- α/β R cross-links using IFN, the cytoplasmic

tails of the receptors trigger the signaling cascade and activate the nuclear IFN-stimulated gene factor-3 (ISGF3), which subsequently stimulates the transcription of IFN-sensitive regulatory element (ISRE) [318]. By now, more than 300 interferon-stimulated genes (ISGs) have been identified, including dsRNA-activated protein kinase R (PKR; translational repression) [319]; 2'-5' oligoadenylate synthetase (OAS; activator of RNaseL for mRNA decay) [320]; and INF-stimulated gene (ISG)15 (a modifier to regulate a number of IFN-stimulated genes) [321]. The main functions of the ISGs include recognizing of the PAMP molecules, regulating the transcription and translation of the host cell, and initiating programmed cell death.

The interaction of innate and adaptive immune responses

The communication between innate and adaptive immune systems is important for the successful defense against the invasion of the influenza virus. During infection, the innate immune components initiate the response against the influenza virus, and then stimulate the adaptive immune system to participate in the battle. Antigen presenting cells (APCs), especially dendritic cells (DCs) are pivotal to the communication between innate and adaptive responses [312].

The macrophages and dendritic cells in the upper respiratory system are generally infected and activated at first by the influenza virus. The activated macrophages secrete many inflammatory cytokines, such as IL-6 and TNF- α , to stimulate the synthesis of acute phase proteins and regulate the immune cells [322].

DCs undergo maturation with the up-regulated expression of receptors CD80 and CD86, and present the specific peptides derived from the influenza virus to the TCR of the naïve T cells via the MHC class II molecule in the draining lymph nodes of the lung; and in turn activate T cells into effector cells. However, the presentation of viral antigens may be affected by the virus and cause the down-regulation of the MHC class II and co-stimulatory receptors on the DCs [323]. NS1, the antagonist of type I IFN, may inhibit and postpone the innate immune response by different mechanisms of blocking the cascade of type I IFN signaling.

Adaptive immune response

The major function of the humoral, or neutralization antibody response against the influenza virus, is blocking the entry to the host cells. Whereas the cellular response is important for clearing the infected cells [312].

Humoral response

Neutralizing antibodies inhibit the viral infection via two different mechanisms: binding the epitopes on the globular head of the HA1, and blocking the attachment of the HA on the receptors; or preventing the viral envelope and cell membrane fusion by binding to the stalk region of the HA [80,81].

Humoral immunity may last from several months to a lifetime [324]. The surface proteins of influenza HA, NA and M2 are targets for the neutralizing antibodies. However, HA is the most important, as the binding of the neutralizing antibodies may directly inhibit the entry of the virus; while NA and M2 are less efficient [325]. Both NA-

specific and M2-specific antibodies may contribute to the elimination of the virus infected cell by antibody-dependent cell-mediated cytotoxicity (ADCC) [326,327].

IgM is the first antibody isotype produced after the primary infection of influenza. It can mediate the neutralization of the virus and activate the complements. IgG antibodies are produced by plasma B cells, and provide the host with long-term protection [322]. More importantly, mucosal secretory IgA antibodies may protect airway epithelial cells from infection by inhibiting membrane fusion, or preventing the attachment of the influenza viruses [328].

Cell-mediated immune response

The APC cells activate naïve CD4⁺ T cells by presenting the influenza virus-derived peptide on MHC II molecules together with the second signal [322]. The activated CD4⁺ T cells differentiate into T helper (Th1) or Th2 cells. Th2 cells secrete IL-4, IL-5 and IL-13, and activate the humoral response against the influenza virus. Th1 cells produce IL-2 and IFN- γ , and promote the cytotoxic (CD8⁺) T lymphocyte (CTL) response [322].

Naïve CD8⁺ T cells are activated by APC cells via recognition of the viral peptides on the TCR-class I MHC molecules in the presence of the second signal, and then differentiated into CTLs. The infected host cells present the processed peptides derived from the influenza virus with class I MHC molecules. The activated CTLs recognize the “foreign” peptides on the class I MHCs and clear the infected cells by programmed cell death [312,322]. Interestingly, human influenza virus-specific CTLs preferentially battle with the epitopes’ highly conserved internal proteins, such as NP, M1

and PB2, which result in CTLs creating the cross-protection among different subtypes of influenza A viruses [322].

Evasion of innate immune response by influenza virus

Influenza virus has evolved multiple strategies to inhibit the innate immune response. Several viral genes, including NS1, PB1-F2, RdRP and NP are involved in antagonizing antiviral activity for successful evasion [322].

In particular, NS1 is a potent antagonist of type I IFN, and has evolved various mechanisms to block the host innate immune response during infection. First, NS1 can inhibit the activation of transcription factors on the IFN- β signaling pathway, such as IRF-3, c-Jun/ATF-2 and NF- κ B, by directly binding dsRNA to its RNA binding domain (RBD), and preventing the recognition by TLR-3 [168,169]. Second, the intracellular sensor RIG-I binds to the viral genome 5'-triphosphate dsRNA, and initiates type I IFN production by interacting with mitochondrial antiviral signaling protein MAVS. NS1 inhibits the activation of RIG-I by directly binding to the RIG-I and forming the NS1-RIG I complex [172,173,174]. TRIM25 activates RIG-I by ubiquitinating the RIG-I N-terminal CARD domain. NS1 inhibits the ubiquitination of the CARD domain and blocks RIG-I signaling [175]. Third, in the nucleus, NS1 can block the processing and nuclear export of all cellular mRNAs by binding to CPSF30 and PABPII [170,171].

Additionally, NS1 can interfere with the function of multiple ISGs. NS1 competitively binds dsRNA with its RBD, and inhibits the activation of two antiviral proteins PKR [329] and OAS [192] in the cytoplasm. ISG15, an IFN- α/β -induced, ubiquitin-like protein, inhibits the nuclear import of the influenza NS1 protein by the ISGylation of residue Lys-41 in the NS1 RBD domain, and blocking the NS1- importin- α

interaction. Interestingly, NS1 binds to Herc5, the major E3 ligase for ISG15 conjugation, and limits the function of ISG15 [178].

NS1 was reported to play both pro- and anti-apoptotic functions during influenza infection in different studies [330,331,332], and NS1 was demonstrated to play important roles in regulating the phosphatidylinositol 3-kinase (PI3K)/Akt pathway [180,181,182,183]. PI3K is a dimeric lipid kinase consisting of a regulatory subunit p85 β and a catalytic subunit p110 [184]. Akt, a serine/threonine protein kinase, is a downstream PIP₃-binding effector of PI3K. In the early phase, the attachment of the virus to the cell surface transiently induces PI3K signaling [186]. In the later phase, PI3K is activated by NS1 and the influenza viral RNA through the stimulation of the cytosolic receptor RIG-I, promoting the production of type I IFN [186,187]. NS1 activates PI3K signaling by directly binding to the inter-HS2 (iSH2) domain of the regulatory subunit p85 β of PI3K to prevent the premature apoptosis of the infected cell and facilitate the viral replication [188,189]. It's reported that NS1 can preferentially interact with phosphorylated Akt in the nucleus and changes the Akt anti-apoptotic activity[190].

Infection with the influenza A virus activates the NF- κ B pathway, and leads to the antiviral response of the host cells. However, NS1 directly interacts with IKK- α and IKK- β and impairs their phosphorylation in both the cytoplasm and nucleus, and subsequently inhibits the NF- κ B-mediated innate immune response [333].

NS1 from the 2009 swine-origin pandemic H1N1 virus cannot inhibit the host gene expression as in other human-adapted influenza A viruses. This feature could be restored in 2009/NS1 by introducing the substitutions R108K, E125D and G189D. The recombinant pandemic 2009 H1N1 virus carrying the NS1 with those substitutions was

more efficiently blocked the innate immune response than the wild-type virus. However, this mutant virus caused less morbidity in mice, and showed a decreased titer in the URT of ferrets when compared to the wild-type virus. The data showed that the NS1 from the 2009 pandemic H1N1 virus seems lack the potential to function more efficiently in human cells [334].

Escaping adaptive immune response by influenza virus

Antigenic drift and antigenic shift are the two main mechanisms causing the antigenic variability of influenza viruses, allowing pathogens to overcome the host adaptive immune responses. Antigenic drift occurs frequently, which enables the virus to cause influenza epidemics by evading the pre-existing immunity in humans. Antigenic shift occurs as gene mixing, or reassortment from different influenza A virus subtypes, such as the 2009 triple-reassortant swine-origin H1N1 [312]. Antigenic shift may cause a human pandemic if the population is immunologically naïve to the new reassortant strains at large [248].

The selective pressure of neutralizing antibodies, mainly against influenza HA, is critical for antigenic shift [322]. For example, a recent study found that the glycosylation residues on HA increased (ranging from 5 to 11 glycosylations) in the past 30 years from the H3N2 isolates [103]. Both HA and NA process post-transcriptional modifications of glycosylation and gain the proper functions in their life cycles. The glycosylation of the globular head region of HA may result in the immune escape from the neutralizing antibody recognition [103].

In the cell-mediated immune response, influenza viruses avoided the recognition by virus specific T cells with mutations inside the CTL epitope regions, or at the TCR contact residues [322]. For example, the variations in the CTL epitopes were analyzed in the seasonal H3N2 isolates. The substitution R384G in the NP (383-391) epitope is an anchor residue which greatly reduces the peptide-MHC I affinity, resulting in the loss of peptide binding [335,336].

Chapter 4: Improved hatchability and efficient protection after *in ovo* vaccination with live-attenuated H7N2 and H9N2 avian influenza viruses

Adapted from: Cai Y, Song H, Ye J, Shao H, Padmanabhan R, Sutton TC, Perez DR. Improved hatchability and efficient protection after *in ovo* vaccination with live-attenuated H7N2 and H9N2 avian influenza viruses. *Virology*. 2011 Jan 21;8:31.

Abstract

Mass *in ovo* vaccination with live attenuated viruses is widely used in the poultry industry to protect against various infectious diseases. The worldwide outbreaks of low pathogenic and highly pathogenic avian influenza highlight the pressing need for the development of similar mass vaccination strategies against avian influenza viruses. We have previously shown that a genetically modified live attenuated avian influenza virus (LAIV) was amenable for *in ovo* vaccination and provided optimal protection against H5 HPAI viruses. However, *in ovo* vaccination against other subtypes resulted in poor hatchability and, therefore, seemed impractical. In this study, we modified the H7 and H9 hemagglutinin (HA) proteins by substituting the amino acids at the cleavage site for those found in the H6 HA subtype. We found that with this modification, a single dose *in ovo* vaccination of 18-day old eggs provided complete protection against homologous challenge with low pathogenic virus in $\geq 70\%$ of chickens at 2 or 6 weeks post-hatching. Further, inoculation of 19-day old egg embryos with 10^6 EID₅₀ of LAIVs improved hatchability to $\geq 90\%$ (equivalent to unvaccinated controls) with similar levels of protection. Our findings indicate that the strategy of modifying the HA cleavage site combined with the LAIV backbone could be used for *in ovo* vaccination against avian influenza. Importantly, with protection conferred as early as 2 weeks post-hatching, with

this strategy birds would be protected prior to or at the time of delivery to a farm or commercial operation.

Introduction

Although depopulation of infected flocks is the method of choice to control the spread of avian Influenza virus (AIV) in poultry, vaccination has become an alternative strategy in order to provide protection to high-risk birds and reduce the possibility of transmission among birds and/or to mammals [253,254]. Thus, in many countries in which avian influenza outbreaks particularly of low pathogenicity have occurred recurrently, selective culling followed by vaccination is used as a measure to control the disease without major economic disruptions. There are only two types of avian influenza vaccines (AIVs) licensed worldwide: inactivated whole AIV vaccine and recombinant fowlpox virus-vectored vaccine expressing the HA gene of AIV. However, both types of vaccines have major limitations: inactivated vaccines cannot elicit strong mucosal and cellular immunity; and previous exposure to fowlpox virus inhibits the host response to the fowl-pox vectored vaccine inhibiting anti-influenza immunity [254,271,272]. In addition, both strategies are heavily time-consuming, requiring each bird to be vaccinated individually by parenteral inoculation.

With the advent of reverse genetics, LAIVs have emerged as a potential alternative to control avian influenza [284]. Several different strategies have been developed to attenuate influenza viruses based on mutations in one or more of the viral internal or surface genes [280,281,282,283]. Several studies have shown that LAIV vaccines protect against influenza viruses of low or high pathogenicity in poultry and

mammals. However, field application of these vaccines is difficult due to the inherent segmented nature of the influenza genome and the fear that LAIVs could expand the plethora of influenza viruses through reassortment. Despite recent reports of the potential genomic manipulation of influenza to prevent undesired reassortments, it is unclear how these viruses will behave under more natural conditions; either by providing adequate protection or reverting to wild type-like viruses. Instead, *in ovo* vaccination using LAIV is an attractive alternative to provide fast and effective protection against influenza while avoiding the potential for reassortment (*in ovo* vaccination is unlikely to produce reassortants as other influenza viruses are not present in the egg).

Several strategies have been developed to generate LAIVs for *in ovo* vaccination. A recombinant LAIV was recently developed that provided immunity against HPAI H5N1 influenza and Newcastle Disease Virus (NDV) [280,337]. This recombinant influenza virus expressed the HA of H5 with a deleted polybasic cleavage site, and the ectodomain of the hemagglutinin-neuraminidase (HN) genes NDV instead of NA gene of HPAI H5N1. With this bivalent virus, a single dose *in ovo* vaccination of 18-day-old eggs provided 90% and 80% protection as early as 3 weeks post-hatching, against NDV and HPAI, respectively. A second strategy employed a non-replicating human adenovirus serotype 5 (Ad5)- vectored vaccine that expressed the HA of a LPAI H5N9 virus. Similarly, this vaccine was delivered *in ovo* and conferred protection in chickens after challenge with either HPAI H5N1 (89% HA homology; 68% protection) or HPAI H5N2 (94% HA homology; 100% protection) viruses. Unfortunately, in both these studies, the hatchability efficiency was not addressed in detail [179].

In our previous reports we demonstrated the potential of a genetically modified

LAIV with the internal gene backbone of A/guinea fowl/Hong Kong/WF10/99 (H9N2) (WF10att) as a vaccine backbone for H5N1 influenza viruses [254]. The WF10att backbone carries mutations in the PB1 (K391E, E581G and A661T) and PB2 (N265S) genes. In addition an HA tag was cloned in frame at the C-terminus of PB1, and enhanced the att phenotype. This backbone results in virus attenuation *in vitro* while attaining high viral growth properties at the permissive temperatures of 33 and 35°C. We also showed that an H5N1 virus carrying the backbone Δ H5N1WF10att was amenable for *in ovo* vaccination and provided optimal protection against H5 HPAI virus. More specifically, a single low (10^4 EID₅₀) or high (10^6 EID₅₀) dose of LAIV resulted in greater than 60% protection at 4-week post-hatching and 100% protection at 9 to 12-week post-hatching. Incorporation of a boost regime with either the low or high virus dose at 2-weeks post-hatching increased the protection efficiency to 100% in 4-week old chickens. The hatchability efficiency of the high-dose (10^6 EID₅₀) *in ovo* vaccination was 85%, compared with 90% in low-dose (10^4 EID₅₀) and mock groups [254,285].

In ovo vaccination with live attenuated viruses is widely used in commercial poultry against various infectious diseases. *In ovo* vaccination was initially introduced into the poultry market to protect against Marek's disease virus (MD) [338,339]. Currently, over 80% of US broilers are immunized *in ovo* with MD vaccine. *In ovo* vaccination is also effective and used commercially to protect poultry from infectious bursal disease virus (IBDV) [340]. Compared with field vaccination, *in ovo* vaccination provides uniform and fast delivery (50,000 egg/h), reduced labor costs, decreased stress to the birds; and most importantly, elicits early immune responses, as soon as 2-week post hatching [341]. From practical and commercial perspectives, *in ovo* vaccination not

only has to be effective in providing protection but also has to maintain high hatchability levels ($\geq 90\%$). In this report, we investigated the effects of changing the H7 and H9 cleavage site to that of the LPAI H6 subtype and the timing of vaccination on levels of protection and hatchability after *in ovo* vaccination with LAIV against H7 and H9 LPAI viruses. Our results indicate that *in ovo* vaccination can result in significant protection against the H7 and H9 virus subtypes while maintaining high hatchability ($>90\%$) when the vaccine is administered in 19-day old chicken embryos.

Materials and methods

Virus, cells and Animals

The influenza virus A/Guinea Fowl/Hong Kong/WF10/99 (H9N2) (WF10) was kindly provided by Robert Webster from the repository at St. Jude's Children's Research Hospital, Memphis, Tennessee; influenza virus A/Chicken/Delaware/VIVA/04 (H7N2) (CK/04) was kindly obtained from Dennis Senne at the National Veterinary Laboratory Services, USDA, Ames, Iowa. The viruses were propagated in 10-day-old embryonated specific-pathogen-free chicken eggs at 35°C and stored at -70°C. The viruses were titrated by the Reed and Muench method to determine the 50% egg infectious dose (EID₅₀). 293T human embryonic kidney and Madin-Darby canine kidney (MDCK) cells were maintained as described previously [254]. White leghorn chickens (Charles River Laboratories, MA) and Japanese quail (Murray McMurray Hatchery, Webster, IA) were hatched at 100°F in a circulating air incubator (G.Q.F. Manufacturing co. Savannah, GA) and maintained under BSL2 conditions.

Generation of recombinant virus by reverse genetics

The 6 internal genes of WF10att were described previously and were used to recover viruses carrying the surface genes of Ck/04 or WF10 [254]. The cloning of the Ck/04 surface genes has been previously described [254]. The H7 HA cleavage site, PEKPKPRG, was substituted with an alternative cleavage site sequence, PQIETRG, from the H6 HA subtype using a two-step PCR reaction and the plasmid pDP2002-H7 (Ck/04) as the template (Figure 4.1A). In brief, two PCR fragments were produced by using primers EcoR I 550-F (5'-CTGTCGAATTCAGATAATTCAGC-3') and H7-H6 CVS-R (5'-GGTCTCCCGCTGTGGAACATTTCTC-3'), and primers H7-H6 CVS-F (5'-CACAGCGGGAGACCAGAGGCCTTTTTG-3') and Pst I 1150-R (5'-GTCAGCTGCAGTTCCTCCCCTTGT-3'). These two fragments were then used as templates for a new PCR product using primers EcoR I 550-F and Pst I 1150-R. The fragment was digested with EcoR I and Pst I, and cloned into pDP-2002-H7 (VIVA/04), to obtain pDP2002-mH7.

The H9 HA cleavage site, PARSSRG, was substituted with the alternative cleavage site sequence PQIETRG (Figure 4.1B) using pDPH9WF10 as the template. Two PCR fragments were produced by using primers: XbaI I 285-F (5'-CCTCATTCTAGACACATGCAC-3') and H9-H6 CVS-R (5'-CCAAATAGTCCTCTAGTTTCGATCTGAGGCACGTTC-3'), and primers H9-H6 CVS-F (5'-GAACGTGCCTCAGATCGAACTAGAGGACTATTTGG-3') and EcoN I 1297-R (5'-CCTCATTCTAGACACATGCAC-3'). These two fragments were then used as templates to generate a new PCR fragment using primers XbaI I 285-F and EcoN I 1297-R. The fragment was digested with XbaI I and EcoN I, and cloned into pDPH9WF10, resulting in the formation of pDP-2002-mH9.

Recombinant viruses were generated using the 8-plasmid system in co-cultured 293T and MDCK cells as described previously [254]. The recombinant viruses (Table 4.1) were propagated in 10-day-old embryonated eggs, titrated by EID₅₀, and stored at -70°C until use. 2mH7N2:6WF10att and 2mH9N2:6WF10att viruses were sequenced using specific primers, the Big Dye Terminator v3.1 Cycle Sequencing kit (Applied Biosystems, Foster City, CA), and a 3100 Genetic Analyzer (Applied Biosystems, Foster City, CA), according to the manufacturer's instructions. The genetic stability of mutations on HA, PB1 and PB2 were evaluated by serial passage of virus stocks at a 1:10,000 dilution for 10 passages in triplicate samples in 10-day-old embryonated eggs. Viruses obtained after ten passages were sequenced as described above.

Hatchability in embryonated chicken eggs

18 or 19-day-old embryonated specific-pathogen-free chicken eggs were inoculated with either 10⁶ or 10⁷ EID₅₀ of virus in 0.1 ml inoculum according to the scheme presented in Table 2. Eggs in the mock group were inoculated with 0.1 ml of PBS. The egg inoculation was performed as described previously [254]. Briefly, eggs were candled, and a small hole was made through the air cell with an electric drill. Next, 0.1 ml of virus dilution or PBS was injected into the allantoic cavity using a 21-gauge needle at a depth of 2.5 cm. The percent hatchability was calculated using the total number of inoculated eggs versus the number of 21-day old eggs that hatched in each group. This experiment was performed under BSL-2 conditions according to protocols approved by the Animal Care and Use Committee of the University of Maryland.

Plaque assay in chicken embryonic kidney (CEK) cells and immunostaining

To investigate if the replacement of amino acids at the HA cleavage site affected the temperature sensitive phenotype of the new live-attenuated viruses, plaque assays were performed in CEK cells at 37°C, 39°C, and 41°C. Confluent CEK cell monolayers in six-well plates were infected with 0.5 ml of 10-fold dilutions of virus 2mH7N2:6WF10att or 2H7N2:6WF10att in M199 medium. The cells were incubated with the virus dilutions for 1 h at 37°C, washed, and overlaid with M199 medium containing 0.9% agar and 0.1 µg/ml TPCK-trypsin. The plates were then incubated at 37°C, 39°C, and 41°C with 5% CO₂. At 4 days post-inoculation (dpi) the overlay was removed and immunostaining was performed as described previously [254]. In brief, the cells were fixed, permeabilized, and blocked with bovine serum albumin (BSA) in PBS. The cells were then incubated with mouse anti-WF10 monoclonal NP antibody prepared in our laboratory, followed by incubation with peroxidase-conjugated goat anti-mouse IgG (Jackson Immuno Research, West Grove, PA). The presence of viral antigen was revealed by adding several drops of aminoethylcarbazol (BD Biosciences, San Diego, CA). The size and number of plaques at each temperature were compared to determine the temperature sensitive phenotype of the new recombinant virus.

Viral replication in MDCK cells

Viral replication was studied to examine the temperature sensitive phenotype of the new recombinant viruses in MDCK cells. Confluent monolayers of MDCK cells in 6-well plates were infected with 2m2H7N2:6WF10att or 2H7N2:6WF10att at a MOI = 0.001 and cultured at 35°C and 39°C, respectively. Supernatant samples were collected at

12, 24, 48, 72, 96 and 120 h post-inoculation, and the viral titer of these samples was determined by TCID₅₀ in MDCK cells[254].

Virus replication and transmission in quail

To evaluate the vaccine's attenuated phenotype *in vivo*, 2mH7N2:6WF10att was compared to the recombinant virus 2H7N2:6WF10att. Six 4-week-old Japanese quail were inoculated by the ocular, intranasal, and intratracheal routes with 10⁶ EID₅₀/0.5 ml of either 2mH7N2:6WF10att or 2H7N2:6WF10att vaccine viruses. Two control quail were inoculated with 0.5 ml of PBS. At 1 dpi, 3 naïve quail were introduced into the same isolators, and placed in direct contact with the inoculated quail to assess virus transmission. At 3 dpi, 3 inoculated quail per group were sacrificed, lungs were homogenized and virus titers were determined by EID₅₀. For the remaining quail, tracheal and cloacal swabs were collected from both the inoculated and direct contact birds at 1, 3, 5, 7, and 9 dpi. The swab samples were stored in glass vials in 1.0 ml freezing Brain Heart Infusion (BHI) medium (BD, Sparks, MD) and titrated for infectivity in 10-day-old embryonated chicken eggs and MDCK cells. Sera were collected 2 weeks post-infection and HA inhibition tests (HI) were performed to quantify antibodies against HA [254].

Challenge studies

Chickens that hatched after *in ovo* vaccination were randomly divided into two groups with the same number of individuals. Early protection was assessed in the first group of chickens by challenge at 2-weeks post-hatching. Challenge virus consisted of 5 × 10⁵ EID₅₀ of virus (equal to 500 chicken infectious dose 50 (CID₅₀)) and was delivered via intranasal inoculation. Late protection was assessed in the second group of chickens

following the strategy described above, but in chickens that were 6 weeks old. Tracheal and cloacal swab samples were collected at 3, 5, and 7 days post-challenge (dpc). Virus shedding was titrated in MDCK cells by TCID₅₀. Sera samples were collected at 2-weeks post-hatching pre-challenge, and 2 weeks post-challenge. HI titers were determined as previously described. Animal studies were conducted under BSL-2 conditions, and performed according to protocols approved by the Animal Care and Use Committee of the University of Maryland.

Results

Chicken hatchability is impaired after *in ovo* vaccination with H7N2 and H9N2 WF10att viruses

Our previous studies showed that *in ovo* vaccination with 10⁶ EID₅₀ of the ΔH5N1:6WF10att virus resulted in effective protection against HPAI H5N1 virus [254]. We wanted to determine whether similar levels of protection could be obtained against other HA subtypes following the same strategy. We were particularly interested in the H7 and the H9 subtypes because they have been responsible for recurrent outbreaks, particularly in Eurasia (although in our studies a H7 virus of the North American lineage was used). Thus, 18-day-old egg embryos were inoculated with 10⁶ EID₅₀ of either 2H7N2:6WF10att or 2H9N2:6WF10att vaccine viruses (Tables 4.1 and 4.2). Unfortunately, the hatchability of vaccinated eggs was poor, 30% and 37% in eggs vaccinated with 2H7N2:6WF10att and 2H9N2:6WF10att, respectively (Table 4.2) compared to 85% in eggs vaccinated with the 2ΔH5N1:6WF10att virus (not shown and [254]).

Chicken hatchability after modification of the HA cleavage site in H7N2 and H9N2 WF10att viruses

The 2 Δ H5N1:6WF10att virus carries the H5 HA protein from A/Vietnam/1203/04 (H5N1) but its polybasic cleavage site, characteristic of HPAI viruses, has been replaced with that from the LPAI H6 HA virus subtype, as described in previous reports [342]. In order to determine if incorporation of the H6 HA cleavage site in the H7 and H9 subtypes would result in more attenuated vaccine viruses and improved hatchability, we generated the recombinant viruses 2mH7N2:6WF10att and 2mH9N2:6WF10att. Modifications at the cleavage site in these viruses did not have major effects on the *in vitro* properties of these viruses. Both recombinant viruses reached titers of 10^6 TCID₅₀/ml at 120 h post-infection in MDCK cells inoculated at an MOI = 0.001 and cultured at 35°C (Figure 4.2 and data not shown). In contrast, viral replication at 39°C was severely restricted, with viral titers reduced more than 1000-fold relative to those at 35°C (Figure 4.2 and data not shown). This indicates that modifications in the HA cleavage site did not change the temperature sensitive phenotype of these viruses in MDCK cells. Likewise, plaque assays, performed using CEK cells (Figure 4.3), showed that 2mH7N2:6WF10att formed significantly smaller plaques than 2H7N2:6WF10att at 37° and 39°C. As expected, these viruses were highly restricted at 41°C (yields of $<10^3$ PFU/ml) consistent with their *att* phenotype. Interestingly, the lower virus titers and smaller plaque sizes of 2mH7N2:6WF10att compared to 2H7N2:6WF10att indicate an additive effect on attenuation provided by the modified HA cleavage site. Similar results were obtained when we compared the 2mH9N2:6WF10att to 2H9N2:6WF10att (not shown). However, despite the additional attenuation, only a slight improvement in

hatchability (50% and 63%) was observed when 18-day-old egg embryos were inoculated with 10^6 EID₅₀ of the 2mH7N2:6WF10att and 2mH9N2:6WF10att vaccine viruses, respectively (Table 4.2).

Stability of new recombinant viruses

The genetic stability of the mutations on HA, PB1, and PB2, was verified by serial passage of the 2mH7N2:6WF10att and 2mH9N2:6WF10att viruses in 10-day-old embryonated eggs. Amino acids 391E, 581G, 661T and the HA tag on PB1, and 265S on PB2 remained unchanged after serial propagation in eggs. More importantly, the amino acids at the HA cleavage site remained unchanged and corresponded to the H6 HA cleavage sequence (PQIETRG).

Modification of the HA cleavage site reduces replication of 2mH7N2:6WF10att virus in quail

We have previously shown that quail are more susceptible than chickens to avian influenza viruses. Thus quail represent a better host to test whether modifications in our vaccine viruses would have any effect on replication and transmissibility. To investigate if modification of the HA cleavage site altered the degree of attenuation and transmissibility in quail, 2 groups of quail (n = 6) were inoculated with either the 2mH7N2:6WF10att virus or the 2H7N2: 6WF10att virus. At 24 h after infection, 3-naïve quail/group were brought in direct contact with inoculated quail to monitor for transmission (Table 4.3). At 3 dpi, 3 inoculated quail from each group were sacrificed to determine virus load in the lungs. No virus was detected in the lungs of inoculated quail regardless of the virus used. This finding is consistent with our previous study showing

that the WF10att backbone prevents the virus from replicating in the lower respiratory tract (not shown and [254,285]). In addition, no virus was detected in cloacal swabs for any of the quail in the study (not shown). In contrast, tracheal swabs showed the presence of virus in the 2H7N2:6WF10att group, with peak virus titers of $10^{2.9}$ (at 1 dpi) and $10^{1.6}$ TCID₅₀/ml (at 3 dpi) in the inoculated and direct contact quail, respectively. Inoculated quail remained positive until 5 dpi but were negative by 7 dpi. Only 2 out of the 3 direct contact quail showed trace amounts of 2H7N2:6WF10att and were negative by 9 dpi. With respect to the 2mH7N2: 6WF10att inoculated group, only trace amounts of virus were observed, and just 1 of 3 quail remained positive by 7 dpi and it became negative by 9 dpi. Direct contacts in the 2mH7N2: 6WF10att virus group were negative except for trace amounts of virus on a single day, 7 dpi, in 2 of the 3 quail. The levels of virus replication in the different groups corresponded with the levels of seroconversion observed. Thus, inoculated quail in the 2H7N2:6WF10att group had the highest neutralizing antibody response, followed by inoculated quail in the 2mH7N2: 6WF10att group, whereas the direct contacts in the 2H7N2:6WF10att showed low, but significant seroconversion. Also consistent with the transient presence of the 2mH7N2: 6WF10att virus in the direct contact group, very low seroconversion was observed. These studies suggest that alterations in the HA cleavage site have an effect on replication in vivo further attenuating these viruses and limiting the ability to replicate after transmission (Table 4.3). We did not perform similar studies in quail with the H9N2 vaccine viruses. However, we must note that similar studies in white leghorn chickens did not result in detectable transmission, when the viruses carry the att backbone in the context of H7N2 or H9N2 surface genes (not shown).

Single dose *in ovo* vaccination provides protection in chickens from homologous challenge with H7 and H9 LPAI viruses at 2 and 6 weeks post-hatching

To further evaluate whether *in ovo* immunization would result in protection against H7 or H9 viruses, vaccinated chickens were divided into two groups, and subsequently challenged with homologous virus at either 2 or 6 weeks post-hatching (Tables 4.4 and 4.5).

Pre-challenge sera collected at 2 weeks post-hatching showed limited seroconversion in chickens that received the 2mH7N2:6WF10att (Table 4.4), both in terms of the number of seropositive chickens as well as the level of HI responses. However, sera collected at 6 weeks post-hatching showed increased numbers of seropositive chickens and increased HI titers (Table 4.4). Relative to 2mH7N2:6WF10att, improved and more consistent antibody responses were obtained in chickens that were vaccinated with 2mH9N2:6WF10att (Table 4.5). In terms of protection, significant protection was observed in chickens challenged with 500 CID₅₀ of Ck/04 (H7N2) at 2 or 6 weeks post-hatching but only in the 19-day old embryo vaccinated groups. Tracheal virus shedding was detected in only 2 out 8 and 1 out of 5 chickens in the 19-day old embryo groups that received 10⁶ or 10⁷ EID₅₀, respectively, of 2mH7N2:6WF10att. There was also a sharp decrease in cloacal virus shedding in these groups, with just 1 out 8 (10⁶ EID₅₀ group) and 1 out 5 (10⁷ EID₅₀ group) virus positive chickens and only at 7 dpc (Table 4.4). In contrast, in the 18-day old embryo vaccinated group only 1 out 4 and 2 out 4, at 2 and 6 weeks post-hatching, respectively, showed protection and no detectable virus replication. Similar protective responses were observed in the WF10 (H9N2)

challenged chickens. Chickens in the 19-day old embryo vaccinated groups showing the best protection, and those in the 18-day old embryo vaccinated groups showed the decreased protection (Table 4.5). Significant seroconversion in all the groups at 14 dpc indicated that lack of virus shedding in protected chickens was not due to a failure in our challenge approach. Considering the 10^6 EID₅₀ vaccine dose in the 19-day old embryo vaccinated groups for both *att* vaccines, there was between 70 and 80% protection efficiency in chickens challenge at 2 or 6 weeks post-hatching, respectively. Slightly better protection efficiency (82%) was observed in the 10^7 EID₅₀ vaccine dose groups; however, it was achieved at the expense of lower hatchability rates (~91% for the 10^6 EID₅₀ versus ~80% for the 10^7 EID₅₀ groups). In contrast, an average of only 55% protection efficiency was observed in the groups vaccinated with a dose 10^6 EID₅₀ in 18-day old embryos.

Discussion

The HA is perhaps the most important protein in influenza viruses, as it is a critical determinant of host range and virulence [50,51]. The HA protein, encoded in segment 4, is expressed on the virus surface as homotrimers. It is initially produced as a precursor, HA0, that requires post-translational modifications, including cleavage and glycosylation in order to become fully active [57]. Cleavage of the HA0 precursor leads to two subunits, HA1 - N-proximal - and HA2 - C-proximal -, which are maintained covalently linked via disulfide bonds. Trypsin-like host proteases found in the lumen of the respiratory and intestinal tracts are involved in the cleavage of the HA of low pathogenic avian influenza viruses - LPAIV - (and mammalian influenza viruses) [57]. Intracellular furin-like proteases have been implicated in the cleavage of the HA of

highly pathogenic avian influenza viruses - HPAIV [57]. The number of basic amino acid residues preceding the cleavage site determines recognition by either trypsin-like or furin-like proteases, with a string of basic amino acids allowing the latter to cause intracellular maturation of the HA at the level of the endoplasmic reticulum [343]. Furin-like protease cleavage produces mature virions that can spread cell to cell without having to reach the lumen of the respiratory or intestinal tracts. This permits the development of a fatal systemic infection, hence the so-called highly pathogenic influenza. Therefore, the cleavability of HA is one of the critical factors for viral tissue tropism and pathogenicity [344,345]. In this study, we modified the cleavage site of the influenza virus H7 and H9 HA protein genes to encode sequences corresponding to the H6 HA cleavage site (mH7 and mH9) in order to improve hatchability after *in ovo* vaccination. It has been previously shown that the H6 HA cleavage site can transform a HPAIV of the H5N1 subtype into a LPAIV [342]. We have previously shown that a LPAI H5N1 virus carrying *att* mutations is amenable for *in ovo* vaccination resulting in $\geq 60\%$ protection while maintaining at least 85% hatchability [254]. In this study we sought to examine whether the mH7 and mH9 *att* viruses showed similar replication yields as unmodified H7 and H9 *att* viruses, and if these modified viruses were more amenable for *in ovo* vaccination without decreased immunogenicity. Growth kinetic studies in tissue culture cells showed similar yields for the mH7 compared to the unmodified H7 viruses (Figure 4.2) and similar results were obtained comparing the mH9 with the unmodified H9 pairs (not shown). As the safe "window" for *in ovo* vaccination of chicken embryos is between day 17 at 12-14 hours to day 19 at 2-4 hours [341], we chose days 18 and 19 for vaccination to test the effects on hatchability of the *att* vaccines. Hatchability studies clearly demonstrated that

the mH7 and mH9 *att* viruses allowed for hatchability (90-93%, 19-day old embryos) similar to the PBS inoculated controls (93-96%), which were much higher than those obtained with the unmodified H7 or H9 *att* viruses (43-60%, 19-day old embryos). We found that the combination of the modified HA cleavage site, vaccine dose, and time of vaccine delivery, had a significant impact on hatchability rates. Thus, 18-day old chicken embryos vaccinated with the mH7 or the mH9 *att* viruses showed improved hatchability rates compared to the unmodified HA *att* counterparts, but they were significantly lower than the rates obtained after vaccinating 19-day old embryos (Table 4.2). Likewise, increasing the dose to 10^7 EID₅₀ of either mH7 or mH9 *att* viruses resulted in 10% hatchability loss compared to the same age embryos inoculated with 10^6 EID₅₀ of the same viruses.

We speculate that the introduction of the alternative H6 HA cleavage site in the mH7 and mH9 *att* viruses (and perhaps in the Δ H5 *att* virus) leads to reduced HA cleavage efficiency and, thus, these viruses exhibit growth restrictions at higher temperatures *in vitro* (Figure 4.3) and *in vivo* in 18-19-day old chicken embryos (Table 4.2). However, these viruses showed no defects in terms of virus yield at the permissive temperatures of 33 and 35°C in tissue culture (Figure 4.2) or in 10-day old chicken embryos. These characteristics are important because efficient immunogenicity was maintained without sacrificing virus yield. In fact, 2mH7N2:6WF10*att* and 2mH9N2:6WF10*att* viruses can easily achieve titers on the order of 10^8 EID₅₀/ml when grown in 10-day old embryonated chicken eggs (data not show), thus making them ideal for mass production.

In ovo vaccination is an attractive approach for vaccination of chickens, particularly broilers [341,346]. It helps to 'close the window' of susceptibility between vaccination and early exposure to infectious agents compared with post-hatch vaccination [346]. Because chickens already develop certain immunologic functions before hatching, *in ovo* vaccination stimulates both the innate and adaptive immune responses. Thus, *in ovo* vaccinated chicks develop an appreciable degree of protection by the time of hatching [346]. This indeed appears to be the case since in our approach chickens showed significant protection ($\geq 70\%$) when challenged as early as 2 weeks post-hatching. It is tempting to speculate that under industrial settings higher protection efficiencies could be obtained since automated systems would result in more accurate, controlled and efficient administration of the vaccine compared to our manual approach. In addition, because the mH7 and mH9 *att* viruses are more attenuated *in vivo* than the unmodified *att* counterparts, we further speculate that these HA genes are not likely to outcompete wild type influenza viruses through reassortment, and thus, should be safe to use in the field. The unprecedented spread of low pathogenic H7 and H9 influenza viruses in commercial settings, calls for the implementation of alternative prevention and control strategies. Our report provides for a viable alternative to the classical vaccination approaches against avian influenza.

Table 4.1. The gene constellations of the recombinant viruses.

Virus	HA	NA	Internal genes (PB1, PB2, PA, NP, M and NS)
2m2H7N2:6WF10att	mH7 (VIVA/04)	N2 (VIVA/04)	WF10att
2H7N2:6WF10att	H7 (VIVA/04)	N2 (VIVA/04)	WF10att
2mH9N2:6WF10att	mH9 (WF10)	N2 (WF10)	WF10att
2H9N2:6WF10att	H9 (WF10)	N2 (WF10)	WF10att

Table 4.2. Comparison of the hatchability of new recombinant viruses in embryonated chicken eggs vs. the viruses with wild type HAs and the optimization of the dose and timing for *in-ovo* vaccination.

Vaccine		Dose (EID50)	Embryo age (Day)	% Hatchability (# hatched/total #)	
H7N2 (VIVA/04) Vaccine	2mH7N2:6WF10att	10 ⁶	18	50% (15/30) (P=0.016)	
		10 ⁶	19	93% (42/45) (P=0.061)	
		10 ⁷	19	80% (24/30) (P=0.066)	
	2H7N2:6WF10att	10 ⁶	18	30% (9/30)	
		10 ⁶	19	43% (13/30)	
		10 ⁷	19	37% (11/30)	
	H9N2 (WF10) Vaccine	2mH9N2:6WF10att	10 ⁶	18	63% (19/30) (P=0.0161)
			10 ⁶	19	90% (27/30) (P=0.260)
			10 ⁷	19	83% (25/30) (P=0.154)
2H9N2:6WF10att		10 ⁶	18	37% (11/30)	
		10 ⁶	19	60% (18/30)	
		10 ⁷	19	37% (11/30)	
PBS (Mock)	0	18	93% (28/30)		
	0	19	96% (43/45)		

* 3 chickens dead at 2-5 days post-hatching

Table 4.3. Replication and transmission study of recombinant virus 2H7N2:6WF10att and 2mH7N2:6WF10att in quail

Virus	Quail group	# of positive tracheal swab/total # post-inoculation					# of seroconverted/total # (Average HI titer at 14 dpi)
		(log ₁₀ TCID ₅₀ /ml± SD) at peak viral shedding					
		1 dpi	3 dpi	5dpi	7 dpi	9 dpi	
2H7N2:6WF10att	Inoculated	6/6 (2.9±0.4)	6/6*	3/3	0/3	0/3	3/3 (133)
	Contact	NA	3/3 (1.6±1.4)	3/3	2/3	0/3	3/3 (47)
2mH7N2:6WF10att	Inoculated	6/6 (<0.7)	6/6*	1/3	1/3	0/3	3/3 (87)
	Contact	NA	0/3	0/3	2/3 (<0.7)	0/3	2/3 (10)

* 3 quail from each inoculated group were sacrificed at 3 dpi to determine virus load in the lungs.

Table 4.4. Single-dose 2mH7N2:6WF10att *in ovo* vaccination study in chickens challenged with low-pathogenic H7N2 (Ck/04) at 2 and 6-week post-hatching

Vaccine dose embryo age	# positive HI/total # pre-challenge	Age in weeks at time of challenge	# Shedding virus/total # in swabs (\log_{10} TCID ₅₀ /ml±SD)						# positive HI/total # at 14 dpi
			Tracheal			Cloacal			
			3 dpc	5 dpc	7 dpc	3 dpc	5 dpc	7 dpc	
			0 (Mock)	0/8	2	8/8 (3.4±0.8)	8/8 (2.9±0.6)	0/8	
10 ⁶ EID ₅₀ 18-Day	1/4 (3)	2	3/4 (3.3±1.0)	3/4 (2.9±0.9)	0/4	2/4 (4.5±0.7)	3/4 (3.7±1.0)	3/4 (3.7±0.7)	4/4 (320)
10 ⁶ EID ₅₀ 19-Day	6/8 (13)	2	2/8 (3.5±0.7)	1/8 (2.3)	0/8	0/8	0/8	1/8 (2.0)	8/8 (240)
10 ⁷ EID ₅₀ 19-Day	3/5 (5)	2	1/5 (2.7)	0/5	0/5	0/5	0/5	1/5 (2.3)	5/5 (272)
0 (Mock)	0/7	6	7/7 (3.5±0.7)	7/7 (3.4±0.7)	0/7	3/7 (3.9±0.5)	5/7 (3.7±1.0)	5/7 (3.3±0.8)	7/7 (525)
10 ⁶ EID ₅₀ 18-Day	2/4 (50)	6	2/4 (4.1±0.6)	2/4 (3.9±0.6)	0/4	1/4 (3.5)	2/4 (4.3±0.4)	2/4 (3.6±0.1)	4/4 (360)
10 ⁶ EID ₅₀ 19-Day	5/7 (51)	6	2/7 (3.4±0.2)	0/7	0/7	1/7 (3.7)	1/7 (3.5)	1/7 (3.3)	7/7 (525)
10 ⁷ EID ₅₀ 19-Day	4/5 (64)	6	1/5 (3.7)	1/5 (3.7)	0/5	0/5	0/5	0/5	5/5 (640)

Table 4.5. Single-dose 2mH9N2:6WF10att *in ovo* vaccination study in chickens challenged with low-pathogenic H9N2 (WF10) at 2 and 6-week post-hatching

Vaccine dose and inoculation time	# positive HI/total # before challenge	Age in weeks at time of challenge	# Shedding virus/total # in swabs			
			(log ₁₀ TCID ₅₀ /ml±SD)			
			Tracheal			# positive
			3 dpc	5 dpc	7 dpc	HI/total # at 14 dpi
0 (Mock)	0/7	2	7/7 (2.7±0.6)	7/7 (2.5±0.3)	0/7	7/7 (217)
10 ⁶ EID ₅₀ ^a 18-Day	3/5 (14)	2	2/5 (2.2±0.2)	2/5 (2.3±0.4)	0/5	5/5 (192)
10 ⁶ EID ₅₀ ^a 19-Day	6/7 (32)	2	1/7 (2.5)	0/7	0/7	7/7 (286)
10 ⁷ EID ₅₀ ^a 19-Day	3/4 (32)	2	1/4 (2.3)	0/4	0/4	4/4 (260)
0 (Mock)	0/7	6	7/7 (2.5±0.3)	7/7 (2.5±0.2)	0/7	7/7 (320)
10 ⁶ EID ₅₀ ^a 18-Day	2/5 (30)	6	3/5 (2.6±0.7)	3/5 (2.2±0.9)	0/5	5/5 (224)
10 ⁶ EID ₅₀ ^a 19-Day	5/7 (71)	6	2/7 (2.4±0.5)	0/7	0/7	7/7 (446)
10 ⁷ EID ₅₀ ^a 19-Day	3/3 (67)	6	0/3	0/3	0/3	3/3 (227)

A



B

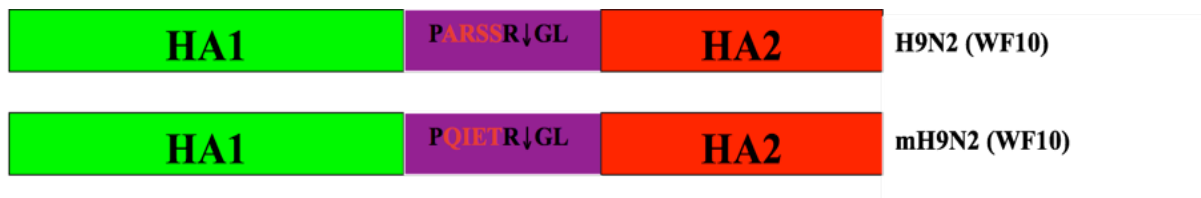


Figure 4.1. Strategy of modifying the HA cleavage site. (A). The substitution of H7N2 (VIVA/04) HA amino acid cleavage site with alternative cleavage site sequences of H6's. (B). The substitution of H9N2 (WF10) HA amino acid cleavage site with alternative cleavage site.

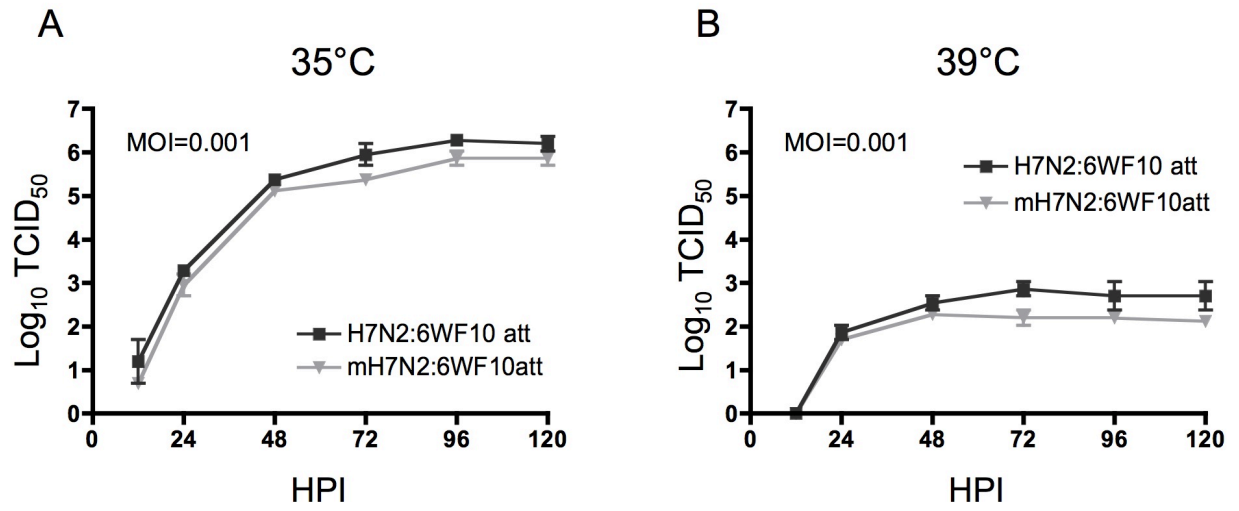


Figure 4.2. Viral replication kinetics of the live-attenuated viruses in MDCK cells at (A) 35°C and (B) 39°C using MOI of 0.001. Viral titers at different time points were determined by TCID₅₀.

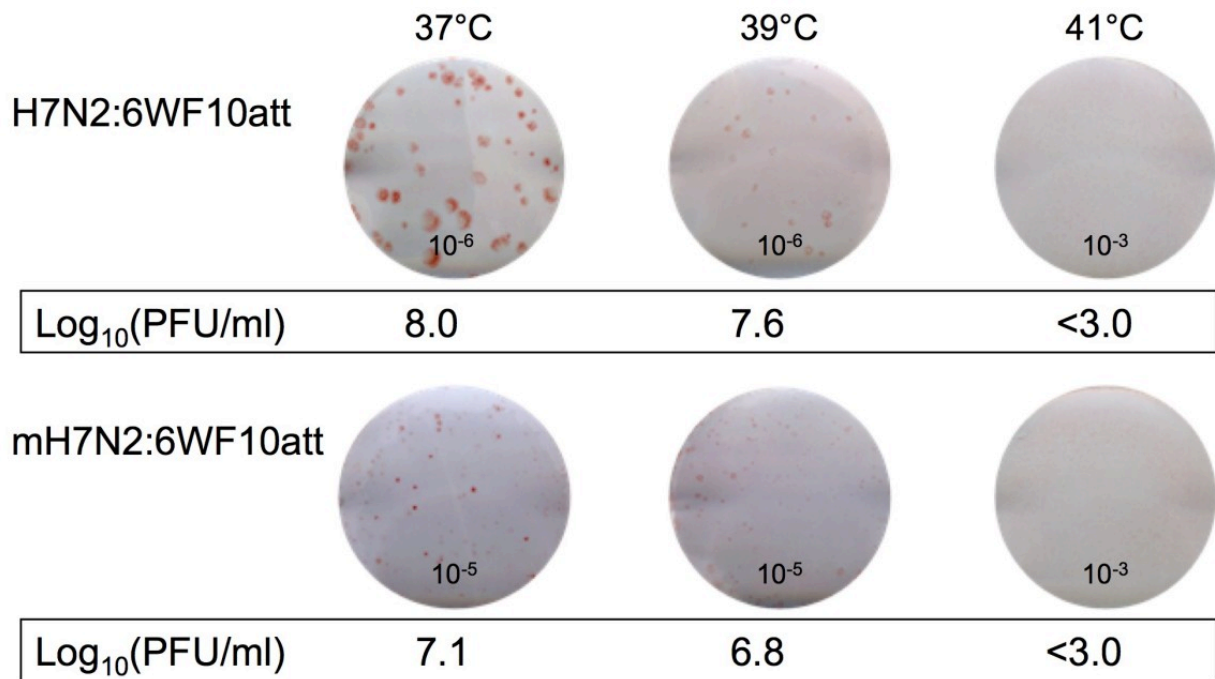


Figure 4.3. Plaque morphology of the live-attenuated viruses in CEK cell at different temperatures. Confluent CEK cells in six-well plates were infected with 2mH7N2:6WF10att or 2H7N2:6WF10att. The numbers 10^{-6} , 10^{-5} , and 10^{-3} on the plaque pictures indicate the virus dilution used to infect cells at the indicated temperature. The cells incubated at 37°C, 39°C, or 41°C, respectively, for 4 days post infection and then fixed and the viral antigen was visualized by immunostaining as described in Materials and Methods. The plaques sizes were observed and the plaque numbers were counted and calculated as the \log_{10} PFU/ml, as indicated below the individual plaque picture. A titer of $<3.0 \log_{10}$ PFU/ml indicates that no virus was detected at 10^{-3} dilution.

Chapter 5: Glutamic acid to valine substitution at position 59 in PA enhances growth of live-attenuated influenza vaccines in eggs and mammalian cells

Abstract

During the emergence of the 2009 pandemic H1N1 (pH1N1) influenza virus, a live attenuated vaccine candidate was produced by reverse genetics in the background of an experimental alternative live attenuated influenza strain, WF10*att*. However, the recombinant virus 2ma-Ca/04:6WF10*att* yielded low hemagglutination (HA) titer after amplification in 10-day-old egg embryos. In order to improve virus yield, the first passage virus (P1) was serially propagated in eggs for eight total passages (P8). The P8 virus showed significant increased in HA titer (>30-fold) compared to the P1 virus. Sequence analysis of the entire 2ma-Ca/04:6WF10*att* viral genome revealed a single amino acid mutation in the PA gene, at position 59, in which glutamic acid was substituted to valine (PA E59V). Inoculation of this virus into eggs resulted in 20-fold increase in HA titer and a 4.6-fold increase in viral titer relative to the wild-type (wt) PA virus. Upon culture in MDCK cells, the PA E59V virus had an HA and viral titer that increased 16 and 3.9-fold, respectively, compared to wt. Western blot analysis and quantitative analysis of viral mRNA showed that the PA E59V virus led to earlier and higher production of viral protein and viral mRNAs compared to the wt virus. The PA E59V mutation did not impair the temperature sensitive phenotype of WF10*att*. The PA E59V mutation moderately enhanced the HA and viral titer of wt WF10 and another alternative live-attenuated backbone, Ty/04*att*. However, it had no effect on two commercially licensed influenza vaccine internal backbones, PR/8 and

cold-adapted (*ca*) Ann Arbor/60. Interestingly, although the E59V had no significant effect on increasing HA/NP ratio of the wt WF10 or WF10*att* based live-attenuate vaccine; both of these backbones resulted in higher antigenic content (higher HA/NP ratio) on viral particles than PR/8- or *ca* Ann Arbor/60-based virus particles.

Introduction

In April 2009, a novel swine-origin pandemic influenza virus (pH1N1) rapidly spread around the world. By August 2010, human cases of pH1N1 had been reported from more than 214 countries, and caused more than 18,000 deaths worldwide [7].

The available seasonal H1N1 vaccines provided little to no protection against the novel pH1N1 virus [26]. Both classical reassortment and reverse genetics methods were applied to readily generate the vaccine candidates against the pH1N1 virus, such as: X-179A (New York Medical School (NYMC)(US)), IVR-153 (Commonwealth Serum Laboratories (CSL) Ltd (AU)), NIBRG-121 (National Institute for Biological Standards and Control (NIBSC)(UK)) and IDCDC-RG15 (Centers for Disease Control and Prevention (CDC)(US)) [262]. Due to the low viral protein yield of those vaccine strains in chicken egg embryos, more efforts were carried out to achieve higher protein yield and functional HA yield resulting in strains NIBRG-121 xp and X-181[262].

In order to generate live attenuated influenza vaccine (LAIV) against pH1N1, Chen et al. generated several reassortants with 6:2 gene constellation (2 surface genes from A/California/4/09 or A/ California /7/09, and 6 internal genes from cold-adapted (*ca*) A/Ann Arbor/6/60 (H2N2) strain) using reverse genetics. To improve the viral

replication in egg embryos and MDCK cells, those reassortant vaccines were propagated two times in MDCK cells and the large plaques were isolated for the sequence analysis. The mutations in the HA gene contributed to the improved viral replication in eggs were identified. The reassortant variants carrying those mutations were further detected in receptor binding assay and animal study. And the results demonstrated that the mutations on residue 119 and 186 may largely improve the viral growth in eggs without affecting the antigenicity and immunogenic of the vaccines [347].

Other strategies were also applied to develop LAIV to protect against pH1N1. Additional experimental vaccines were developed, such as a mutant pH1N1 virus with the M2 protein lacking 11 amino acids at the cytoplasmic tail could protect mice from infection [348]; an engineering temperature sensitive LAIV was successfully developed by directly introducing point mutations into PB1 and PB2 genes of a pH1N1 like-virus [349].

Previsously, we reported the development of alternative LAIVs based on introduction of amino acid mutations on the PB1 (K391E, E581G, and A661T) and PB2 (N265S) genes and an additional HA-tag at the C-terminus of the PB1 gene in the background of influenza viruses A/Guinea Fowl/Hong Kong/WF10/99 (H9N2) and A/turkey/Ohio/313035/2004 (H3N2), herein referred to as WF10*att* and Ty/04*att*, respectively. Using the WF10*att* background we generated a LAIV for the pH1N1 virus based on the surface HA and NA genes from A/California/04/2009 (H1N1) (Ca/04). The new virus, 2Ca/04:6WF10*att*, produced low HA titers (4.4 ± 0.4) when amplified in eggs. Serial propagation of this virus in eggs, however, significantly

improved the HA titer (10.0 ± 0.38). Sequencing results revealed no changes on the surface genes but instead a single amino acid mutation in the PA gene: the codon encoding residue 59 changed from glutamic acid to valine.

PA, a subunit of the influenza virus RNA-dependent RNA polymerase (RdRP), contains an N-terminal domain with endonuclease and protease activities and a C-terminal domain that interacts with the RdRP's PB1 subunit. The N-terminal 209 amino acids of PA possess a type II restriction endonuclease activity, with active site that coordinated with two manganese ions (Mn^{2+}), similar to other two-metal-dependent endonucleases. Chelation of Mn^{2+} by PA involves participation of two sites: Mn^{2+} site 1 involves amino acids Glu80 and Asp108; whereas Mn^{2+} site 2 binding involves His40, Asp108 and Glu109 [134,135,136,137]. The endonuclease activity of PA complements the process of binding and snatching of host-derived capped mRNA 10-13 nt long primers used for the synthesis of viral mRNAs [134,138,139,140].

In this study, the amino acid substitution E59V in PA is demonstrated to be responsible for the enhanced HA titer and viral yield in eggs and MDCK cell on the live attenuated vaccine WF10att background. PA E59V virus resulted in earlier and higher production of viral protein and viral mRNAs compared to the wt virus. Introduction of this substitution could also moderately enhance the HA and viral titer of the wild-type WF10 backbone and another alternative LAIV backbone, Ty/04att; however, it had no significant effect on two licensed influenza vaccine internal backbones PR/8 and *ca* Ann Arbor/60. Interestingly, although the PA E59V mutation had no significant effect on increasing HA/NP ratio of WF10 or WF10att based live-

attenuated background; both of these backbones led to more antigenic content on the viral particles (higher HA/NP) than PR/8 or *ca* Ann Arbor/60 backgrounds.

Materials and methods

Virus, plasmid and cells

The pH1N1 virus (Ca/04), wt-WF10, WF10*att*, wt-ty/04, and Ty/04*att* viruses have been previously described [254,350,351]. Virus stocks were prepared in specific pathogen free 9-day old embryonated chickens eggs following standard techniques for growth of influenza viruses. Madin-Darby canine kidney (MDCK) cells were maintained in Modified Eagle's medium (MEM) (Sigma-Aldrich, St. Louis, MO) containing 5% fetal bovine serum (FBS) (Sigma-Aldrich). Human embryonic kidney 293T cells were cultured in Opti-MEM I (GIBCO, Grand Island, NY) containing 5% FBS. The reverse genetics 8-plasmid system for influenza A/Puerto Rico/8/1934 (H1N1) (PR8) virus was a gift from Peter Palese, Mount Sinai School of Medicine, New York, NY. The RG system for the *ca* A/Ann Arbor/6/60 (H2N2) virus was produced from the homologous strain provided by Ruben Donis, CDC, Atlanta, GA, and cloned into the pDP2002 vector (Sutton et al, unpublished). The E59V mutation in PA genes from various virus backgrounds was introduced using the QuickChange II site-directed mutagenesis kit (Stratagene, Inc., La Jolla, CA) according to manufacturer's protocols. The presence of each mutation was confirmed by sequencing.

Generation of recombinant virus by reverse genetics

The recombinant viruses were generated using the 8-plasmid system in co-cultured 293T and MDCK cells as described previously [254]. 10 μ l of pDP-2002 plasmids (100 ng/ml) carrying the cDNA from each of 8 RNA segments were incubated with 18 μ l TransIT LT-1 (Mirus, Madison, WI) at room temperature for 45 min, and then the mixture was transfected into co-cultured 293T and MDCK cells. 8 h later, the DNA-transfection mixture was replaced by Opti-MEM I. 24 h after transfection, 1 ml of Opti-MEM I containing TPCK-trypsin of 1.0 μ g/ml was added to the cells. All recombinant viruses were propagated in 10-day-old embryonated eggs, titrated by TCID₅₀, and stored at -70°C until use. All viruses were sequenced using specific primers.

Sequence analysis

The cDNA of the virus was prepared as previously described [254]. The total RNA of each sample was extracted using RNeasy Mini Kit (Qiagen, Gaithersburg, MD), and RNAs were eluted in 40 μ l RNase-free water. The reverse transcription (RT) was performed with the 4 μ l of RNA sample and 1 μ l Uni12 primer using AMV Reverse Transcriptase (Promega, Madison, WI) at 42°C for 2 h and then 70°C for 10 min. The specific fragment was amplified and sequenced using a combination of universal and custom made primers (available upon request, see Appendices). Sequencing was performed using the Big Dye Terminator v3.1 Cycle Sequencing kit (Applied Biosystems, Foster City, CA) on a 3100 Genetic Analyzer (Applied Biosystems, Foster City, CA) according to the manufacturer's instructions. The sequencing reaction system contains 2.0 μ l of the cDNA, 1.5 μ l of the sequencing

primer, 2.0 µl of RR-100 (Life technologies, Grand Island, NY) and 3.0 µl of 5x Sequencing buffer (Life technologies, Grand Island, NY). The cycle conditions of sequencing were 96 °C 4 min, followed by 60 cycles of 96 °C 30 s, 56 °C 10s, and 60 °C for 4 min. The reaction products were precipitated with 5µl EDTA (0.125 mM) and 60 µl 100% ethanol, and spin down at 3000xg for 15 min, following a wash with 80 µl of 70% ethanol, and spin down at 3000xg for 15 min. The pellet was dried and dissolved in 10 µl of Hi Di formamide (HiDi, Fisher Scientific, Waltham, MA) for sequencing.

Viral replication study in eggs and mammalian cells

10-day-old embryonated eggs were inoculated with 100 or 1000 TCID₅₀ virus in 0.1 ml PBS. The allantoic fluids were collected at 24, 48, 72 and 96 h post inoculation from 3 egg embryos. For the MDCK cells infection. The cells were washed with PBS for 3 times. Confluent monolayers of MDCK cells (10⁶ cell/well) in 6-well plates were infected with 1000 TCID₅₀ of the viruses in 1.0 ml of Opti-MEM I (MOI = 0.001). The plate was put in 4 °C for 15 min, and then transferred to 37°C incubator for 45 min. The cells were washed with PBS for 3 times, and then 1.0 ml of Opti-MEM I containing TPCK-trypsin of 1.0 µg /ml was added to each well. The viral supernatants were collected at 12, 24, 48, 72, 96 and 120 h post-inoculation. TCID₅₀ from egg embryos and MDCK cells were detected as described previously [254].

The inoculation of the egg embryos was carried out in triplicate; the infection of MDCK cells was performed in duplicate. All experiment results were confirmed with at least one more experiment.

Western blot

MDCK cells were seeded in 6-well plate overnight, and then infected with viruses at MOI=0.1. The cells were harvested every 4 h after infection up to 24 h with 250 μ l of 2x Laemmli Sample Buffer (Bio-Rad, Hercules, CA) containing 50 μ l β -mercaptoethanol (Fisher Scientific, Waltham, MA)/ml. The samples were heated at 100°C for 5 min and sonicated for 20 seconds, and then 20 μ l of the samples were loaded into a Mini-PROTEAN TGX Precast Gel (Bio-Rad, Hercules, CA). The gel was run for 60 min at 150 V using PowerPac basic power supply (Bio-Rad, Hercules, CA). Then the protein samples were transferred into supported nitrocellulose membrane (Bio-Rad, Hercules, CA) at 18 V for 45 min using Trans-Blot SD System and PowerPac HC Power Supply System (Bio-Rad, Hercules, CA). The viral protein HA and NS1 were detected with the monoclonal antibodies S-OIV-3B2 (prepared in the lab (1:500)) and Clone NS1-1A7 (from NIH (1:500)) as the primary antibody, respectively; and then with HRP-conjugated goat anti-mouse IgG (SouthernBiotech, Birmingham, Alabama (1:5000)) as the secondary antibody. The image was developed using SuperSignal West Pico chemiluminescent substrate (Fisher Scientific, Waltham, MA). The image was scanned and the optical density of each sample was quantitated using densitometry software Quantity One version 4.6.5 (Bio-Rad, Hercules, CA), and then the relative amount of the proteins were further calculated. GAPDH was taken as the cellular internal control.

This experiment has been repeated 2 times. However, quantitative densitometry has been performed only once.

Reverse transcription and real-time PCR

MDCK cells were seeded in 6-well plate overnight, and then infected with viruses at MOI=0.1. The cells were collected at the early phase of infection at 1, 5, 9 and 13 h.p.i. using Trypsin-EDTA solution (Sigma-Aldrich, St. Louis, MO). The total RNA of each sample was extracted using RNeasy Mini Kit (Qiagen, Gaithersburg, MD), and RNAs were eluted in 40 μ l RNase-free water. The reverse transcription (RT) was performed with the 4 μ l of RNA sample and 1 μ l specific tagged RT primers as listed in Table 5.3 using AMV Reverse Transcriptase (Promega, Madison, WI) at 42°C for 2 h and 70°C for 10 min. The reverse transcription of the internal control MDCK 18s rRNA was performed with a random 15- oligomer (Sigma-Aldrich, St. Louis, MO).

Quantitative real-time PCR (qPCR) was performed with Lightcycler 480 SYBR Green I Master (Roche Applied Science, Indianapolis, IN), on a CFX96 Real-time System (Bio-Rad, Hercules, CA). 2 μ l of 10-fold dilution of the cDNA was added to the qPCR reaction mixture (10 μ l Lightcycler 480 SYBR Green I Master (2 \times), 1.5 μ l forward primer (10 μ M), 1.5 μ l reverse primer (10 μ M), and 5 μ l millipore water). The cycle conditions of qPCR were 95 °C 10 min, followed by 40 cycles of 95 °C 15 s and 63 °C for 1 min. The internal control MDCK 18s rRNA was used for normalization, the real-time PCR of the virus samples was performed with specific primers as listed in Table 5.3. Data were analyzed using the Bio-Rad iQ5 software version 2.1 (Bio-Rad, Hercules, CA). The relative level of mRNA, vRNA and cRNA were calculated via the $2^{-\Delta\Delta C_T}$ method [352].

This experiment has been performed once in triplicate. “Relative Quantity (mean)” and “Relative Quantity SD (standard deviation)” produced by Bio-Rad iQ5 software version 2.1(Bio-Rad, Hercules, CA). “2-sample t-test” was performed for the t-statistic of the RNA samples:

$$t = \frac{\bar{x}_1 - \bar{x}_2}{\sqrt{(s_1^2 / n_1 + s_2^2 / n_2)}}$$

Here: $SD_1 = (3/2)^{1/2} * S_1$; $SD_2 = (3/2)^{1/2} * S_2$. $n_1 = n_2 = 3$. Therefore, $t = (\text{Mean}_{mPA} - \text{Mean}_{PA}) / ((SD_{mPA}^2/2) + (SD_{PA}^2/2))^{1/2}$. $Df = n_1 + n_2 - 2 = 4$.

I calculated the t-statistic for each RNA sample at different time points with $t = (\text{Mean}_{mPA} - \text{Mean}_{PA}) / ((SD_{mPA}^2/2) + (SD_{PA}^2/2))^{1/2}$ using Microsoft EXCEL (All Means and SDs have been already determined by Bio-Rad iQ5 software version 2.1). With degrees of freedom =4, I compared the t-value of mRNA, vRNA and cRNA at 1, 5, 9 and 13 h.p.i. I calculated from above to the “t distribution table” at the chosen confidence level and decide whether to accept or reject the null hypothesis.

The comparison of HA/NP ratio of the purified viruses using ELISA

1000 TCID₅₀ virus was inoculated into thirty 10-day-old embryonated eggs. 200 ml of the allantoic fluid of each virus was harvested at 3 d.p.i., and then purified using sucrose cushion centrifugation with Ultra-Clear centrifuge tubes (Beckman Coulter, Sykesville, Maryland) and L-90K Ultracentrifuge (Beckman Coulter, Sykesville, Maryland) at 25,000×g for 2h. The concentrated pellet was dissolved in 8 ml of PBS for ELISA.

In the ELISA, the purified virus was lysed with lysis buffer (0.5% Tween-20 in PBS). The lysed virus was used as coating antigen, the mouse monoclonal antibody against HA: S-OIV-3B2 (prepared in the lab, specific to HA of A/California/04/2009 (H1N1)) or NP: 2F4 (prepared in the lab, specific to NP of influenza virus) was used as first antibody, and the HRP-conjugated goat anti-mouse IgG (Southern biotech, Birmingham, AL) was used as detection antibody. The virus (diluted in carbonate/bicarbonate buffer, pH 9.6) was coated to 96-well plates for 12h at 4°C. After one wash with PBST (0.05% Tween-20 in PBS), the plate was blocked with 5% (w/v) non-fat milk in PBS for 1h at 37°C. After one wash with PBST, the first antibody was diluted (1:5000) in dilution buffer (0.5% BSA in PBS) and added to the wells (100µl/well). The mixture was incubated at 37°C for 1 h. After wash three times with PBST, 100µl HRP-conjugated goat anti-mouse IgG (1:10000) diluted in dilution buffer was added to well and the mixture was incubated for 1 h at 37°C. After five washes with PBST, the development was performed using the TMB substrate system (KPL, Gaithersburg, Maryland) for 15 min. The ratio of the OD650 value of the sample wells (S) to that of the negative control wells (N) was determined, and the ratio of HA to NP from the same sample was calculated. However, this experiment was performed only once.

Statistical analysis

All figures were generated and all statistical analyses were performed with GraphPad Prism software version 5.0c (GraphPad Software Inc., San Diego, CA). Comparison between the means of two groups was carried out with a paired two-tailed Student's t-test, the multiple comparisons were performed by analysis of

variance (ANOVA) with Tukey's multiple comparison test, unless otherwise specified. P values of <0.05 were considered significant difference. The statistical analysis of the "real-time PCR" was performed with "2-sample t-test" using Microsoft EXCEL, and compared with "t distribution table".

Results

Preparation of an alternative pH1N1 live attenuated influenza virus (LAIV) based on the WF10att background (pH1N1 WF10att)

During the emergence of pH1N1, a LAIV was produced carrying the two surface genes from A/California/04/2009 (pH1N1) (Ca/04) in the WF10att background (2 Ca/04:6 WF10att) (Table 5.1). The amplification of virus in 10-day-old eggs, however, resulted in low HA titer (4.4 ± 0.4). To enhance the viral growth, the first passage virus (P1) was further serially propagated in eggs for a total of eight passages (P8). The results showed the viral HA titer of the P8 (10 ± 0.38) virus increased at least 30 fold compared to P1 (Table 5.2).

Cooperated with Hongjun Chen, I finished the whole genome sequencing of P1 and P8 viruses at 3x coverage. Five nucleotide substitutions were found in the PA and PB2 segments in P8 virus. However, only one nucleotide substitution in PA is non-synonymous, and rest four nucleotide substitutions caused no amino acid change (Table 5.3). Generally during egg adaptation of influenza viruses amino acid substitutions on the surface of HA and NA proteins are expected, which can enhance virus growth, sometimes in detriment of the antigenic profile of the virus.

Interestingly, full-length genome sequencing of the P8 virus revealed no mutations resulting in amino acid changes on HA and NA. Instead, a single amino acid mutation was detected in the PA gene: amino acid 59 changed from glutamic acid to valine (E59V).

The enhanced HA and viral titer of live-attenuated virus was confirmed in egg embryos and MDCK cells using reverse genetics

To investigate if PA E59V is responsible for the enhanced HA titer, we generated the viruses containing either mutated PA (E59V) or wild-type (wt) PA using reverse genetics (Table 5.1). The viruses were inoculated into 10-day-old egg embryos, and HA and viral titer were detected at 3 d.p.i. The HA titer of virus 2ma Ca/04:mPA(E59V):5WF10att increased at least 20-fold compared with that of the recombinant virus with the wt PA (Figure 5.1A and E); and the viral titer increased 4.6-fold than that of the recombinant virus with the wild-type PA at HA peak (Figure 5.1B and F). Similarly, when infected MDCK cells, the HA titer and the viral titer of 2 ma Ca/04:mPA(E59V):5WF10att increased 16 and 3.9-fold, respectively, compared with those of the virus with the wild-type PA (Figures 5.1C and G, and Figures 5.1 D and H).

We further confirmed the role of PA E59V on viral HA synthesis using western blot. MDCK cells were infected with either E59V or wt PA virus at MOI=0.1; the viral supernatants were collected every 4 h after infection up to 24 h. The expression level of HA (CA/04) and NS1 (WF10) were detected using western blot (Figure 5.2A-C). Densitometry results showed that NS1 could be detected as

early as 8 h.p.i. in E59V samples; while no signals could be detected from the wt PA samples at the same time point (Figure 5.2D and E). The strong HA signal could be detected in the E59V infected cell lysate from 12 h.p.i. (Figures 5.2C and D). The results suggested HA expression level was greatly up-regulated by PA E59V during the infection with live-attenuated virus.

The substitution of PA E59V increased mRNA, cRNA and vRNA level during early phase of infection in MDCK cells using strand-specific real-time RT-PCR

To investigate the role of PA E59V on viral RNA transcription and replication, we applied strand-specific real-time RT-PCR to evaluate the mRNA, cRNA and vRNA levels during early phase of infection; and selected HA and NP as the target genes for detection. The reverse transcription of HA (ma Ca/04) and NP (WF10) genes were performed with specific tagged primers “RT mRNAtag”, “RT vRNAtag” or “RT cRNAtag” (Table 5.4). The quantitative real-time PCR performed with specific primers “mRNAtag”, “vRNAtag” or “cRNAtag” which was reverse complement to the partial sequence of the tagged primer in the RT process, and the internal primers as listed (Table 5.4). The result showed: for HA gene, 2ma Ca/04:mPA(E59V):5WF10att increased the mRNA level 8- and 2.5-fold, and increased the vRNA level 9- and 4.3-fold at 9 and 13 h.p.i., respectively, compared to those of wt-PA virus at 9 and 13 h.p.i. (Figures 5.3A and B). Similarly, for the NP gene, at 9 and 13 h.p.i., 2ma Ca/04:mPA(E59V):5WF10att increased the mRNA level 6.5- and 2.5-fold and increased vRNA level 7.9 and 7.1-fold, respectively, compared to those of wt-PA virus (Figures 5.3D and E).

The substitution of PA E59V did not impair the temperature sensitive phenotype of the live-attenuated backbone

To study if PA E59V affects the temperature sensitive phenotype of WF10*att*, MDCK cells were infected with PA E59V or wt PA virus, and cultured at 35°C and 39°C. The kinetic curve of the viral replication suggested that the viral replication at 39°C was severely restricted, with viral titers reduced more than 1000-fold relative to those at 35°C (Figure 5.4), which indicated that the substitution E59V did not impair the temperature sensitive phenotype of the backbone.

The substitution of PA E59A had no effect on the viral replication of live-attenuated virus in egg embryos and MDCK cells

To investigate if position 59 on PA gene is critical to the viral replication in the live-attenuated viruses, we substituted this amino acid to alanine, and generated 2ma Ca/04:mPA(E59A):5WF10*att* (Table 5.1) using reverse genetics. The viral kinetics of live-attenuated viruses carrying PA 59V, 59E and 59A were compared in egg embryos and MDCK cells. However, no significant difference in HA or viral titer has been detected between the viruses with PA 59E and 59A during infection (Figure 5.5), which indicated that PA position 59 may not be the critical amino acid responsible for the viral RNA-dependent polymerase activity in the live-attenuated influenza viruses. Take together, PA 59V may contribute to a regulation mechanism which confers the attenuated backbone enhanced HA yield under the temperature sensitive phenotype.

The substitution of PA E59V moderate enhanced the HA titer of vaccines with WF10 and Ty/04att backbones; but had no effect in PR/8 and Ann Arbor backbones

To investigate if PA E59V has the effect of enhancing the HA and viral titers in other live-attenuated and inactivated influenza vaccine systems, we introduced this substitution into PA of wild-type WF10, PR8, *ca* Ann Arbor/60 and Ty/04att backbones (Table 5.1); and inoculated egg embryos and MDCK cells with the recombinant viruses. However, amongst those four systems, only wild-type WF10 and Ty/04att backbones with PA E59V displayed moderately enhanced HA and viral titers in egg embryos and MDCK cells (Figures 5.6A-D, and Figures 5.6E-H); while introducing of this substitution did not affect the HA titer of virus with PR8 or *ca* Ann Arbor/60 backbone in egg embryos (Figures 5.6I and K, and Figures 5.6J and L).

WF10att and wild-type WF10 backbones have higher HA/NP ratio than that of PR8 and Ann Arbor/60

To investigate if substitution PA E59V can cause the particles to incorporate more HA proteins into the live-attenuated virus, and to compare which vaccine backbone may include more HA content, we detected the HA and NP level of purified live-attenuated and inactivated viruses, and compared the HA/NP ratio of each virus. However, in the WF10att and wt-WF10 system, the result revealed that the introduction of E59V did not significantly increase the HA/NP ratio (Table 5.5). As the amount of NP is generally taken as a constant in a viral particle, the result indicated that E59V could not increase the number of HA molecules on the surface of the viral particle.

Interestingly, compared with HA/NP ratio of PR8 (3.27) and *ca* Ann Arbor/60 (3.86) system, WF10*att* and wt-WF10 has the HA/NP ratio more than 5.0 (Table 5.5), which suggested that these two system may incorporate more HA content than other two systems when produce recombinant vaccines. However, this experiment has been performed only once, and repeating is needed to confirm the result.

Discussion

The embryonated chicken eggs have been widely used for influenza vaccines production. However, the amplification of the human-like virus isolates, especially H1N1 and H3N2 subtype, generally showed low viral protein yield in eggs [262,353,354,355]. Several approaches are employed to improve the virus growth in eggs. To further serially pass in eggs is the most straightforward method to improve the viral growth [262,353,356,357]. For example, a live-attenuated vaccine strain against seasonal influenza H3N2 A/Fujian/411/02 was generated by reassorting the HA and NA segments of H3N2 virus with the internal segments of *ca* A/Ann Arbor/6/60. Inoculation of reassortant vaccine in chicken eggs resulted in poor replication. Three more passages in eggs dramatically increased the virus titer from $1.5 \log_{10}$ PFU/ml to $8.2 \log_{10}$ PFU/ml. Two amino acid substitutions in the HA (H183L and V226A) contribute to the improved virus replication in eggs, as well as the enhanced receptor-binding activity [357]. The first available candidate vaccine viruses against an A/California/7/2009-like virus, such as NIBRG-121 showed disappointingly low virus protein yield in eggs. The protein yield was greatly improved by serial passage of NIBRG-121 for ten more times. The substitution K119N in HA was indentified to be responsible for the enhanced HA and total protein

yield observed in the egg-adapted vaccine [353]. Propagating the virus in mammalian cells, isolating the large-morphology for the test of viral replication in eggs is also been applied to improve the vaccine virus replication in eggs. A live attenuated influenza virus A/California/7/9 (H1N1) vaccine strain carrying the HA and NA gene segments of the 2009 pandemic virus and the six internal gene segments of *ca* A/Ann Arbor/6/60 (H2N2) replicated poorly in chicken eggs. The reassortant viruses were propagated twice in MDCK cells with different MOI, and the supernatants were detected by plaque assay. The HA segments from the MDCK-passaged viruses with much larger size of the plaques were further sequenced. The results revealed that several amino acid substitutions were responsible for the enhanced viral replication in MDCK cells and eggs. However, only the substitutions at residues 119 and 186 did not change the antigenicity or immunogenicity of the virus [347].

The previously identified amino acid substitutions in HA which are responsible for the improved the viral growth in eggs can also be a good reference for the novel vaccine strain with the same subtype [347,356]. For example, the substitutions G186V and V226I or H183L and V226A in the HA have been discovered to contribute to the improved virus replication of live attenuated vaccine against seasonal influenza H3N2 A/Fujian/411/02 in eggs. Those substitutions were introduced into the HA of another H3N2 virus A/Singapore/21/04 by reverse genetics. The results showed that G186V also has the effect on enhancing the virus replication of this strain in eggs [356]. However, the vaccine strains needs to be further evaluated as the amino acid mutation(s) in HA after adaptation may appear on

the HA antigenic site or/and receptor binding site, affect the antigenicity and immunogenic of the vaccine, and protection efficacy [358,359].

In order to evaluate the live attenuated Influenza virus as a candidate to protect human and animals from the infection of newly emergent pH1N1 2009, our lab selected ma Ca/04 strain as an alternative to A/California//04/2009. This strain contains two mutations D131E and S186P on HA, which are responsible for the increased virulence for mice; and these two mutations were also found in increased human cases after 2009 ([350] and Ye et al, unpublished).

Our lab generated live attenuated influenza virus 2ma-Ca/04:6WF10*att* against pH1N1 2009 replicated poorly in eggs firstly. After passed the virus 7 more times in eggs, the virus had dramatic increased in HA titer. Interestingly, the whole genome sequencing result of the egg-adapted virus showed that the amino acid substitution did not appeared on the surface glycoprotein HA or NA, but on the internal gene PA: residue 59 mutated from glutamic acid to valine. We obtained the live attenuated WF10*att* virus contained this amino acid substitution using reverse genetics, and confirmed the effect of E59V on increasng the HA yeild and viral growth.

PA is the subunit of influenza virus RdRP heterotrimer, and characterized to be a type II restriction endonuclease in the crystal structure study. The function of PA residue 59 is unclear, but according to the crystal structure of PA_N, E59 is also coordinated with Mn1 and Mn2 from close molecule, which suggest that amino acid residue 59 may also related to the endonuclease activity.

The kinetic study in 35 and 39°C showed that PA E59V did not impair the temperature sensitive phenotype of live attenuated WF10att backbone. As the single mutation is on the internal gene, this mutation is not likely to affect the antigenicity and immunogenic.

The conventional real-time RT-PCR approach performed with the strand-specific primers, and generally showed low specificity. In contrast, the novel strand-specific reverse transcription method developed recently greatly improved the product specificity using tagged primers to add a 18-20 nucleotides “tag” on the 5'-end which is not related to influenza sequences [360]. We selected canine 18S rRNA as the reference gene (internal control) for the normalization of real-time RT PCR data, as compared with other tested housekeeping genes, 18S rRNA was the most stable in the influenza virus infected cells [361]. To generate the viral RNA synthesis profiles during infection, we applied this tagged primer strand-specific real-time PCR method. The results showed, both viral mRNA transcription level and vRNA replication level were significantly up-regulated in HA and NP genes by the substitution of PA E59V at the early phase of infection; which indicated that this mutation enhanced RdRP activity of the live attenuate WF10att vaccine when carrying the pH1N1 2009 surface glycoprotein.

However, the alignment of PA genes from different subtypes of Influenza viruses displayed that glutamic acid at residue 59 is highly conserved in most of the virus strains, and PA E59V substitution did not enhance the HA and viral titers in PR8 and *ca* Ann Arbor/60 backbones. In another experiment, the replacement of PA residue 59 into alanine did not affect the viral replication of the WF10att virus in eggs

and MDCK cells. All together, the amino acid substitution of E59V on PA gene is the result of viral adaptation under the selection stress of embryonated chicken eggs; this substitution could be backbone-specific, not critical to the RdRP activity, but confer the live attenuated system enhanced HA yeild and better viral growth without imparing the temperature sensitive phenotype of WF10*att*. The substitution PA E59V also confer WF10*att* backbone higher capbility to replicate better in eggs with the glycoprotein derived from human-like influenza virus.

To compare the HA yield and viral growth of pH1N1 2009 vaccines with different backbone systems, as well as to investigate if the substitution of PA E59V could cause the viral particle to incorporate more HA molecules on the surface, we purified and concentrated the viruses in this study and then determined the HA titer, viral titer and HA/NP ratio of each virus. In the live attenuated vaccine group, WF10*att* backbone with PA E59V mutation achieved the best HA titer (4096) and viral titer (5.6×10^9); while in the inactivated vaccine group, PR8 system obtained the highest HA titer (4096) and viral titer (1.8×10^{10}) (Table 5.5). Unlike our hypothesis, PA E59V did not provide higher HA/NP ratio in either WF10*att* or wt WF10 systems, which indicated E59V could not increase the number of HA molecules on the surface since the amount of NP is generally unchanged in a viral particle. Interestingly, we found the HA/NP ratios of WF10*att* wt WF10 are more than 5.0, which are much higher than that of PR8 or *ca* Ann Arbor/60 systems (Table 5.5). HA is the most important antigen to elicit the neutralization antibody in the host immune response. The live attenuated vaccine system WF10*att* which was developed by our lab may be

proved to be valuable to contain more antigen content from embryonated chicken eggs and mammalian cells.

I also planned to study the mechanism of PA E59V on HA and viral titer promotion using the endonuclease activity assay. I cloned N-terminal 210 amino acids of WF10 mPA (E59V) and wt-PA into pET-15b vector. However, the expression of PA-Nter in BL-21 *E.coli* was not successful. After pre-culture, the bacteria strains were inoculated 1:50 into 5 ml of LB media. I tried culture at 37°C for 5-8 h or at room temperature (around 25°C) for overnight until the OD₆₀₀ was 0.4~0.7. The induction of protein express was carried out by the addition of 0.2, 0.5 or 1.0 mM Isopropyl β-D-1-thiogalactopyranoside (IPTG) into the media. The bacteria were harvested at 6 and 12 h after induction, and the expression of the protein was detected using SDS-PAGE gel. However, compared with blank plasmid, no extra band has been found around the molecular weight 33 kDa (PA-Nter). Other conditions, such as culturing at 16°C or inducing with 2.0 mM IPTG should be try to optimize the protein expression.

Table 5.1. Gene constellations of recombinant viruses used in this study.

Virus	HA and NA	Internal Genes (PB1, PB2, NP, M and NS)	PA
2ma Ca/04: 6WF10 <i>att</i>	mouse-adapted Ca/04 H1and N1	WF10 <i>att</i>	PA (WF10 <i>att</i>)
2ma Ca/04:mPA(E59V):5WF10 <i>att</i>	mouse-adapted Ca/04 H1and N1	WF10 <i>att</i>	PA E59V (WF10 <i>att</i>)
2ma Ca/04: 6WF10	mouse-adapted Ca/04 H1and N1	WF10	PA (WF10)
2ma Ca/04:mPA(E59V):5WF10	mouse-adapted Ca/04 H1and N1	WF10	PA E59V (WF10)
2ma Ca/04: 6PR8	mouse-adapted Ca/04 H1and N1	PR8	PA (PR8)
2ma Ca/04:mPA(E59V):5PR8	mouse-adapted Ca/04 H1and N1	PR8	PA E59V (PR8)
2ma Ca/04: 6 <i>ca</i> Ann Arbor	mouse-adapted Ca/04 H1and N1	<i>ca</i> Ann Arbor	PA (<i>ca</i> Ann Arbor)
2ma Ca/04:mPA(E59V):5 <i>ca</i> Ann Arbor	mouse-adapted Ca/04 H1and N1	<i>ca</i> Ann Arbor	PA E59V (<i>ca</i> Ann Arbor)
2ma Ca/04: 6Ty/04 <i>att</i>	mouse-adapted Ca/04 H1and N1	Ty/04 <i>att</i>	PA (Ty/04 <i>att</i>)
2ma Ca/04:mPA(E59V):5Ty/04 <i>att</i>	mouse-adapted Ca/04 H1and N1	Ty/04 <i>att</i>	PA E59V (Ty/04 <i>att</i>)
2ma Ca/04:mPA(E59A):5WF10 <i>att</i>	mouse-adapted Ca/04 H1and N1	WF10 <i>att</i>	PA E59A (WF10 <i>att</i>)

Table 5.2. Enhanced HA titers after serially propagated recombinant influenza virus ma-CA/04 H1N1:6WF10att in egg embryos.

Passage	HA Titer (log2)	Mean±standard error of the mean
1	5, 4, 3, 5, 5	4.40 ±0.40
2	5, 5, 5, 5, 6	5.20±0.20
3	6, 3, 7, 8, 7, 7	6.33±0.72
4	9, 6, 7, 7, 6	7.00±0.55
5	8, 9, 9, 9, 8	8.60±0.25
6	9, 9, 8, 11, 9, 6, 8	8.57±0.57
7	11, 9, 11, 9	10.00±0.58
8	10, 11, 8, 11, 10, 10, 10	10.00±0.38

Table 5.3. The nucleotide changes in the genes of P8 virus.

Gene	Nucleotide position	Nucleotide change	Amino acid	Synonymous or non-synonymous mutations
PA	215	A → T/A	Glu → Val/Glu	Non-synonymous
	495	A → A/T/C	Gly → Gly	Synonymous
	2061	A → A/T	Leu → Leu	Synonymous
PB2	1162	C → C/T	Leu → Leu	Synonymous
	1302	C → T/C	Phe → Phe	Synonymous

Table 5.4. The primer sets for strand-specific real-time RT-PCR using tagged primers for quantification of the vRNA, cRNA, and mRNA of HA and NP of 2 mouse-adapted(ma) Ca/04 H1N1:6WF10att

Target	RNA	Purpose	Primer name	Sequence (5'-3')	Position (nt)
Segment 4 HA (ma Ca/04)	vRNA	RT	vRNAtag-Ca/04HA-884F	GGCCGTCATGGTGGCGAAT CAGATACACCAGTCCACCGATTGC	884-907
		Real-time PCR	vRNAtag	GGCCGTCATGGTGGCGAAT	
	cRNA	RT	Ca/04HA-968R	GTATATTCTGAAATGGGAGGCTG	968-946
		Real-time PCR	cRNAtag-Ca/04HA-1743R	GCTAGCTTCAGCTAGGCATC AGTAGAAAACAAGGGTGTTTTCTC	1776-1743
Segment 5 NP (WF10)	mRNA	RT	cRNAtag	GCTAGCTTCAGCTAGGCATC	1681-1713
		Real-time PCR	Ca/04HA-1681F	CAGTTTCTGGATGTGCTCTAATG	1760-1744
		RT	mRNAtag-Ca/04-1760R	CCAGATCGTTCGAGTCGTTTTTTTTTTTTTCTCATGCTTCTG	
	vRNA	Real-time PCR	mRNAtag	CCAGATCGTTCGAGTCGT	1681-1713
		RT	Ca/04-1681F	CAGTTTCTGGATGTGCTCTAATG	740-763
		Real-time PCR	vRNAtag-WF10NP-740F	GGCCGTCATGGTGGCGAAT CAGCAGCACAAAAGAGCAATGATGG	
cRNA	RT	vRNAtag	GGCCGTCATGGTGGCGAAT	847-824	
	Real-time PCR	WF10NP-847R	CTCTCAGGATGAGTGCAGACCGTG	1565-1541	
	RT	cRNAtag-WF10NP-1565R	GCTAGCTTCAGCTAGGCATCAGTAGAAAACAAGGGTGTTTTCTTC		
	Real-time PCR	cRNAtag	GCTAGCTTCAGCTAGGCATC		
mRNA	RT	WF10NP-1466F	CGATCGTGCCTCCCTTTG	1466-1483	
	Real-time PCR	mRNAtag-WF10NP-1549R	CCAGATCGTTCGAGTCGTTTTTTTTTTTTTCTCAATTGTC	1549-1534	
mRNA	RT	mRNAtag	CCAGATCGTTCGAGTCGT	1466-1483	
	Real-time PCR	WF10NP-1466F	CGATCGTGCCTCCCTTTG		

Table 5.5. The comparison of HA to NP ratios of the pH1N1 vaccines with different internal backbones

Category of the viruses	Virus	HA titer of	TCID50	EID50
Live-attenuated vaccine	ma-Ca/04 H1N1: mPA:5WF10 <i>att</i>	4096	5.0×10^7	5.6×10^9
	ma-Ca/04 H1N1: 6WF10 <i>att</i>	256	2.3×10^6	3.2×10^8
	ma-Ca/04 H1N1: 6ca Ann Arbor	128	5.6×10^5	3.2×10^7
Inactivated vaccine	ma-Ca/04 H1N1: mPA:5WF10	4096	5.0×10^7	5.6×10^9
	ma-Ca/04 H1N1: 6WF10	2048	2.3×10^7	3.2×10^9
	ma-Ca/04 H1N1: 6PR/8	4096	1.6×10^8	1.8×10^{10}

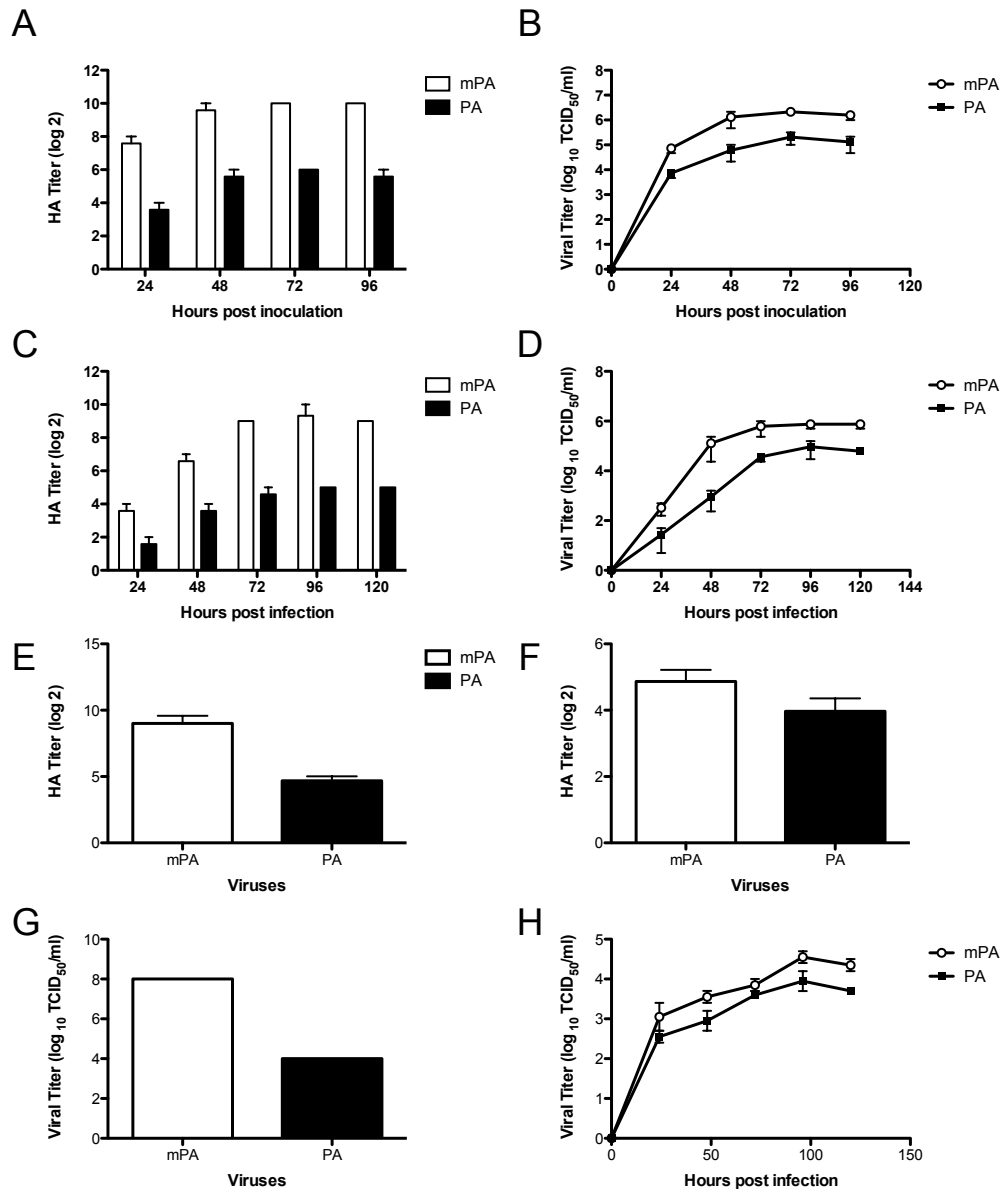
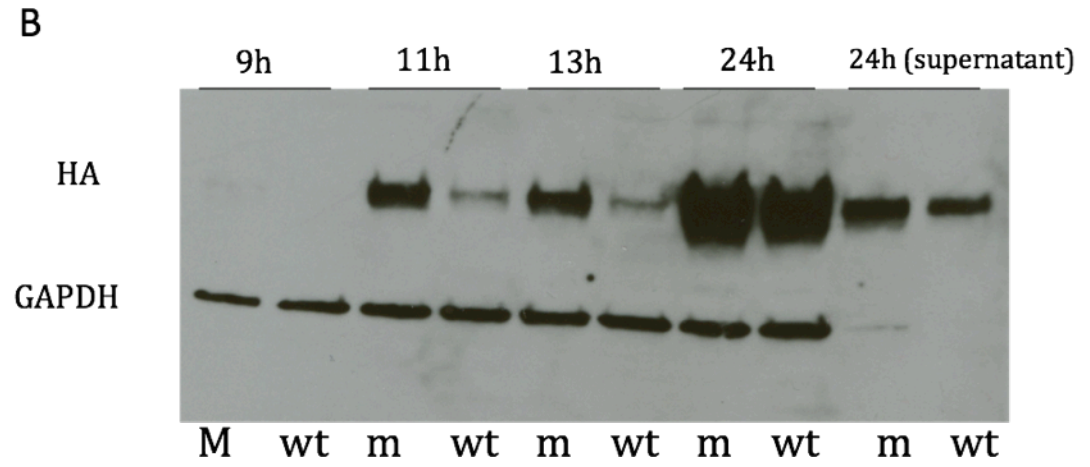
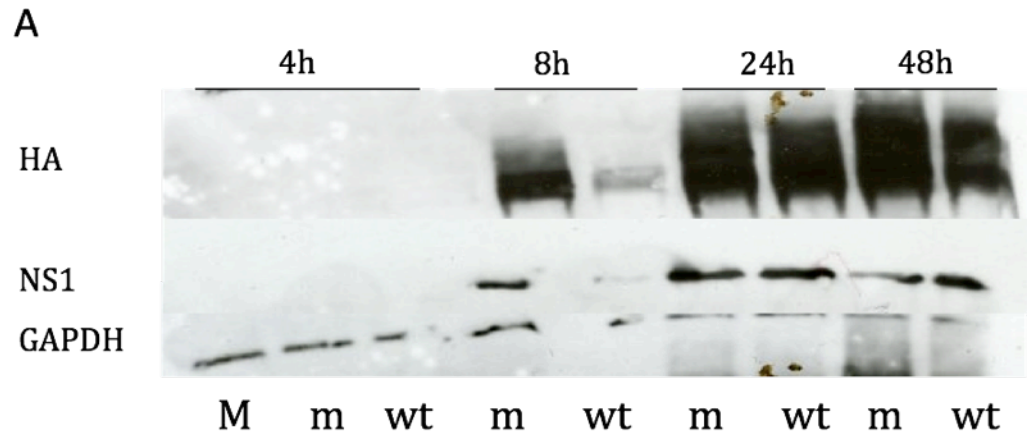


Figure 5.1. Comparison of the HA and viral titers of mPA (E59V) and wt-PA viruses in 10-day-old embryonated eggs and MDCK cells. 100 TCID₅₀ of the viruses were inoculated in 10-day-old embryonated eggs and the HA titers of the allantoic fluid were detected every 24 hpi (A), or (E) at 4 d.p.i., and the viral titers of the samples were detected using TCID₅₀ method in MDCK cells (B and F). MDCK cells were infected with the viruses at MOI=0.005. The HA titers of the supernatants were detected at 24, 48, 72, 96 and 120 hpi (C) or at 96 h.p.i (G), and the viral titers of the samples were detected using TCID₅₀ method in MDCK cells (D and H).



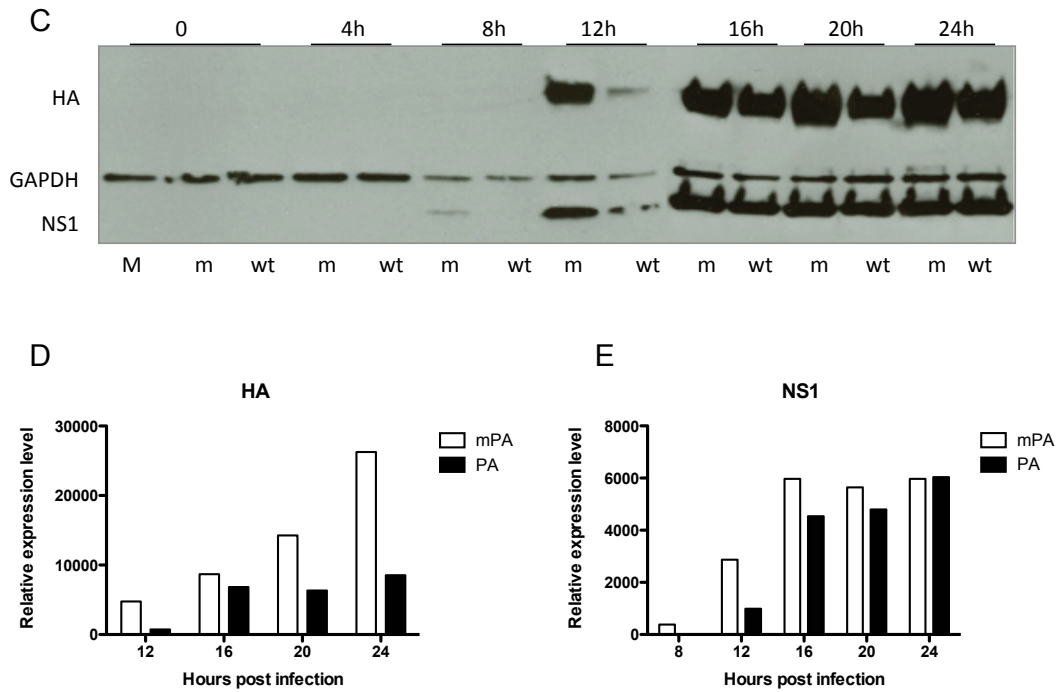
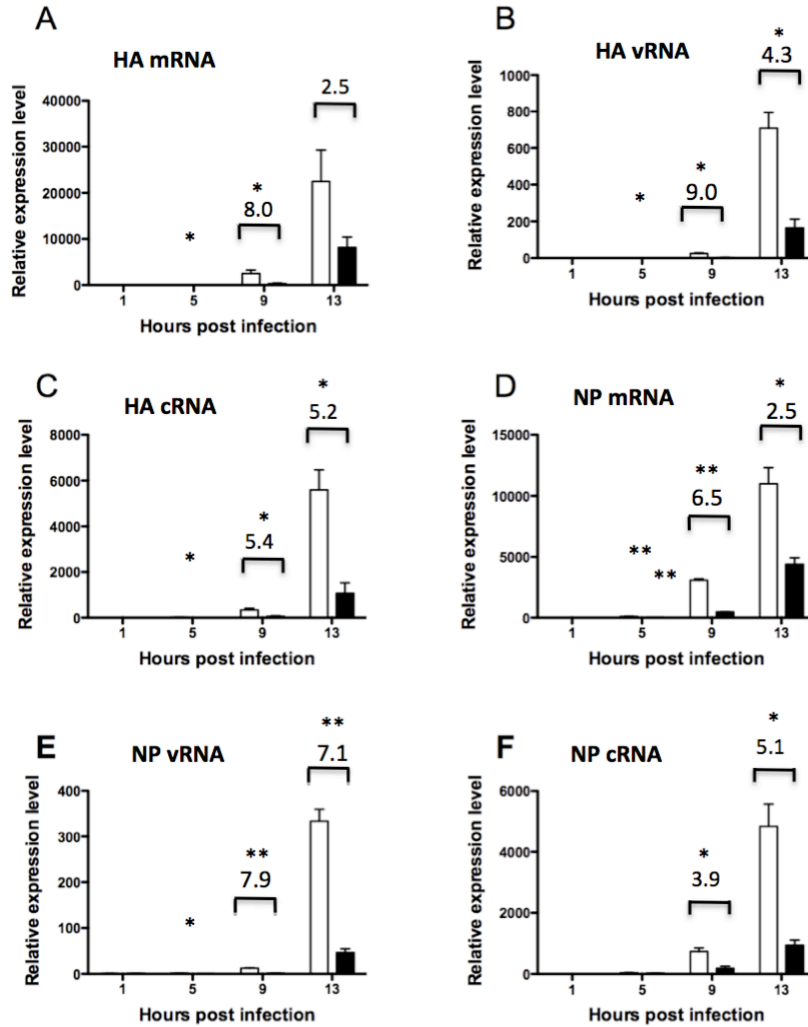


Figure 5.2. Comparison of the viral protein: HA and NS1 synthesis level in MDCK cells during infection. MDCK cell were infected with 2ma-Ca/04 H1N1:mPA (E59V):5WF10att (m) or 2ma-Ca/04 H1N1:6WF10att (wt) at MOI=0.1. The protein synthesis levels of HA and NS1 were detected (A) at 4, 8, 24 and 48 h.p.i; (B) at 9, 11, 13, and 24 h.p.i; and (C) at 4,8,12,16,20 and 24 h.p.i. using western blot. Cells were mock (M) infected with PBS. The protein synthesis levels of the HA (D) and NS1 (E) in (C) were quantitative by densitometry, and the relative expression levels were showed.



* indicates a P-value < 0.05, ** indicates a P-value < 0.005.

Figure 5.3. Evaluation of HA and NP viral mRNA, cRNA and vRNA level at early phase of infection in MDCK cells at different time points using RT real-time PCR. MDCK cells were infected with 2ma-Ca/04 H1N1:mPA (E59V):5WF10att and 2ma-Ca/04 H1N1:6WF10att. The cell samples were harvested at 1, 5, 9 and 13 h.p.i. The viral RNA expression levels of HA and NP were detected by using influenza virus segment specific tagged primers. The relative mRNA (A), vRNA (B) and cRNA (C) levels of the HA, and the relative mRNA (D), vRNA (E) and cRNA (F) levels of the NP were calculated by comparing the expression level of mPA samples to that of wt-PA samples at the same time point.

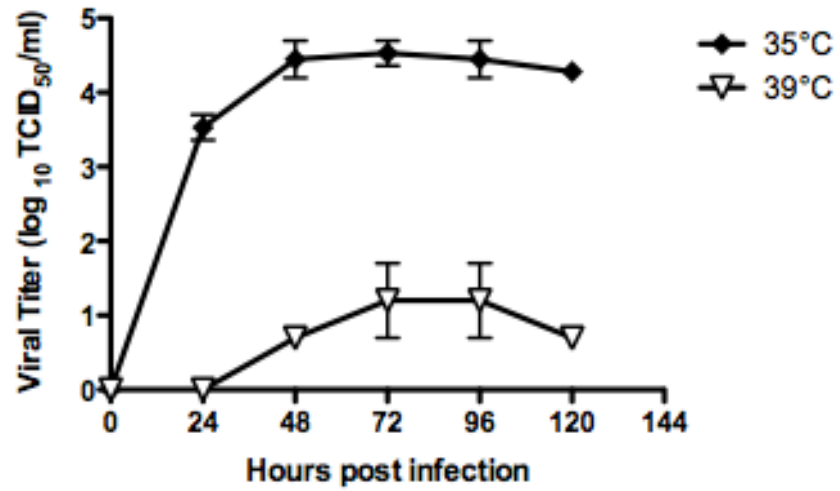


Figure 5.4. Viral replication kinetics of the live-attenuated viruses in MDCK cells at 35°C and 39°C using MOI of 0.001. Viral titers at different time points were determined by TCID₅₀.

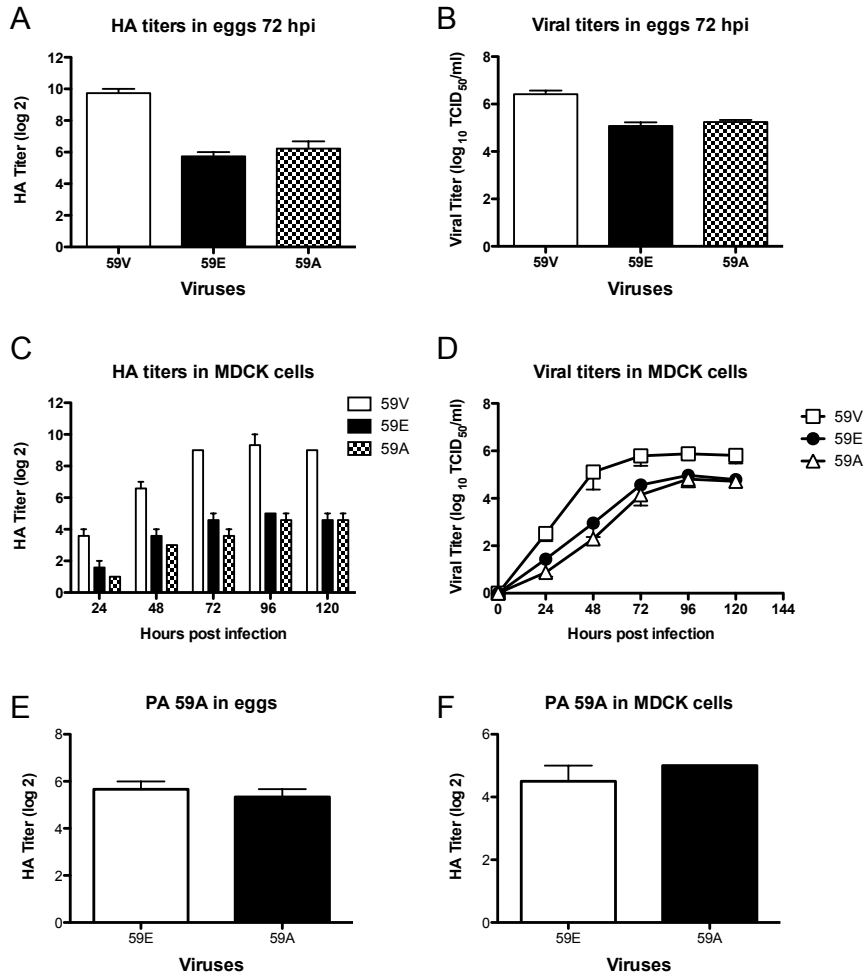


Figure 5.5. The comparison of live-attenuated viruses of PA 59A with 59E and 59V in egg embryos and MDCK cells. 100 TCID₅₀ of the viruses were inoculated in 10-day-old eggs and the HA titers of the allantoic fluid were detected at 3 d.p.i. (A), and the viral titers were detected using TCID₅₀ method in MDCK cells (B). MDCK cells were infected with the viruses at MOI=0.01. The HA titers of the supernatants were detected at 24, 48, 72, 96 and 120 h.p.i. (C), and the viral titers were detected using TCID₅₀ method in MDCK cells (D). The virus replications of PA 59E and 59A were also compared (E) in eggs by inoculated with 100 TCID₅₀ of the virus and (F) in MDCK cells by infected with the virus at MOI=0.01. The peak HA titers of the viruses in eggs and MDCK cells were showed.

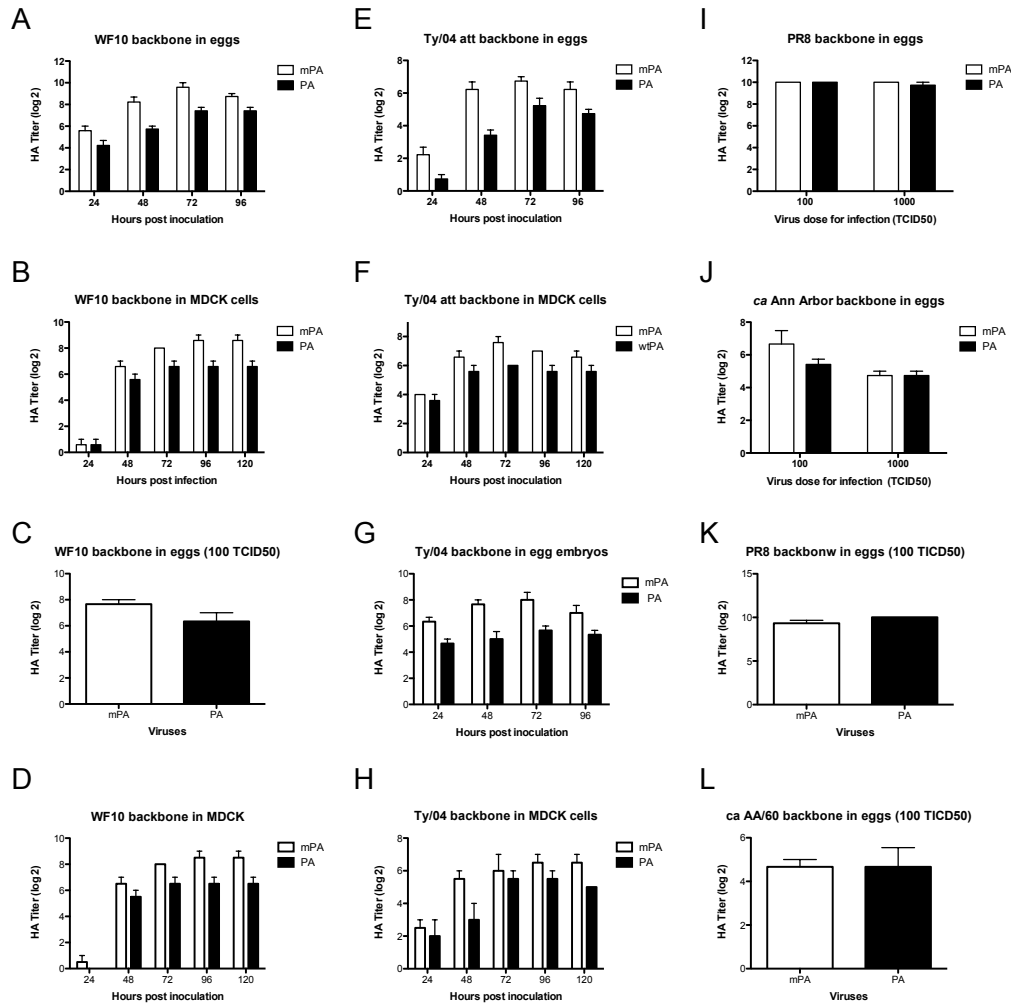


Figure 5.6. Evaluation of the effect of PA amino acid 59 substitution on WF10, Ty/04att, PR8 and *ca* Ann Arbor/60 internal backbones. (A) and (C) 100 TCID₅₀ of the virus 2ma Ca/04 H1N1:mPA(E59V):5WF10 or 2ma Ca/04 H1N1: 6WF10, or (E) and (G) 2ma Ca/04 H1N1: 6Ty/04att or 2ma Ca/04 H1N1:mPA(E59V):5Ty/04att were inoculated in 10-day-old eggs and the HA titers of the allantoic fluid were detected every 24 h.p.i. MDCK cells were infected with the viruses of (B) and (D) WF10 or (F) and (H) Ty/04att backbones at MOI=0.005 and the HA titers of the supernatants were detected at 24, 48, 72, 96 and 120 h.p.i. (I) and (K) 100 TCID₅₀ of the virus 2ma Ca/04 H1N1:mPA(E59V):5PR8 or 2ma Ca/04 H1N1: 6PR8, and (J) and (L) 2maCa/04 H1N1:mPA(E59V):5*ca* Ann Arbor/60 or 2maCa/04 H1N1: 6*ca* Ann Arbor/60 were inoculated in 10-day-old eggs and the HA titers of the allantoic fluid were detected every 24 h.p.i.

Chapter 6: Cytoplasmic Accumulation of NS1 Enhances the Viral Replication and Anti-apoptotic activity of an Avian Influenza Virus (H9N2)

Abstract

To better understand the molecular mechanism of the adaptation and interspecies transmission of influenza viruses, our lab previously generated two adapted viruses from wildtype duck H9N2, A/duck/Hong Kong/702/79 (WT702) virus, through 23 serial passages in lung of quail, and followed by 10 serial passages in the chickens. The quail-adapted virus is named as QA23, and the virus further adapted in chickens is named as QA23CkA10. QA23CkA10 gained the new phenotype of replicating and transmitting efficiently in both chickens and quail. And more importantly, both QA23 and QA23Ck10, unlike WT702, were able to infect mice without any further adaptation. We were particularly interested in the mutated NS1 gene of QA23, as NS1 has multiple functions, such as antagonizing host immune responses during viral infection. Three amino acid substitutions M106T, K217E and K219E were identified in QA23 NS1 as well as QA23Ck10 NS1. The localization study and the nuclear and cytoplasmic protein distribution assay demonstrated that QA23 NS1 mainly accumulated in the cytoplasm; in contrast, WT702 NS1 predominantly accumulated in the nucleus. In this H9N2 influenza virus strain, residue 219 played the critical role on the nucleus importing of NS1, and nuclear localization sequence 2 (NLS2) is the major import

signal instead of NLS1. Minigenome assay in DF1 cells demonstrated that QA23 NS1 up-regulated the viral protein synthesis. The enhanced cytoplasmic accumulation of QA23 NS1 did not affect the inhibition of IFN- β , while the apoptotic activity level of the cell was greatly reduced during the infection. However, the mutated NS1 did not affect the virus replication and transmission in Japanese quail. Take together, the increased cytoplasmic accumulation of NS1 may enhance the viral replication and reduce apoptotic activity in the host cells.

Introduction

NS1 protein contains 230-237 amino acids, depending on the strains, and has a molecular weight around 26 kDa. According to the biological function, NS1 can be divided into the N-terminal (residues 1-73) RNA-binding domain (RBD) and C-terminal (residues 84-207) effector domain (ED), which are connected by a linker. The structure of the 20 amino acids on the C-terminal domain may be naturally disordered.

The structures of RBD domain and ED domain, and the locations and key residues of NLS1, NLS2, NES and NoLS have been discussed in Chapter 1 and 3. One of the major functions of NS1 is to antagonize the innate immune response of the host during influenza infection, especially to limit the production of interferon beta (IFN- β) induction by interacting with multiple host factors, such as CPSF30, PABPII, RIG I, TRAM25, OSA and PKR (discussed in Chapter 1 and 3).

To our notice, several important functions of NS1, such as the PDZ domain-binding and the activation of PI3K pathway, appear to be strain-specific.

Some of those functions are associated with the virulence of the influenza virus. I summarized the strain-specific functions of NS1 from the references, and listed in Table 1.2.

The nucleus/cytoplasm accumulation pattern of NS1 may affect its interaction with the host factors, because some host factors distribute only in the nuclear or cytoplasm. For example, compared to the NS1 of its low pathogenic precursor H7N1 (A/chicken/Italy/1082/99), the NS1 of the highly pathogenic H7N1 (A/ostrich/Italy/984/00) carried two mutations in NES, and a 6-amino acid truncation at the C-terminus resulted from the third mutation. The cytoplasmic accumulation of NS1 is responsible for the enhanced pathogenicity of this HP H7N1 strain [199].

Our lab previously generated two adapted viruses QA23 and QA23CkA10 from a wildtype duck H9N2 (WT702) virus. Both viruses gained the new phenotype of replicating and transmitting efficiently in both chickens and quail, and directly infecting mice. These two viruses also showed faster growth kinetics in MDCK and CEK cells [98]. The comparison of the deduced amino acid sequences from the ORF of QA23, QA23Ck10 and WT702 revealed that 14 and 17 amino acid substitutions and throughout the viral genome and a 21-amino acid deletion in NA in the adapted viruses QA23 and QA23Ck10 compared with WT702 [98]. Of particular interest, however, were the amino acid mutations on NS1, as NS1 is one of the most important pathogenesis factors and has multiple functions during viral infection. Three amino acid substitutions were identified in QA23 NS1 as well as QA23Ck10 NS1: M106T, K217E and K219E. NS1 protein

localization study using Immunofluorescence assay and dissociation of nuclear and cytoplasmic fractions displayed that QA23 NS1 predominantly accumulated in the cytoplasm; in contrast, WT702 NS1 predominantly distributed in the nucleus. Residue 219 played the critical role on the nucleus importing of NS1, and nuclear localization sequence 2 (NLS2) is the major signal instead of NLS1. Minigenome assay in DF1 cells demonstrated that QA23 NS1 up-regulated the viral protein synthesis. The enhanced cytoplasmic accumulation of QA23 NS1 did not affect the inhibition of IFN- β , while the apoptotic activity level was greatly reduced during the early phase of the infection. However, there is no evidence showing that QA23 NS1 is associated with the enhanced replication and transmission of the virus in quail. Take together, the increased cytoplasmic accumulation of NS1 may enhance the viral replication and reduce apoptotic activity in the host cells.

Materials and methods

Virus, plasmid and cells

The A/Duck/Hong Kong/702/79 (H9N2) virus (WT702) was kindly provided by Dr. Robert G. Webster, St. Jude Children's Research Hospital, Memphis, TN. The quail-adapted (QA23) virus was generated and isolated as previously described [98]. The virus stocks were prepared in specific pathogen free 9-day old embryonated chickens eggs following standard techniques for growth of influenza viruses. The RG 8-plasmid system for the WT702 and QA23 virus were cloned into the pDP2002 vector (Hickman et al, unpublished). MDCK,

A549 and HeLa cells, as well as DF1 cells, MDCK cells were maintained in Modified Eagle's medium (MEM) (Sigma-Aldrich, St. Louis, MO) containing 10% fetal bovine serum (FBS) (Sigma-Aldrich). Human embryonic kidney cell-line 293T (HEK293T) were cultured in Opti-MEM I (GIBCO, Grand Island, NY) containing 5% FBS.

The green fluorescence protein eGFP-NS1 fusion plasmids were constructed as following: the amplified full-length of WT702 and QA23 NS1 gene were digested with PstI and BamHI, and cloned into pEGFP-C1 expression vector (Clontech, Mountain View, CA) digested with identical enzymes. The C-terminus of the eGFP protein is connected with the N-terminus of the NS1.

All mutations were introduced using the QuickChange II site-directed mutagenesis kit (Stratagene, Inc., La Jolla, CA) according to manufacturer's protocols with the specific primers. The presence of each mutation was confirmed by sequencing.

Generation of recombinant virus by reverse genetics

The recombinant viruses were generated using the 8-plasmid system in co-cultured 293T and MDCK cells as described previously [254]. All recombinant viruses were propagated in 10-day-old embryonated eggs, titrated by TCID₅₀, and stored at -70°C until use. All viruses were sequenced using specific primers.

Sequence analysis

The cDNA of the virus was prepared as previously described [254]; the specific fragment was amplified and sequenced using a combination of universal and custom made primers (available upon request, see Appendices). Sequencing

was performed using the Big Dye Terminator v3.1 Cycle Sequencing kit (Applied Biosystems, Foster City, CA) on a 3100 Genetic Analyzer (Applied Biosystems, Foster City, CA) according to the manufacturer's instructions.

Immunofluorescence assay

For the eGFP-NS1 fusion protein localization, 293T, MDCK, A549 and DF1 cells were seeded on glass coverslips overnight. 200ng of eGFP-NS1 plasmid was incubate with 3.6 μ l TransIT LT-1 (Mirus, Madison, WI) at room temperature for 45 min, and then the mixture was transfected into the cells. 8 h later, the DNA-transfection mixture was replaced by Opti-MEM I. At 24 h post transfection, the cells were fixed with 4% paraformaldehyde solution, washed with PBS, incubated with 0.2% Triton X-100 in PBS. After further washes with PBS, cells were incubated with 4',6-diamidino-2-phenylindole (DAPI ; 1 mg /ml; Thermo Scientific, West Palm Beach, FL), and processed for immunofluorescence microscopy using a Zeiss SM510 confocal microscope (Carl Zeiss Microscopy, Thornwood, NY).

For the immunostaining assay, DF1 cells were seeded in Nunc Lab-Tek II chamber slides (Thermo Scientific, West Palm Beach, FL) overnight, and infected with virus WT702 or QA23 NS:7WT702 at MOI=1. At 9 h.p.i., cells were fixed with 4% paraformaldehyde solution, washed with PBS, incubated with 0.2% Triton X-100 in PBS, and blocked with 5% bovine serum albumin (BSA). Incubation with primary mouse NS1 monoclonal antibodies (Clone NS1-1A7 (from NIH (1:250)) was followed by incubation with goat anti-mouse-fluorescein

isothiocyanate (FITC) -labeled secondary antibody (Southern Biotech, Birmingham, AL (1:5000)). Cells were visualized using a Zeiss SM510 confocal microscope (Carl Zeiss Microscopy, Thornwood, NY).

Dissociation of nuclear and cytoplasmic fractions

MDCK cells were seeded in 6-well plate to 80% confluence and infected with recombinant virus WT702 or QA23 NS:7WT702 at MOI=1, and harvested the cell at 8 and 24 h.p.i. using Trypsin-EDTA solution (Sigma-Aldrich, St. Louis, MO). The nuclear and cytoplasmic fractions were separated using the NE-PER Nuclear and Cytoplasmic Extraction kit (Thermo Scientific, West Palm Beach, FL) according to the manufacturer's protocol. Added 200 μ l of ice-cold CER I to the cell pellet, and resuspended. Incubated the tube on ice for 10 min. 11 μ l of ice-cold CER II was added to the tube. Vortexed and incubated the tube on ice for 1 min. The tube was spin down at 16,000xg for 5 min and transferred the supernatant (cytoplasmic extract) fraction to a new tube. The insoluble (pellet) fraction was resuspended in 100 μ l of ice-cold NER. The sample was kept on ice and continue vortexed for 15 s every 10 min, for a total of 40 min. Spin down the tube at 16,000xg for 10 min, and immediately transfer the supernatant (nuclear extract) fraction to a new tube.

The samples were added 50 μ l of 2x Laemmli Sample Buffer (Bio-Rad, Hercules, CA) containing 50 μ l β -mercaptoethanol (Fisher Scientific, Waltham, MA)/ml, heated at 100°C for 5 min, and then loaded into a Mini-PROTEAN TGX Precast Gel (Bio-Rad, Hercules, CA). The gel was run for 60 min at 150 V using PowerPac basic power supply (Bio-Rad, Hercules, CA). Then the protein samples

were transferred into supported nitrocellulose membrane (Bio-Rad, Hercules, CA) at 18 V for 45 min using Trans-Blot SD System and PowerPac HC Power Supply System (Bio-Rad, Hercules, CA). The NS1 expression were detected with the Clone NS1-1A7 (from NIH (1:500)) as the primary antibody, and then with HRP-conjugated goat anti-mouse IgG (SouthernBiotech, Birmingham, Alabama (1:5000)) as the secondary antibody. The image was developed using SuperSignal West Pico chemiluminescent substrate (Fisher Scientific, Waltham, MA). The image was scanned and the optical density of each sample was quantitated using densitometry software Quantity One version 4.6.5 (Bio-Rad, Hercules, CA), and then the relative amount of the proteins were further calculated. GAPDH was taken as the cellular internal control.

Minigenome assay

The minigenome assay was performed as described previously [351]. 200 ng of the plasmid pMACK-GLuc encoding the influenza virus-like NS vRNA carrying the GaussiaLuciferase (GLuc) reporter gene and chicken polymerase I promoter (Poli) was transfected in DF1 cells along with 200 ng of plasmids encoding WT702 PB1, PB2, PA, NP and QA23 or WT702 NS or NS1 (only) using the TransIT-LT1 (Mirus, Madison, WI) reagent. The SEAP plasmid, which expresses the secreted alkaline phosphatase, was co-transfected into cells to normalize the transfection efficiency. The supernatants were collected at 24, 48 and 72 h post transfection, and luciferase and secreted alkaline phosphatase activities were detected from 25 μ l of the samples using the BioLux Gaussia Luciferase Assay Kit (NEB, Ipswich, MA) and the Phospha-Light Secreted

Alkaline Phosphatase Reporter Gene Assay System (A&D, FosterCity, CA) according to the manufacturers' instructions. Relative polymerase activity was calculated as the ratio of luciferase to SEAP luminescence. Two independent experiments were performed in duplicate. The statistical analyses were performed with GraphPad Prism software version 5.0c (GraphPad Software Inc., San Diego, CA). The multiple comparisons were performed by analysis of variance (ANOVA) with Tukey's multiple comparison test.

IFN- β ELISA

Beta interferon (IFN- β) expression level in mammalian and avian cells were detected using Dog/Canine Interferon Beta INF-Beta ELISA Kit (Novateinbio, Woburn, MA), and Chicken Interferon β , IFN- β /IFNB ELISA Kit (Novateinbio, Woburn, MA), respectively, according to the manufacturer's protocol. Confluent MDCK and DF1 cells in 12-well plates were infected with the recombinant viruses at MOI=0.1, and at 12, 24 and 48 h.p.i., 10 μ l of supernatant diluted in 40 μ l of Sample Diluent or 50 μ l standards were added to 96-well plates, and then add 50 μ l horseradish peroxidase (HRP)-labeled IFN- β antibody and incubated for at 37°C 30 min. After 5 washes, the 50 μ l chromogenic Substrate A and 50 μ l chromogenic Substrate B solution were added to develop the color, and incubated at 37°C for 15 min. 50 μ l of Stop Solution was added immediately to each well to stop the reaction. The optical density was measured at 450 nm (OD₄₅₀). Cells transfected with Poly(I:C) (InvivoGen, San Diego, California) or infected with inactivated virus were taken as the positive control in these two assays, respectively.

Apoptosis Assay

The terminal deoxynucleotidyltransferase-mediated dUTP-biotin nick-end-labeling (TUNEL) staining for apoptotic nuclei was carried out using the DeadEnd colorimetric TUNEL kit (Promega, Madison, WI) according to the instructions of the manufacturer. A549 and HeLa cells were infected with recombinant virus WT702 or QA23 NS:7WT702 at MOI=1. At 16 h.p.i., the cells were fixed in 4% paraformaldehyde and incubated with 0.2% Triton X-100 in PBS. Labeling reactions were performed with 100 μ l of TdT reaction mix for 1h at 37°C in a humidified chamber. After washed with PBS, cells were incubated with 100 μ l Streptavidin HRP at room temperature for 30 min. The Color development was accomplished with diaminobenzidine (DAB) for 7 min. The image of stained positively apoptotic nuclei was captured using a Zeiss Axiovert 200M (Carl Zeiss Microscopy, Thornwood, NY, USA). Apoptosis was evaluated as the average number of positively stained cells per field at high-power magnification (\times 400). The cells added Staurosporine reagent (0.2 μ M; Sigma-Aldrich, St. Louis, MO) was taken as the positive control.

To determine the role of QA23 NS1 on regulation the cellular apoptotic activity, the Akt and phosphorylated Akt levels were detected in HeLa cells infected with the viruses carrying either QA23 or WT702 NS1. HeLa cells were seeded in 6-well plate overnight, and then starved the cells by culturing with non-serum media for 24 h. The cells were infected with viruses QA23 NS:7WT702 or WT702 at MOI=0.1. The cells were harvested at 12, 24 and 36 h.p.i by adding 250 μ l of 2x Laemmli Sample Buffer (Bio-Rad, Hercules, CA) containing 50 μ l

β -mercaptoethanol (Fisher Scientific, Waltham, MA) and 10 μ l sodium fluoride (BioLabs, Ipswich, MA) /ml. The samples were heated at 100°C for 5 min and sonicated for 20 sec, and then 20 μ l of the samples were loaded into a Mini-PROTEAN TGX Precast Gel (Bio-Rad, Hercules, CA). The gel was run for 60 min at 150 V using PowerPac basic power supply (Bio-Rad, Hercules, CA). Then the protein samples were transferred into supported nitrocellulose membrane (Bio-Rad, Hercules, CA) at 18 V for 45 min using Trans-Blot SD System and PowerPac HC Power Supply System (Bio-Rad, Hercules, CA). The total Akt, phosphorylated Akt (Pho-Akt) and viral NS1 were detected with the Akt antibody (Cell Signaling, Boston, MA (1:500)), Phospho-Akt antibody (Ser473) (Cell Signaling, Boston, MA (1:500)), and Clone NS1-1A7 (from NIH (1:500)) as the primary antibody, respectively. Then added HRP-conjugated goat anti-rabbit IgG (SouthernBiotech, Birmingham, Alabama (1:5000)) as the secondary antibody for Akt and Pho-Akt, and added HRP-conjugated goat anti-rabbit IgG (SouthernBiotech, Birmingham, Alabama (1:5000)) as the secondary antibody for NS1. The image was developed using SuperSignal West Pico chemiluminescent substrate (Fisher Scientific, Waltham, MA). GAPDH was taken as the cellular internal control. This experiment has been repeated 2 times.

Quail study

Twelve 4-week-old Japanese quail were inoculated by the ocular, intranasal, intratracheal and cloacal routes with 10^6 EID₅₀ viruses in 1.0 ml. At 1 dpi, 6 naïve quail were introduced into the same isolators, and placed in direct contact with the inoculated quail to assess virus transmission. At 3 and 5 dpi, 3

inoculated quail per group were sacrificed, lungs were homogenized and virus titers were determined by EID₅₀. The tracheal and cloacal swabs were collected from both the inoculated and direct contact birds at 1, 3, 5, 7, 9 and 11 dpi. The swab samples were stored in glass vials in 1.0 ml freezing Brain Heart Infusion (BHI) medium (BD, Sparks, MD) and titrated for infectivity in 10-day-old embryonated chicken eggs and MDCK cells. Sera were collected 2 weeks post-infection and HA inhibition tests (HI) were performed to quantify antibodies against HA [254].

Statistical analysis

All figures were generated and all statistical analyses were performed with GraphPad Prism software version 5.0c (GraphPad Software Inc., San Diego, CA). Comparison between the means of two groups was carried out with a paired two-tailed Student's t-test, the multiple comparisons were performed by two-way analysis of variance (ANOVA) with Tukey's multiple comparison test, unless otherwise specified. P values of <0.05 were considered significant difference.

Results

The mutation K219E enhanced cytoplasmic accumulation of NS1 in mammalian and avian cell lines

After the wildtype duck H9N2 (WT702) virus was serially propagated in lung of quail for 23 times, the quail adapted virus QA23 obtained new phenotype of replicating and transmitting efficiently in both chickens and quail [98]. Three amino acid substitutions were found in NS1: M106T, K217E and K219E [98].

The residue 217 and 219 are located at C-terminal of NS1, and 219 is known as a key amino acid in NLS2 [165]. To find out if these two mutations will affect the distribution of NS1, we firstly analyzed the intracellular location of NS1 using eGFP-NS1 fusion protein, which consisted of full-length NS1 gene. To avoid the interference of NS2, two additional stop codons were introduced after the original stop codon of NS1 (eGFP-QA23 NS1 and eGFP-WT702 NS1) to abolish the NS2 expression. The results demonstrated that QA23 NS1 predominantly distributed in the cytoplasm, while WT702 NS1 predominantly accumulated in the nucleus in 293T cells (Figure 6.1A, E, G, H and I), as well as MDCK (Figure 6.1B), A549 (Figure 6.1C) and DF1 cells (Figure 6.1D). The distributions of NS1 in the nucleus, cytoplasm or both in those cells were analyzed by counting more than 100 single cells in at least 5 different eyesights. The results of NS1 distribution pattern were consistent with the results of eGFP-NS1 localization study (Figure 6.1F). We further introduced three single mutations into pEGFP-C1 vector (eGFP-WT702 NS1-M106T, eGFP-WT702 NS1-K217E and eGFP-WT702 NS1-K219E), and the localization study displayed that 219K is the critical amino acid responsible for NS1 localization change from nucleus to cytoplasm (Figure 6.1E and I).

We alternatively confirmed the enhanced accumulation of QA23 NS1 in the cytoplasm using immunostaining analysis with directly infected cells. We generated the viruses QA23 NS:7WT702 and WT702 using reverse genetics, and infected DF1 and MDCK cells with the virus at MOI=1 for 9h. The immunostaining result showed the change of NS1 distribution pattern from

nucleus (WT702) to cytoplasm (QA23:7WT702) (Figure 6.1J and K), which is consistent with the result of eGFP-NS1 fusion protein localization study (Figure 6.1B and D).

To directly analyze the accumulation of QA23 NS1 in the cytoplasm, we separated the nuclear and cytoplasmic fractions of the infected MDCK cells and detected the distribution of the NS1 in both fractions. MDCK cells were infected with virus QA23NS:7WT702 or WT702, and harvested at 8 and 24 h.p.i. Then the amount of NS1 in nuclear and cytoplasmic fractions was directly compared using Western blot. The result was confirmed the QA23 NS1 accumulated in the cytoplasm of the MDCK cells, while WT702 NS1 predominately distributed in the nucleus (Figure 6.1L and M).

NLS2 is the major functional signal for the nuclear accumulation of NS1 in WT702 strain

Amino acid residue 219 is located on the theoretical NLS 2, which is responsible for importing WT702 NS1 into the nucleus. There is another typical NLS 1 locates on 35 to 41, and conserved in all subtype of influenza viruses. Based on our observation, the single mutation of K219E in NS1 gene of WT702 can change the NS1 accumulation pattern from nuclear to cytoplasmic (Figure 6.1I). To find out whether the theoretical NLS1 plays the role for nuclear transportation of NS1, we substituted two critical amino acids of NLS1, Arginine-38 and Lysine-41, into alanine. pEGFP-WT702 NS1-R38A and /or K41A, and pEGFP-QA23 NS1-R38A and/or K41A were transfected into 293T cells, and the results from Confocal proved the abolishing of theoretical NLS1 did not affect the

NS1 distribution pattern of either QA23 or WT702 (Figure 6.2). Take together, the results indicated NLS2, but not NLS1 is the major functional signal for the accumulation of WT702 NS1 in the nucleus.

QA23 NS1 leads to up-regulated viral protein synthesis in DF1 cells

To investigate if the mutations of QA23 NS1 will affect the viral protein synthesis in the avian cells, we performed the minigenome assay with different NS1. WT702 PB1, PB2, PA and NP genes, the reporter (luciferase) and internal control (SEAP) genes were co-transfected into DF1 cells, as well as WT702 or QA23 NS1 gene. The results showed that at 24 and 48 h post transfection, QA23 NS1 largely increase the viral protein synthesis compared with WT702 NS1 (Figure 6.3A and B), which may related to the enhanced cytoplasmic accumulation of NS1. However, when infected DF1 cells with WT702 and QA23 NS1: WT702 viruses at MOI=0.1, both viruses yield very low viral titer (HA titer of WT702 infected cells was 2, and HA titer of QA23 NS1: WT702 infected cells was 8 at 72 h.p.i.).

This experiment has been performed two times. The statistics analysis was performed using ANOVA with Bonferroni's posttest, and t-test at 24, 48 and 72 h post-transfection was performed to compare the relative activity of QA23 NS1 and WT702 groups. P values of <0.05 were considered significant difference.

The predominant cytoplasmic distribution of NS1 does not affect its inhibition of host IFN- β

NS1 may inhibit the production of interferon beta (IFN - β) induction by both pre-transcription (nucleus) and post-transcription (cytoplasm). The distribution pattern change of QA23 NS1 may affect the host immune response, and therefore, we detected the IFN- β expression level of mammalian and avian cells after infect with WT702 and different mutants. MDCK and DF1 cells were infected with virus QA23 NS: 7WT702, WT702, single mutants 217E or 219E at MOI=1.0. The IFN - β activities were detected at 12, 24 and 48 h.p.i. using ELISA kits. The results showed all viruses strongly decrease the induction of IFN- β in both MDCK cells (Figure 6.4A) and DF1 cells (Figure 6.4B), but there was no significant difference in IFN- β level amongst the different viruses (Figure 6.4A and B). Take together, the enhanced cytoplasmic and decrease nuclear distribution of NS1 did not affect the inhibition the induction of host IFN- β . However, both of the experiments have been performed only once.

The predominant cytoplasmic distribution of NS1 enhanced the anti-apoptotic activity level

During the course of experiment we observed that A549 cells infected with WT702 rounded up and detached much earlier than the cells infected with virus QA23 NS:7WT702. To investigate the role of QA23 NS1 on regulating the apoptotic activity of the infected cell, a TUNEL assay was carried out in A549 and HeLa cells. TUNEL, or Terminal deoxynucleotidyl transferase dUTP nick

end labeling is an approach for detecting DNA fragmentation by labeling the terminal end of nucleic acids. During the infection of influenza viruses, endogenous endonuclease activities cleave the DNA of apoptotic cells into a population of 180- to 200-bp fragments, resulting in the morphological changes of the host cells; TUNEL could label those degraded DNA fragments in situ. Here we applied a DeadEnd colorimetric TUNEL kit to display the apoptotic level of infected A549 (Figure 6.5A) and HeLa cells (Figure 6.5B). The apoptotic DNA fragments were stained into dark brown. Compared with the cells infected with the virus carrying QA23 NS1, the cells infected with the virus carrying WT702 NS1 showed much higher apoptotic level (more dark brown dots) at 16 h.p.i. in both A549 and HeLa cells (Figure 6.5A and B). In contrast, the uninfected (Mock) cells were negative for TUNEL staining, and the cells treated with the apoptosis-inducing agent staurosporine showed severe apoptotic changes (Figure 6.5A and B). The results indicated that the cytoplasmic accumulation of QA23 NS1 may enhance the anti-apoptosis function of the NS1 protein and lead to a reduced apoptotic activity of the host cells.

The analysis of the apoptotic activity levels in DF1 and MDCK cells during infection is more relevant to this study. However, no dark brown dots were observed using the TUNEL staining after I infected DF1 and MDCK cells for 16 h. The optimization of the infection condition is required to obtain the better images from these two cell lines.

PI3K/Akt signaling pathway plays important role in host anti-apoptosis. The activation of PI3K can be detected by phosphorylation of Akt, the

downstream effector of PI3K [185]. To analysis the anti-apoptosis function of QA23 NS1 during infection, I performed the preliminary experiments on detecting phosphorylated Akt (Pho-Akt) level in infected HeLa and A549 cells. However, no Akt and Pho-Akt signal has been detected from infected A549 cell. Whereas, infected HeLa cells showed strong signals for both molecules in the western blot. The results showed Pho-Akt level up-regulated in QA23 NS:7WT702 infected HeLa cells at 12 and 24 h.p.i compared with WT702 infected cells (Figures 6.6 A and B). However, compared with QA23 NS1, the signal of WT702 NS1 during infection was very low, which indicated the Pho-Akt level difference might be caused by the different expression levels between QA23 and WT702 NS1. The kinetics study showed virus QA23 NS:7WT702 replicated more efficiently in Hela cells than WT702 (Figure 6.6C). In contrast, no significant difference on viral replication has been observed in A549 cell (Figure 6.6D).

QA23 NS1 has no significant effect on the viral replication and transmission in Japanese quail

Because the three amino acid substitutions M106T, K217E and K219E were generated through the wildtype duck H9N2 (WT702) virus serially prorogated 23 times in lung of quail, and obtained the capability to effectively infect and transmit in quail and chicken, we wanted to determine whether these three mutations also contribute to the replication and transmission of the adapted virus (QA23) in quail. Twelve 4-week-old Japanese quail were inoculated with virus WT702 or mutants; and the next day, 6 naïve quail were introduced into the

same isolators to directly contact with the inoculated quail. The results showed the all quail inoculated WT702 or mutants and all direct contact quail were positive at 1 and 3 d.p.i and 3 d.p.i , respectively (showed in Table 6.1.). The viral shedding was detected mainly from the upper respiratory tract (trachea), while only trace amount of virus (below the limit of detection in MDCK cells) was isolated from cloaca of some birds (showed in Table 6.1.). However, no significant difference of viral shedding had been detected from the inoculated birds (Figures 6.7A), or from the direct contact birds (Figures 6.7B), which suggested that QA23 NS1 has no significant effect on viral replication and transmission in quail compared with WT702 NS1.

Discussion

To better understand the molecular mechanism of the adaptation and interspecis transmission of influenza virus from wild aquaic birds to land-based poultry in nature, our lab established a model for virus adaptation by serially passing a wildtype duck H9N2, A/duck/Hong Kong/702/79 (WT702) virus, in the lung of Japanese quail for 23 times followed by 10 more passages in the lung of chicken, and generated adapted virus QA23 and QA23CkA10, respectively [98]. Quail carries both α -2,3 SA (avian-like) and α -2,6SA (human-like) receptors in the respiratory tract and thought to be the potential mix vessel to generate reassort influenza virus and an ideal environment for the adaptation of influenza virus from wild birds to land-based poultry and mammals [362,363,364]. Both QA23 and QA23CkA10 gained the new phenotype of replicating and transmitting efficiently in chickens and quail [98]. And more importantly, both QA23 and

QA23Ck10, unlike WT702, were able to infect mice without any further adaptation, and showed faster growth kinetics in MDCK and CEK cells [98]. Amongst all of the amino acid substitutions on virus QA23, we particularly noticed three amino acid substitutions M106T, K217E and K219E on NS1 gene, which generated after the adaptation in quail.

Firstly, we constructed eGFP-QA23 NS and eGFP-WT702 NS and analysis the distribution of NS1 in 4 mammalian or avian cell lines (293T, MDCK A549, and DF1). The result of localization study on Confocal displayed that, in all cell lines, WT702 NS1 predominantly distributed in the nucleus, while QA23 NS1 mainly accumulated in the cytoplasm (Figure 6.1A-M). Three single mutations were introduced into GFP vector, and the result demonstrated 219K is the critical amino acid responsible for NS1 distribution pattern change of QA23 from nucleus to cytoplasm (Figure 6.1E and I). We also infected DF1 and MDCK cells with viruses QA23 NS:7WT702 and WT702, respectively; and confirmed the enhanced cytoplasmic accumulation of NS1 by performed immunostaining assay (Figure 6.1J and K) and dissociation of nuclear and cytoplasmic fractions (Figure 6.1L and M). WT702 NS1 contains both theoretical NLS1 and NLS2. NLS1, containing 3 critical residues: Arg-35, Arg-38 and Lys-41, is highly conserved in most of the influenza strains; while NLS2 is deficient from a large number of the virus strains. However, based on our observation, seems NLS2 plays the important role on nuclear importing of NS1 in this H9N2 strain, because a single mutation K219E could dramatically reduce the accumulation of NS1 in nucleus. Using the eGFP-NS1 fusion protein, we confirmed that to abolish the

function of NLS 1 by substituting residue 38R and/ or 41K into alanine did not affect the predominantly distribution of WT702 NS1 in nucleus (Figure 6.2). The observation is similar to a recent NS1 localization study of a human H3N2 influenza virus (A/Udorn/72), which showed, unlike H1N1 subtype, its C-terminal NLS2/NoLS was the major signal for the transportation of the NS1 protein into the nucleus [365]. Take together, the data indicated that the primary function of NLS1 and NLS2 could be strain-specific.

NS1 can interact with a number of host proteins to overcome the innate protection of host and facilitates the viral replication during infection. The increased accumulation of NS1 in the cytoplasm may promote the interaction between NS1 and cytoplasmic factors. It's reported that NS1 can suppress the host antiviral function by blocking 2'-5'-oligoadenylate synthetase (OAS) [192] and serine/threonine protein kinase R (PKR) [193]. More important, NS1 could inhibit RIG-I function on inducing of IFN- β by directly form the RIG-I-NS1 complex, and binding to TRIM25, which activates RIG-I by ubiquitinating RIG-I N-terminal CARD domain [172,173,174,175]. To determine if the enhanced cytoplasmic distribution affect NS1 function on antagonizing the host type I interferon, we infected MDCK and DF1 cells with WT702 and different mutants, and detected the IFN- β production in the supernatant. However, compared with virus WT702, those mutants did not show significant changes on the interferon expression level (Figure 6.4).

To analyze the effect of cytoplasmic accumulation of NS1 on the viral replication, we first infected DF1 cells with viruses WT702 and QA23

NS:7WT702. However, both viruses replicated poorly in DF1 cells. We alternatively investigate the effect of NS1 on viral protein synthesis using minigenome assay. The results showed that QA23 NS1 up-regulated the viral protein synthesis at 24 and 48 h post transfection (Figure 6.3). In the cytoplasm, NS1 may enhance the viral protein synthesis by binding to Staufen [366] and binding eukaryotic translation initiation factor eIF4GI to viral mRNA 5' untranslated region[191]; meanwhile, limits the expression of the host antiviral gene[137]. The cytoplasmic accumulation of NS1 may enhance the viral protein synthesis by increasing the interaction with those host factors located in the cytoplasm.

NS1 may activate PI3K in the cytoplasm, and limit the programmed cells death. However, the role of NS1 in apoptosis is still unclear as both pro-apoptosis and anti-apoptosis were reported, and the function could be strain-specific or host-specific [160,330,332,367]. In this study, we applied TUNEL assay to investigate whether QA23 NS1 enhance the function of pro-apoptosis or anti-apoptosis during infection. The results showed that, at 16 h.p.i., QA23 NS1 reduced the apoptotic activity level of A549 and HeLa cells (Figure 6.5), and suggested the cytoplasmic accumulation of NS1 may enhance the anti-apoptosis function of the protein during infection. DF1 and MDCK should be more relevant to this apoptosis assay in this study. However, TUNEL assay in these two cells resulted in poor staining. Optimization of the infection and TUNEL condition are needed to improve the signal in DF1 and MDCK cells.

PI3K/Akt is an important intracellular signaling pathway in apoptosis. During influenza infection, NS1 interacts with PI3K by direct binding to the subunit of p85 β , and phosphorylate Akt consequently inhibits the apoptosis of the infected cells. However, when we detected the phosphorylated Akt (Pho-Akt) level in different cell-lines (including A549, MDCK, DF1 and HeLa cells) infected with WT702 or QA23 NS: 7WT702, the difference was only found in HeLa cells. It may be because the commercialized antibodies against Pho-Akt and Akt could only react with human, mouse, and rat; or because the Akt and Pho-Akt expression level are relative low in other cell-lines. More efforts need to be carried out on prove the role of QA23 NS1 on up-regulating the Pho-Akt in HeLa cells, as well as in DF1 and MDCK cells.

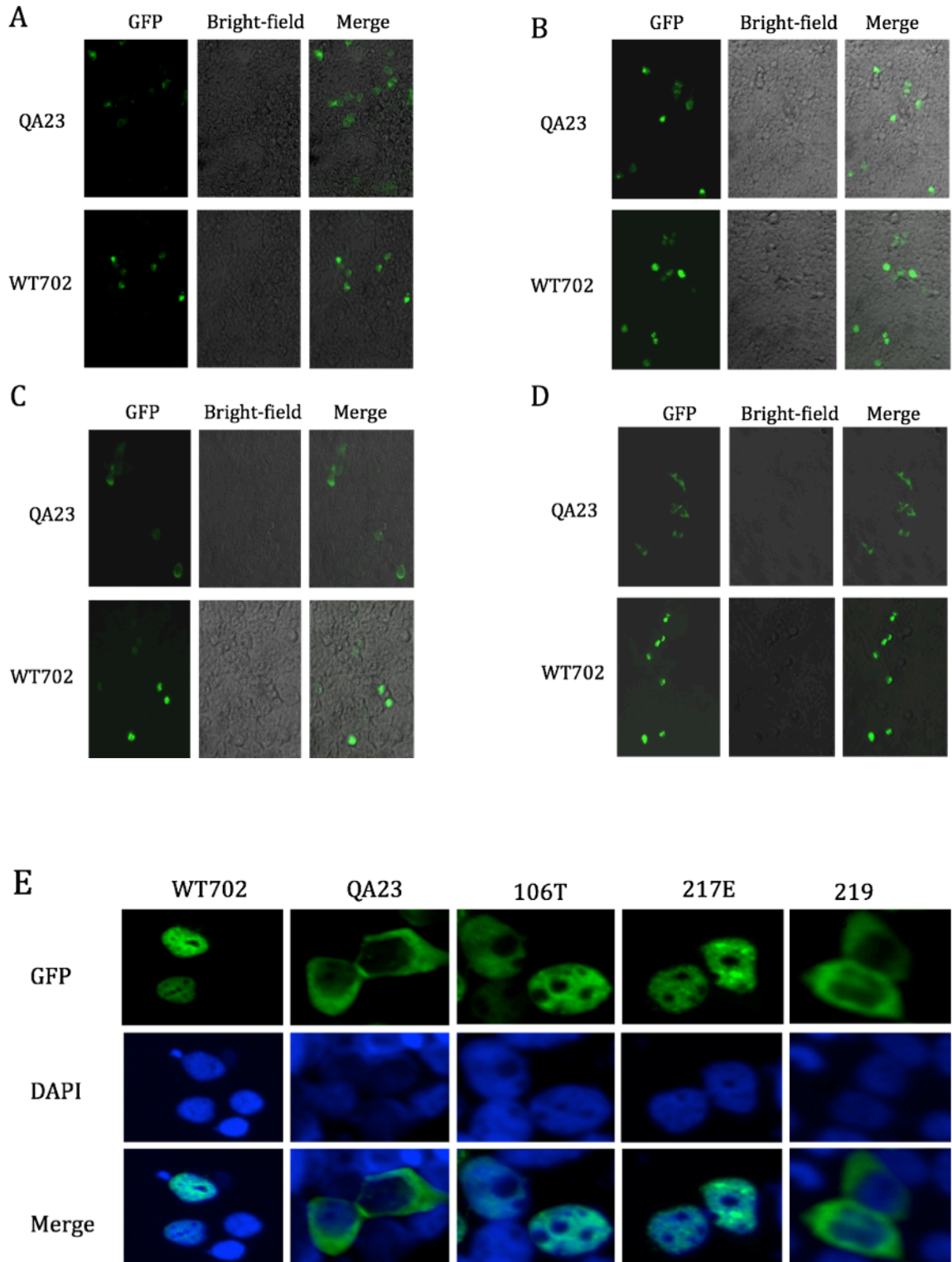
To determine the contribution of QA23 NS1 gene to the adaptation of WT702 in chicken and quail, we performed the viral replication and transmission study in Japanese quail. The results showed: no significant difference in the viral shedding has been detected from the trachea (upper respiratory tract) or lung (lower respiratory tract) of the inoculated birds, or from the trachea of the direct contact birds (Figures 6.6A and B). The results suggested that the accumulation of NS1 in the cytoplasm does not affect the virus replication and transmission in quail.

In this study, we demonstrated, for this H9N2 strain, the increased cytoplasmic accumulation of NS1 may enhance the viral replication and anti-apoptosis activity level in the host cells. As the amino acid mutations on NS1 were the selection result under the certain stress of adapting to a new host, the

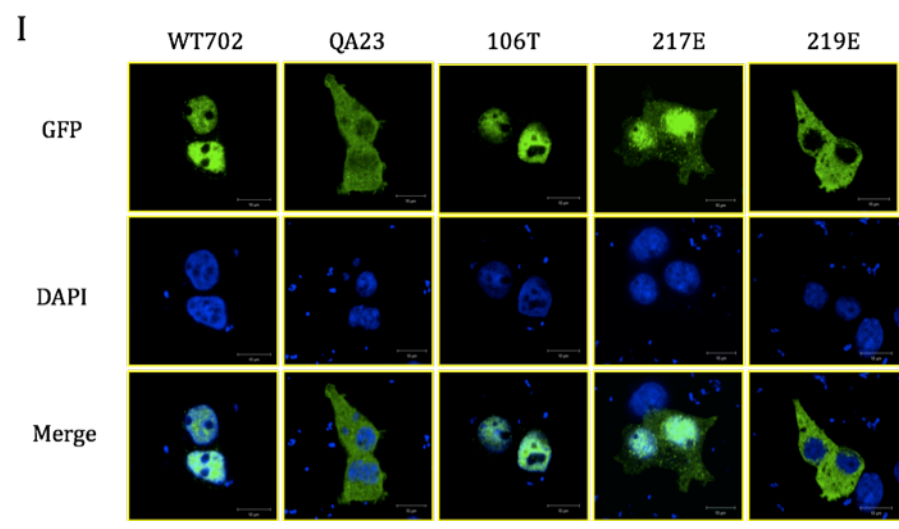
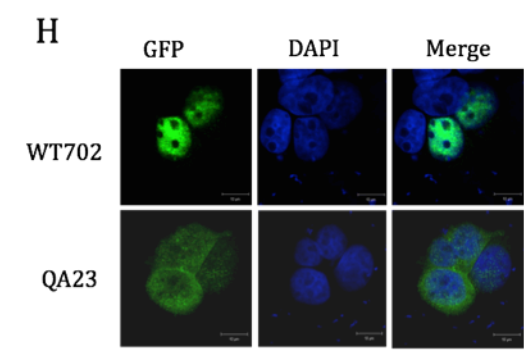
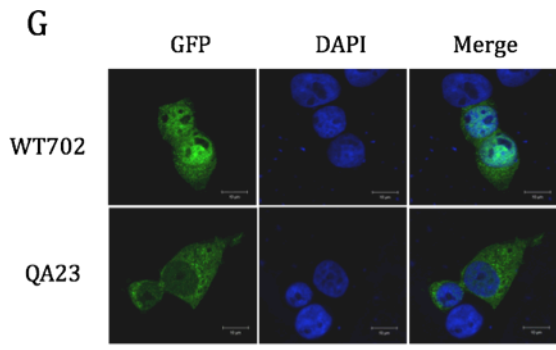
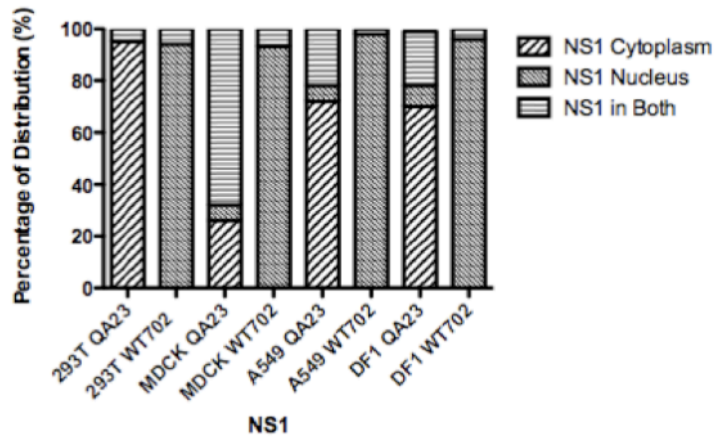
cytoplasmic accumulation of NS1 may facilitate influenza virus to produce more mutants as the candidates for better fitness during this processing by utilize the host cell longer and more efficiently. This could be a strategy for the interspecies transmission of influenza virus. However, some of the experiments in this study were carried out only once, and more evidence needs to be provided before we draw the conclusions.

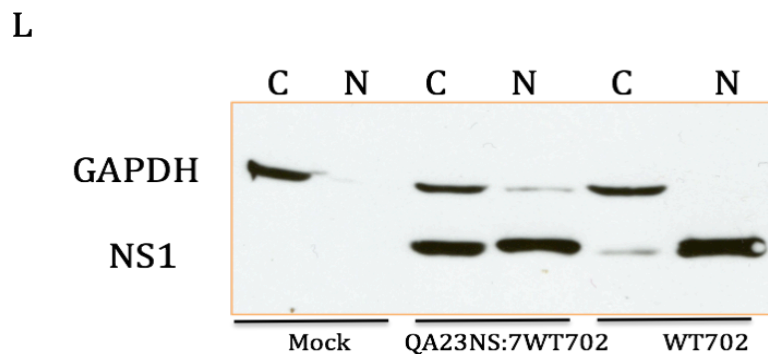
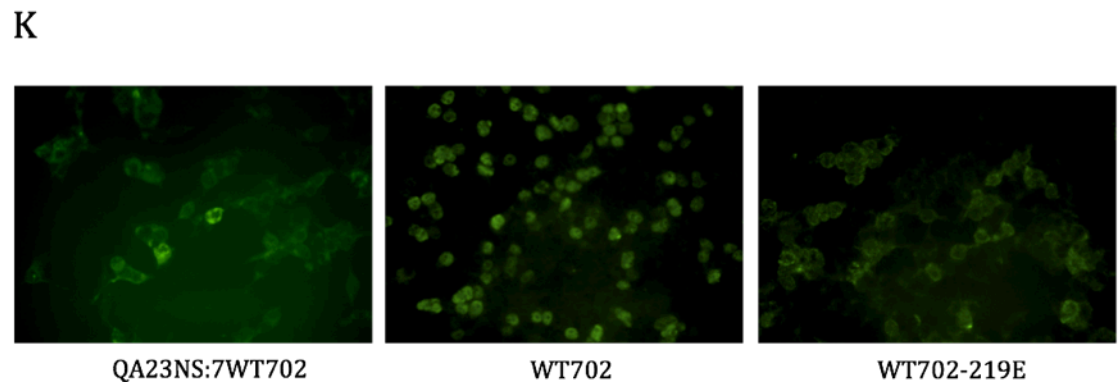
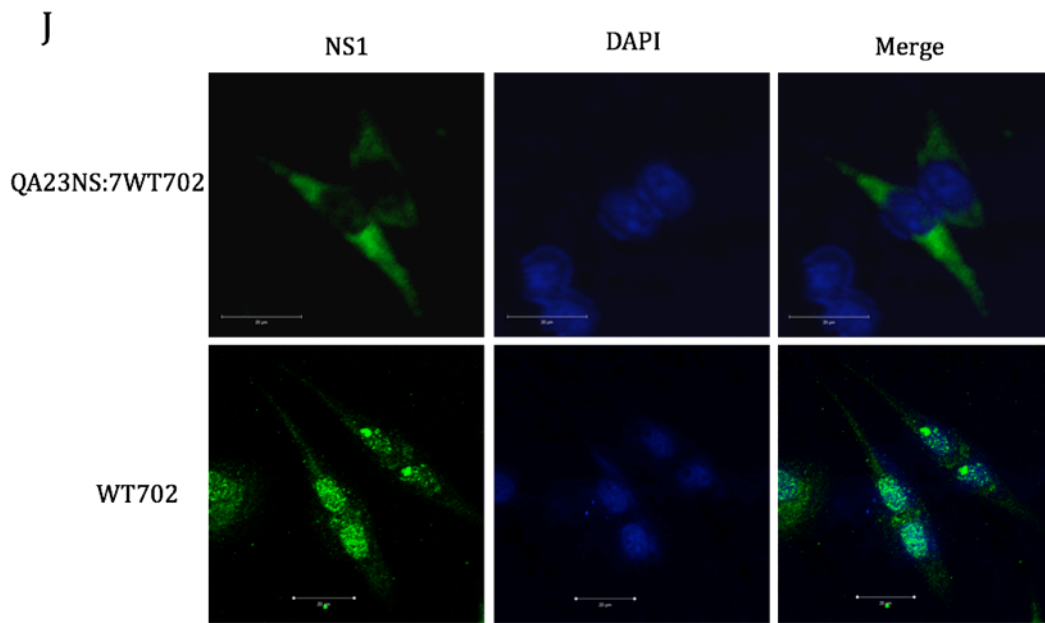
Table 6.1. Replication and transmission of H9N2 viruses in Japanese quail.

Virus/Group	Days post-infection												# of positive HI/total # at 14 dpi	
	1		3		5		7		9		11			
	T	C	T	C	T	C	T	C	T	C	T	C		
WT702														
Infected	12/12	4/12	12/12	6/12	4/9	1/9	0/6	0/6	0/6	0/6	0/6	0/6	0/6	6/6 (26.7)
Contacts	NA	NA	6/6	0/6	4/6	0/6	2/6	1/6	0/6	0/6	0/6	0/6	0/6	6/6 (18)
QA23NS: 7WT702														
Infected	12/12	3/12	12/12	5/12	5/9	1/9	0/6	0/6	0/6	0/6	0/6	0/6	0/6	6/6 (41.3)
Contacts	NA	NA	6/6	1/6	5/6	2/6	2/6	3/6	0/6	0/6	0/6	0/6	0/6	6/6 (4.3)
WT702 NS1 217E														
Infected	12/12	4/12	12/12	5/12	5/9	1/9	0/6	0/6	0/6	0/6	0/6	0/6	0/6	6/6 (30.7)
Contacts	NA	NA	6/6	0/6	5/6	1/6	2/6	2/6	1/6	0/6	0/6	0/6	0/6	6/6 (9.3)
WT702 NS1 219E														
Infected	12/12	4/12	12/12	6/12	6/9	1/9	0/6	0/6	0/6	0/6	0/6	0/6	0/6	6/6 (44.0)
Contacts	NA	NA	6/6	1/6	5/6	2/6	2/6	3/6	1/6	1/6	0/6	0/6	0/6	6/6 (4.7)
WT702 NS1 106T														
Infected	12/12	3/12	12/12	5/12	4/9	0/9	0/6	0/6	0/6	0/6	0/6	0/6	0/6	6/6 (24.0)
Contacts	NA	NA	6/6	0/6	5/6	0/6	1/6	2/6	0/6	0/6	0/6	0/6	0/6	6/6 (14.7)



F





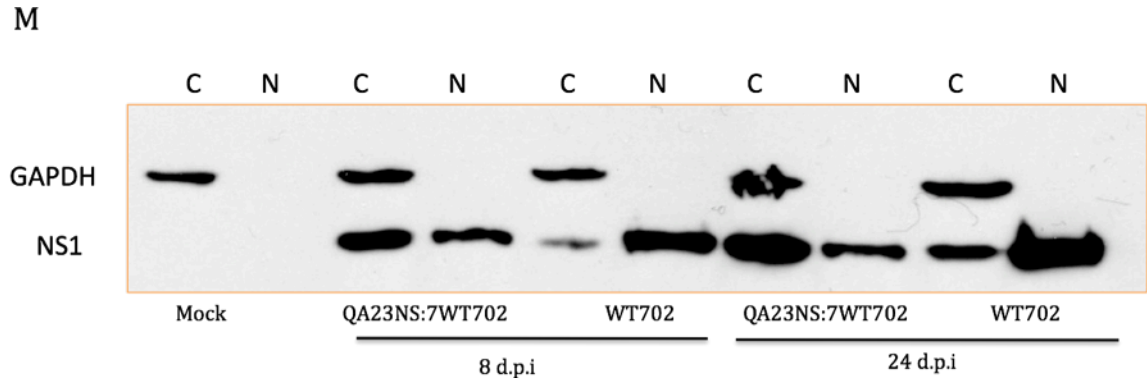


Figure 6.1. Immunofluorescence of NS1 protein localization and cytoplasmic and nuclear and fractions of NS1. (A) 293T, (B) MDCK, (C) A549, and (D) DF1 cells were transfected with plasmids expressing the different GFP-NS1 proteins and fixed at 24 h post-transfection for immunofluorescence analysis using a Zeiss Axiovert 200M (400x). (E) 293T were transfected with plasmids expressing the different GFP-NS1 proteins and fixed at 24 h post-transfection for immunofluorescence analysis using a Zeiss SM510 confocal microscope. (F) The distribution of NS1 in the cytoplasm, nucleus, and in both were analyzed in 293T, MDCK, A549 and DF1 cells by counting more than 100 single cells in at least 5 different eyesights. 293T cells were transfected with plasmids expressing the different GFP-NS1 proteins and fixed at (G) 6 h, (H) 12h, and (I) 24 h post-transfection for immunofluorescence analysis. (J) DF1 cells were infected with recombinant viruses QA23NS:7WT702 or WT702 cells at an MOI=1. At 9 h p.i., the cells were fixed for immunofluorescence analysis. GFP-NS1 fusion protein showed in green and DAPI (the nucleus) showed in blue. (K) MDCK cells were infected with recombinant viruses QA23NS:7WT702 or WT702 cells at an MOI=0.1. At 24 h.p.i., the cells were fixed for immunofluorescence analysis. MDCK cells were infected with the recombinant viruses QA23NS:7WT702 or WT702 at MOI=1.0. The cells were harvested (L) at 8 h.p.i. and (M) at 8 and 24 h.p.i., and then fractionated for detection. Amounts of NS1 in cytoplasmic (C) and nuclear (N) fractions were analyzed by western blot analysis. GAPDH was used as a control.

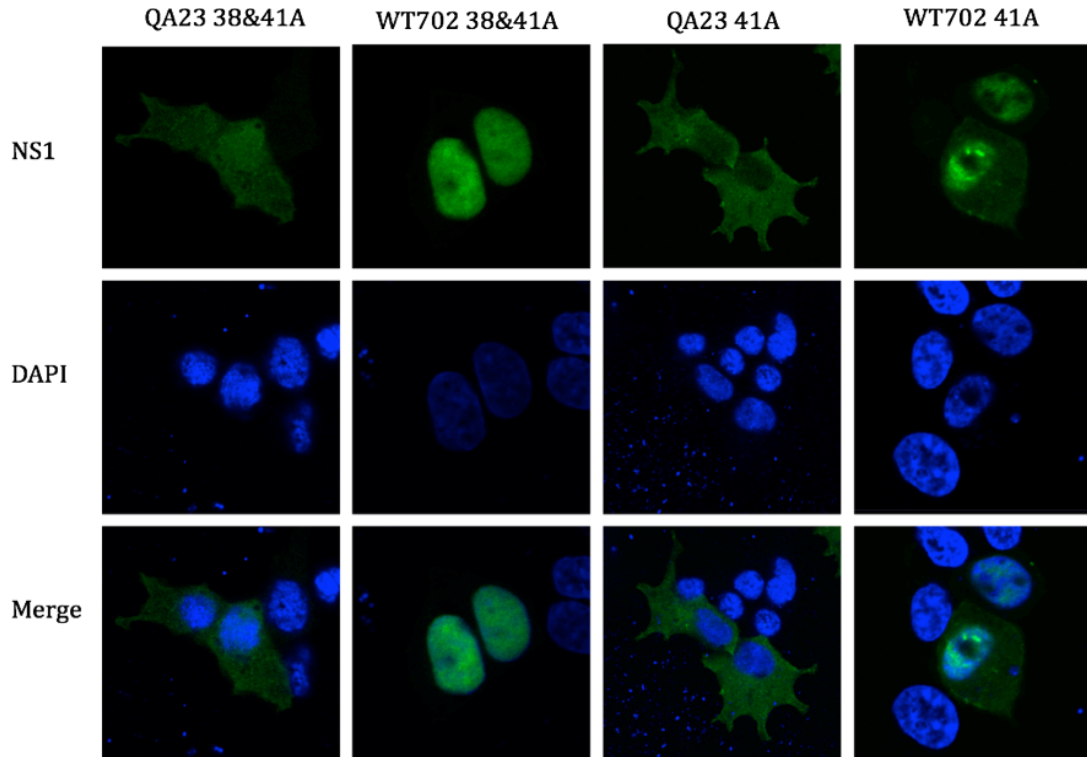


Figure 6.2. Immunofluorescence of NS1 mutants localization. 293T cells were transfected with QA23 and WT702 NS1 plasmids containing 41A and/or 38A mutation(s) and fixed at 24 h post-transfection for immunofluorescence analysis. GFP-NS1 fusion protein showed in green and DAPI (the nucleus) showed in blue.

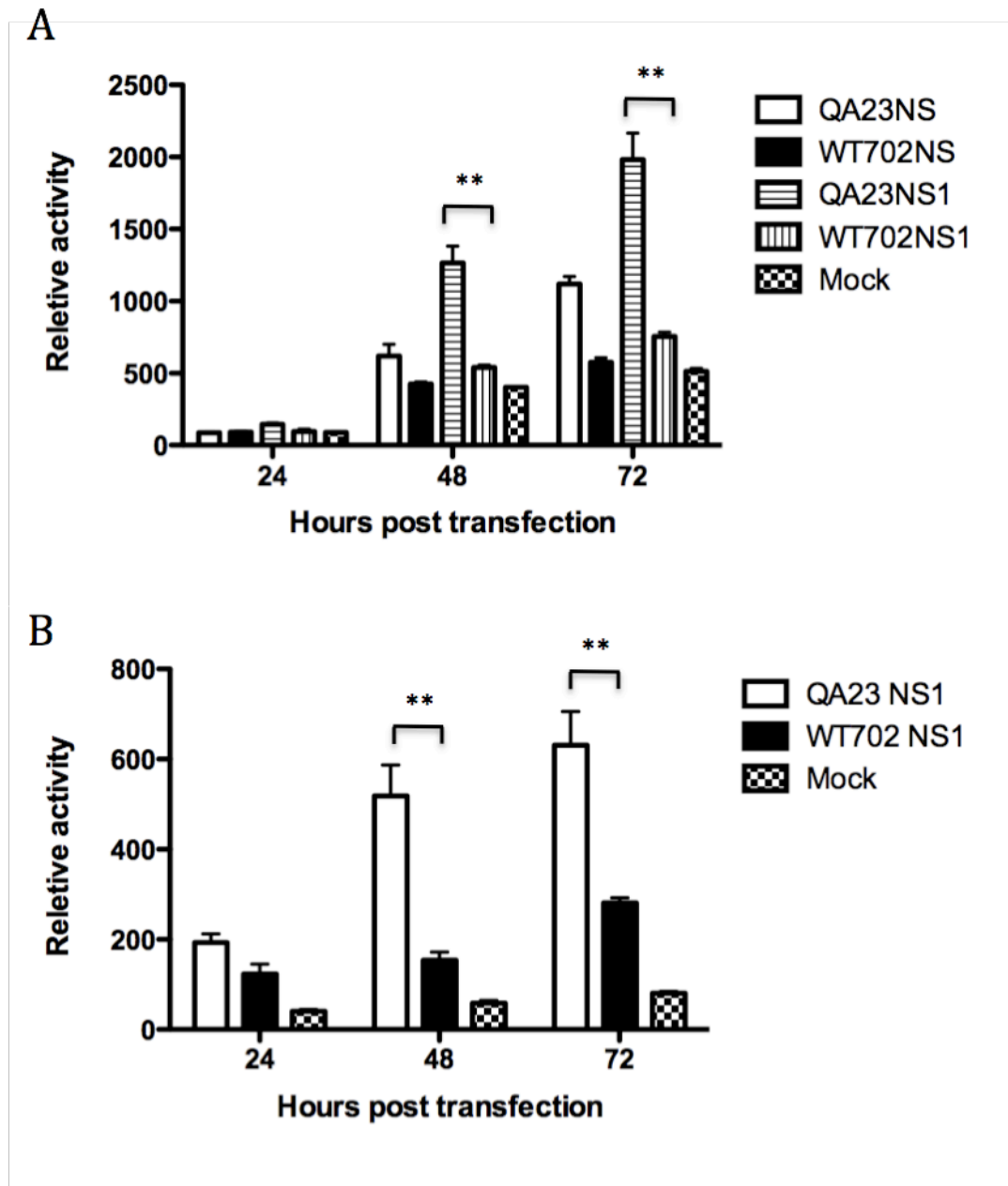


Figure 6.3. Minigenome assay. DF1 cells were transfected with each of the influenza virus driven-luciferase reporter plasmids (GLuc) and PB2, PB1, PA, and NP plasmids, and (A). QA23 or WT702 NS and QA23 or WT702 NS1, and (B). QA23 or WT702 NS1, and pCMV/SEAP, which carries the secreted alkaline phosphatase gene was cotransfected into the cells to normalize transfection efficiency. (The experiments were carried out 2 times.)

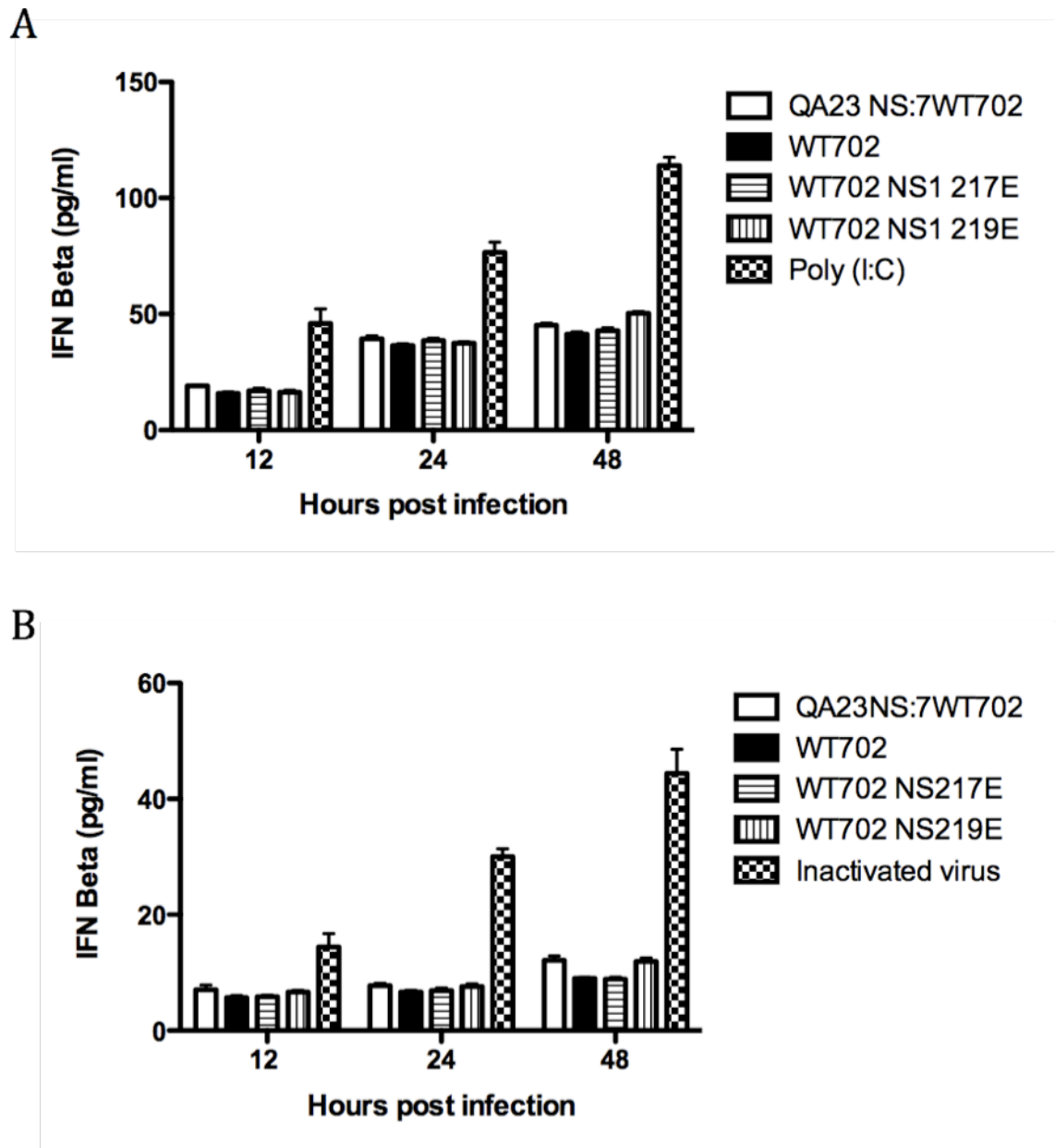
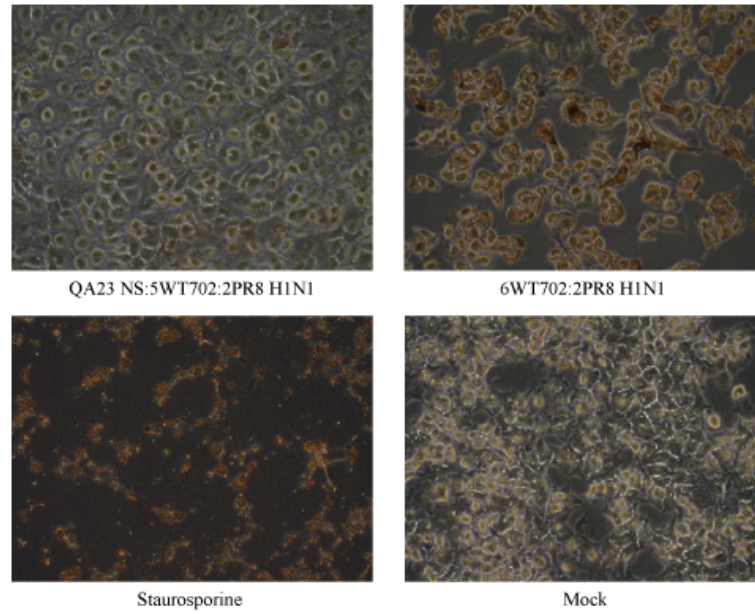


Figure 6.4. IFN- β level induced by recombinant viruses. (A) MDCK cells and (B) DF1 cells were infected with the recombinant viruses at MOI= 1. Supernatants were harvested at 12, 24, and 48 h p.i., and measurements were carried out using an IFN- β ELISA kits were performed. (These 2 experiments were performed only once. The results showed significant difference between positive control and viruses.)

A



B

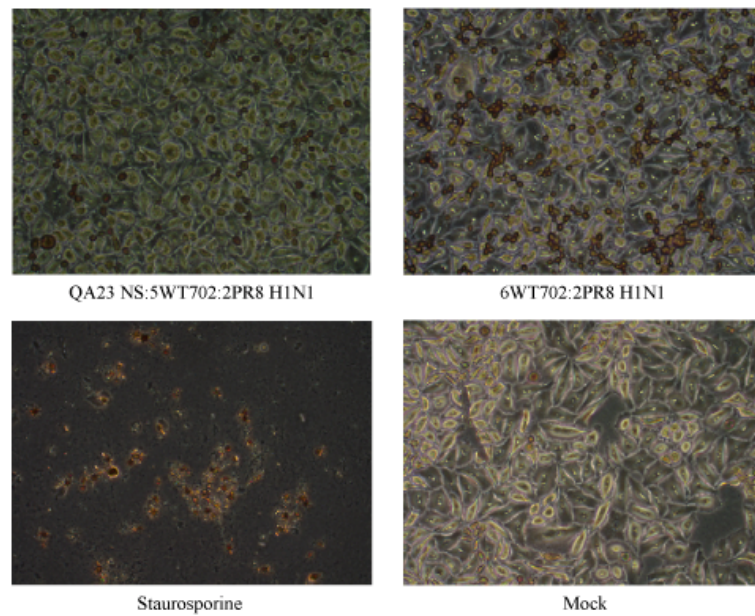


Figure 6.5. Apoptosis assay using TUNEL assay. (A) A549 and (B) HeLa cells were infected with the recombinant viruses QA23NS:5WT702:2PR8 H1N1 or 6WT702:2PR8 H1N1, and fixed the cells at 16 h.p.i. The apoptotic activity level of the cells was detected using TUNEL assay kit. The apoptotic nucleus with the small DNA fragments was stained into dark brown dots. However, this is only one-time experiment.

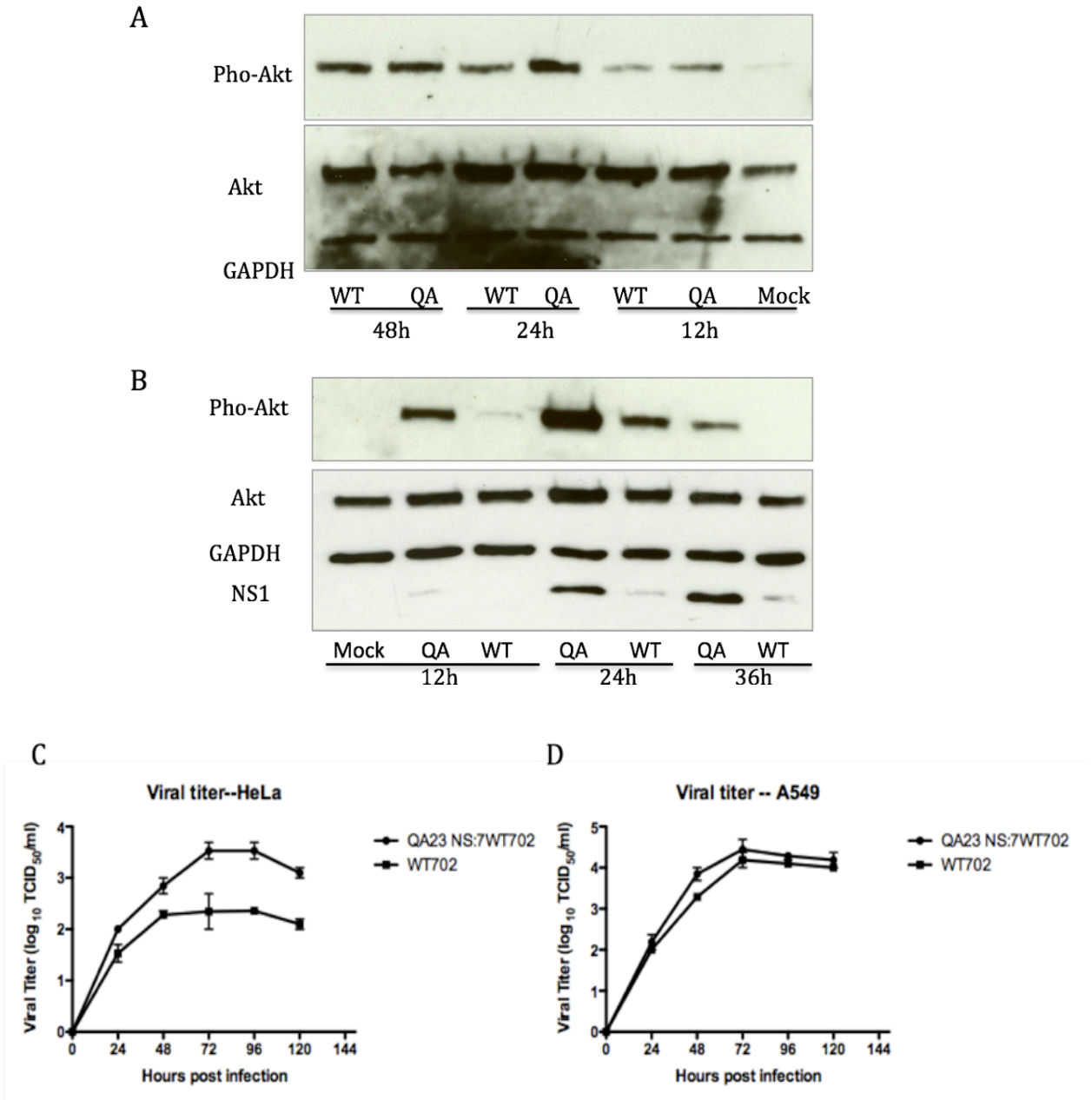
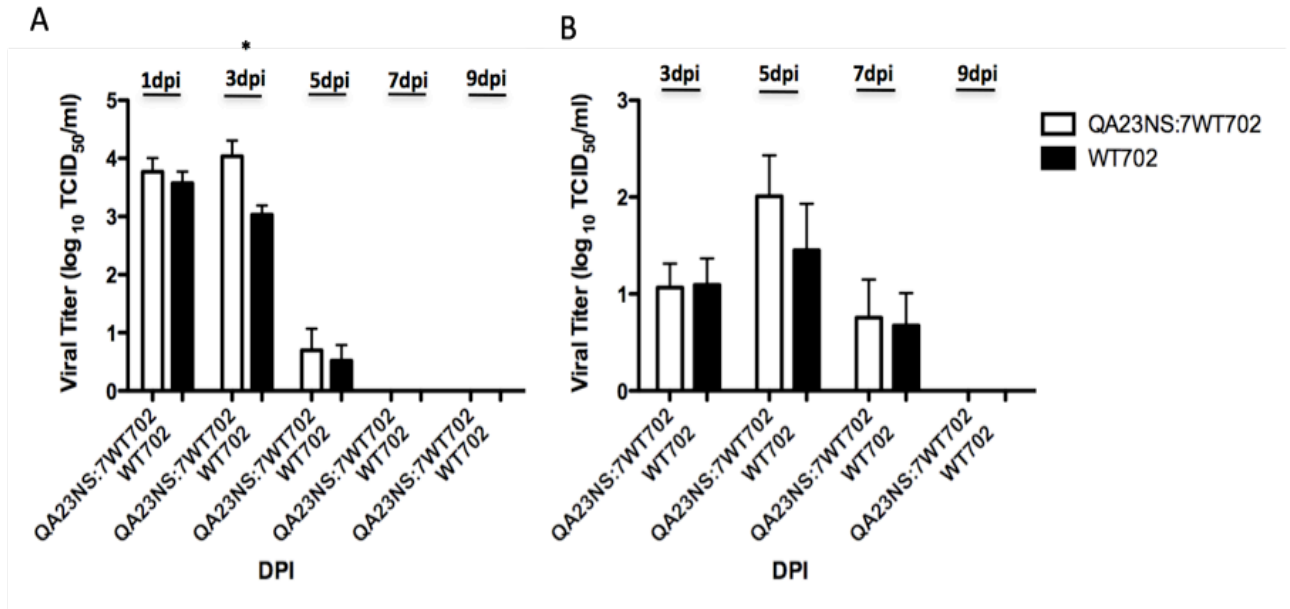


Figure 6.6. Influenza virus infection activates Akt phosphorylation. HeLa cells were infected by virus QA23NS:7WT702 or WT702. Cell lysates were collected at (A) 12, 24, and 48 h.p.i. ; or (B) 12, 24, and 36 h.p.i. The amounts of phosphorylated Akt (pho-Akt) and total Akt evaluated by western blot using Akt and Pho-Akt antibodies. (C) HeLa and (D) A549 cells were infected with QA23 NS:7WT702 or WT702 at MOI=0.1. The supernatants were collected at 24, 48, 72, 96 and 120 h.p.i., and TCID₅₀ was detected the in MDCK cells.



* P Value <0.05

Figure 6.7. Viral shedding from the trachea of quail. The swabs from (A) infected and (B) contacted birds were collected at 1,3,5,7,9 and 11 dpi. The viral titers were detected using TCID₅₀ method in MDCK cells.

Chapter 7: Perspective

Influenza A viruses constantly circulate in a broad range of animal species, such as humans, birds, pigs, horses and dogs. In humans, the seasonal influenza virus infections cause epidemics every year, resulting in millions of cases with severe illness worldwide [368]; whereas the influenza pandemics occur sporadically, generally resulting in millions of death globally [18,19]. Meanwhile, the outbreaks of HPAI and LPAI cause the depopulation of flocks and major economic losses worldwide. Occasionally, the avian influenza viruses overcome the host barrier and directly cause the morbidity and mortality in humans, which highlight the threat of avian influenza viruses to public health.

Vaccination is the main strategy to control and prevent influenza virus infections. Currently, inactivated vaccine, live attenuated vaccine and recombinant virus-like-particles (VLPs) vaccine are licensed in the US against human seasonal influenza epidemics [243,245]. In poultry manufactory, inactivated vaccine, recombinant fowlpox virus-vectored vaccine expressing the H5 HA gene, and recombinant Newcastle disease virus (NDV)-vector with the H5 HA gene insert are approved to use for preventing avian influenza virus infection [255]. However, both licensed human seasonal influenza and avian influenza vaccines have some limitations, which stimulate the development of novel vaccines with other strategies.

Our lab previously demonstrated the potential of an avian live attenuated master backbone WF10*att* for use in epidemic and pandemic influenza vaccines in poultry and mammals [254,285,369]. In this study, I further tested if modifying

the HA gene combined with WF10att backbone could be used for *in ovo* vaccination against avian influenza in chickens. In “Chapter 4: Improved hatchability and efficient protection after *in ovo* vaccination with live-attenuated H7N2 and H9N2avian influenza viruses”, I investigated the strategy of replacing the HA cleavage site of H7 and H9 subtypes with that of H6’s to improve hatchability and protection efficiency. The results showed that the hatchabilities were greatly improved to more than 90% when *in ovo* vaccinated with those genetically modified live-attenuated viruses. More importantly, a single dose *in ovo* vaccination of 19-day-old egg embryos provided the high protectivity (>70%) against low pathogenic H7 and H9 challenge in the chickens at 2- or 6- week post-hatching. However, we conducted the *in ovo* vaccination manually in this study. An automated egg vaccination machine system currently used in poultry industry would deliver the vaccines in a more efficient, accurate and uniform way compared to manual approach. Therefore, further investigation is needed to determine if the automated system would provide a higher protection efficiency for *in ovo* vaccination with our live-attenuated vaccines in a large number of the chicken egg embryos.

Different methods were applied to generate the vaccine candidates in the emergence of the 2009 swine-origin pandemic H1N1 virus [262]. And more efforts were carried out to improve the functional HA yield of those vaccine strains in embryonated chicken eggs [262,347,353]. The amino acid substitutions generally present on the surface HA and NA proteins during egg adaption of influenza viruses. Interestingly, I identified that the amino acid substitution, at

residue 59 in PA, from glutamic acid to valine (PA E59V) is responsible for the enhanced HA and viral titers in egg embryos and MDCK cells on the live-attenuated vaccine WF10*att* backbone (Chapter 5: Glutamic acid to valine substitution at position 59 in PA enhances growth of live-attenuated influenza vaccines in eggs and mammalian cells). The substitution PA E59V confers this backbone higher capability to replicate better in eggs with HA and NA derived from human-like influenza virus under the temperature sensitive phenotype; and PA 59V is not likely to be the critical amino acid responsible for the RNA-dependent RNA polymerase activity of live-attenuated influenza virus. PA 59V may contribute to a regulation mechanism which confers the attenuated backbone enhanced HA yield under the temperature sensitive phenotype. However, the mechanism of PA E59V on enhancing the HA titer and viral replication of WF10*att* backbone in egg embryos needs to be further elucidated. Future study can be carried out to investigate whether the function of PA E59V is related to the amino acid mutations on PB1 and PB2, or HA tag on the c-terminus of PB1 on WF10*att* backbone. Meanwhile, the endonuclease assay with full-length PA or PA Nter (N-terminal 210 amino acid residues) may help us to further figure out the function of PA 59V on viral polymerase activity.

NS1 of Influenza A virus has been identified as a multifunctional protein, which is responsible for the increased pathogenicity and virulence of the viruses. NS1 generally possesses two nuclear localization sequences (NLS1 and NLS2) and one nuclear export sequence (NES), which are responsible for the shuttling of the protein between cytoplasm and nucleus of the host cells [370,371].

Antagonizing the host innate immune response is one of the major functions of NS1: NS1 blocks the cellular mRNA maturation by binding to CPSF30 and PABII [170,171], and inhibits the activation of transcription factors in the IFN- β signaling pathway by binding to dsRNA [169,282]. NS1 could also directly bind to the cytosolic sensor RIG-I, form a complex, resulting in the inhibition of the IFN- β induction [172,173,174]. Meanwhile, NS1 has other important functions during infection, such as regulating PI3K/Akt pathway, which is involved in the host apoptotic activity [180,181,182,183].

In “Chapter 6: Cytoplasmic accumulation of NS1 enhances the viral replication and anti-apoptosis of an avian influenza virus (H9N2)”, I had a particular interest in the NS1 from a quail-adapted H9N2 virus QA23. Compared with the wild-type virus WT702, the NS1 accumulation pattern of the quail-adapted virus QA23 (containing three identified mutations: M106T, K217E and K219E in the NS1 gene) changed from nucleus to cytoplasm in the infected cells. The theoretical nuclear localization sequence 2 (NLS2) and 219K in NS1 are critical to the accumulation of the protein in the nucleus.

Both QA23 and WT702 NS1 have the effect on reducing the IFN- β induction level in DF1 cell and MDCK cells. However, no significant difference in the IFN- β expression level between QA23 and WT702 NS1 has been found. The results indicated that the cytoplasmic accumulation of NS1 does not affect NS1 function on blocking the induction of host IFN- β . We also observed that different cell-lines, such as A549 and MDCK cells, infected with recombinant WT702 rounded up, detached and suffered morphological changes much earlier

than the cells infected with recombinant QA23 NS: 7WT702. The results indicated that cytoplasmic accumulation of QA23 NS1 might relate to the reduced apoptotic activity of the host cells. PI3K/Akt is an important intracellular signaling pathway in apoptosis. During influenza infection, NS1 interacts with PI3K by direct binding to the subunit of p85 β , and phosphorylate Akt consequently inhibits the apoptosis of the infected cells. However, when we detected the phosphorylated Akt (Pho-Akt) level in different cell-lines (including A549, MDCK, DF1 and HeLa cells) infected with WT702 or QA23 NS: 7WT702, the difference was only found in HeLa cells. It may be because the commercialized antibodies against Pho-Akt and Akt could only react with human, mouse, and rat; or because the Akt and Pho-Akt expression level are relative low in other cell-lines.

Investigating the role of QA23 NS1 on pro- or anti-apoptosis may help us to better understand how this protein contributes to the pathogenesis by modulating the host-cell signalings during infection. We may also alternatively detect expression level of other important host factors, which involve in either pro-apoptotic or anti-apoptotic function in the life cycle of the cells. For example, p53 and cytochrome c play the pro-apoptotic role, while Bcl-2, Bcl-X_L, Bcl-W function as anti-apoptosis factors.

Appendices

The primers used for sequencing and reverse genetics

Primer name	Primer sequence	Function
Ba-PB2 1F	TATTGGTCTCAGGGAGCGAAAGCAGGTC	Universal primer
Ba-PB2 2341R	ATATGGTCTCGTATTAGTAGAAAACAAGGTCGTTT	Universal primer
Bm-PB1 1F	TATTCGTCTCAGGGAGCGAAAGCAGGCA	Universal primer
Bm-PB1 2341R	ATATCGTCTCGTATTAGTAGAAAACAAGGCATTT	Universal primer
BmPA-1F	TATTCGTCTCAGGGAGCGAAAGCAGGTAC	Universal primer
BmPA-2233R	ATATCGTCTCGTATTAGTAGAAAACAAGGTA CTT	Universal primer
Bm-NP-1F	TATTCGTCTCAGGGAGCAAAAAGCAGGGTA	Universal primer
BmNP-1565R	ATATCGTCTCGTATTAGTAGAAAACAAGGGTATTTTT	Universal primer
Bm-NS-1F	TATTCGTCTCAGGGAGCAAAAAGCAGGGTG	Universal primer
Bm-NS-890R	ATATCGTCTCGTATTAGTAGAAAACAAGGGTGT TTT	Universal primer
Bm-M-1F	TATTCGTCTCAGGGAGCAAAAAGCAGGTAG	Universal primer
Bm-M-1027R	ATATCGTCTCGTATTAGTAGAAAACAAGGTAGTT TTT	Universal primer
PB2 412R	CCATGTTTCAACCTTTCAACC	Internal primers
PB2 1774R	CAA ACTCCATCTTATTGTA	Internal primers
WFPB2-1454BseR	GCTAACTCTCACTCCTCTTAGTGAC	Internal primers
WF10 PB2 1381F	GAACCCATCGACAATGT CATG	Internal primers
Ba-PB2-1768F	TATTGGTCTCAGGGACAATCCTTGGTACCTA	Internal primers
WF10PB1-1195WTF	CGAGAAAGAAAATTGAGAAAATAAGACCTC	Internal primers
WF10PB1-1766WTR	CTTTGAGCGGGTCTGCTCCCACAGCTTCTTCAA	Internal primers
PB1 419R	GTCCAATCATAAGTCTGGC	Internal primers
Bm-PB1-1473F	TATTCGTCTCAGGGACATAAATAGGACAGG	Internal primers
BmPB1-620F	TATTCGTCTCTGGTCACACAAAGAACAATAG	Internal primers
PA735F	AACCGAACGGCTGCATTGAGGGC	Internal primers
PA1769R	ATCATGCTCTCAATCTGTTG	Internal primers
PA336R	CTTGGGCTTCTCAACCCCG	Internal primers
PA-1807F	AGCATGATTGAGGCCGAGTC	Internal primers
PA-930-953F	CCACTATACGATGCAATCAAATGC	Internal primers
Sw HA 752F	TAGAGCCGGGAGACAAAATAACAT	Internal primers
Sw HA 1213F	ACACAGTTCACAGCAGTAGGTAAA	Internal primers
Sw HA 931R	TCTGAAATGGGAGGCTGGTGTT	Internal primers
Sw HA 521R	GGATTTGCTGAGCTTTGGGTATG	Internal primers
NP-700F	GCACAAAGAGCAATGATGGA	Internal primers
NP-446R	GTGAGACCAGCAGTTGCGTCTTCTCCATTGTTCCG	Internal primers
NP529F	AGAATGTGCTCTCTGATGCAAGG	Internal primers
NP669R	CTCCAGAAGTTCCGGTCATT	Internal primers
Sw NA 949F	ATATGCAGTGGGATTTTCGGAGAC	Internal primers
Sw NA 1022R	ACCCTTTTACTCCATTTGCTCCAT	Internal primers
Sw NA 451R	GGGTTCGATATGGGCTCCTGTC	Internal primers
M-772F	GCGATTCAAGTGATCCTCTCGTTA	Internal primers
M-915R	CTCCTTCCGTAGAAGGCCCTC	Internal primers
NS1_294-313F	GTCAAGGGATTGGTTAATGC	Internal primers
pCAG 2066-2085R	GGTCCACTCTAATGCAAAGG	Internal primers

Bibliography

1. Presti RM, Zhao G, Beatty WL, Mihindukulasuriya KA, da Rosa AP, et al. (2009) Quarantil, Johnston Atoll, and Lake Chad viruses are novel members of the family Orthomyxoviridae. *J Virol* 83: 11599-11606.
2. Hay AJ, Gregory V, Douglas AR, Lin YP (2001) The evolution of human influenza viruses. *Philos Trans R Soc Lond B Biol Sci* 356: 1861-1870.
3. Osterhaus AD, Rimmelzwaan GF, Martina BE, Bestebroer TM, Fouchier RA (2000) Influenza B virus in seals. *Science* 288: 1051-1053.
4. Jakeman KJ, Tisdale M, Russell S, Leone A, Sweet C (1994) Efficacy of 2'-deoxy-2'-fluororibosides against influenza A and B viruses in ferrets. *Antimicrob Agents Chemother* 38: 1864-1867.
5. Youzbashi E, Marschall M, Chaloupka I, Meier-Ewert H (1996) [Distribution of influenza C virus infection in dogs and pigs in Bavaria]. *Tierarztl Prax* 24: 337-342.
6. Cox NJ, Subbarao K (2000) Global epidemiology of influenza: past and present. *Annu Rev Med* 51: 407-421.
7. Organization WH (2011) Pandemic influenza A (H1N1).
http://www.who.int/csr/resources/publications/swineflu/h1n1_donor_032011.pdf.
8. Abdel-Ghafar AN, Chotpitayasunondh T, Gao Z, Hayden FG, Nguyen DH, et al. (2008) Update on avian influenza A (H5N1) virus infection in humans. *N Engl J Med* 358: 261-273.
9. Chen W, Calvo PA, Malide D, Gibbs J, Schubert U, et al. (2001) A novel influenza A virus mitochondrial protein that induces cell death. *Nat Med* 7: 1306-1312.
10. Wise HM, Foeglein A, Sun J, Dalton RM, Patel S, et al. (2009) A complicated message: Identification of a novel PB1-related protein translated from influenza A virus segment 2 mRNA. *J Virol* 83: 8021-8031.
11. Yewdell JW, Ince WL Virology. Frameshifting to PA-X influenza. *Science* 337: 164-165.

12. Klenk E, Faillard H, Lempfrid H (1955) [Enzymatic effect of the influenza virus]. *Hoppe Seylers Z Physiol Chem* 301: 235-246.
13. Gottschalk A (1957) Neuraminidase: the specific enzyme of influenza virus and *Vibrio cholerae*. *Biochim Biophys Acta* 23: 645-646.
14. Calisher CH, Childs JE, Field HE, Holmes KV, Schountz T (2006) Bats: important reservoir hosts of emerging viruses. *Clin Microbiol Rev* 19: 531-545.
15. Rohm C, Zhou N, Suss J, Mackenzie J, Webster RG (1996) Characterization of a novel influenza hemagglutinin, H15: criteria for determination of influenza A subtypes. *Virology* 217: 508-516.
16. Webster RG, Berton MT (1981) Analysis of antigenic drift in the haemagglutinin molecule of influenza B virus with monoclonal antibodies. *J Gen Virol* 54: 243-251.
17. Skehel JJ, Wiley DC (2000) Receptor binding and membrane fusion in virus entry: the influenza hemagglutinin. *Annu Rev Biochem* 69: 531-569.
18. Crosby AW (1989) America's Forgotten Pandemic: The Influenza of 1918.
19. Potter CW (2001) A history of influenza. *J Appl Microbiol* 91: 572-579.
20. Taubenberger JK (2006) The origin and virulence of the 1918 "Spanish" influenza virus. *Proc Am Philos Soc* 150: 86-112.
21. Tscherne DM, Garcia-Sastre A (2011) Virulence determinants of pandemic influenza viruses. *J Clin Invest* 121: 6-13.
22. Medina RA, Garcia-Sastre A (2011) Influenza A viruses: new research developments. *Nat Rev Microbiol* 9: 590-603.
23. Goldsmith C (2007) Influenza: The Next Pandemic?
24. Starling A (2006) Plague, SARS, and the Story of Medicine in Hong Kong.
25. Paul WE (1993) *Fundamental Immunology*.
26. World Health Organization (2009) Characteristics of the emergent influenza A (h1N1) and viruses and recommendations for vaccine development. <http://www.who.int/csr/resources/publications/swineflu/H1N1Vaccinevirusrecommendation26May2009.pdf>.

27. Dunham EJ, Dugan VG, Kaser EK, Perkins SE, Brown IH, et al. (2009) Different evolutionary trajectories of European avian-like and classical swine H1N1 influenza A viruses. *J Virol* 83: 5485-5494.
28. Garten RJ, Davis CT, Russell CA, Shu B, Lindstrom S, et al. (2009) Antigenic and genetic characteristics of swine-origin 2009 A(H1N1) influenza viruses circulating in humans. *Science* 325: 197-201.
29. Sims LD, Ellis TM, Liu KK, Dyrting K, Wong H, et al. (2003) Avian influenza in Hong Kong 1997-2002. *Avian Dis* 47: 832-838.
30. Ku AS, Chan LT (1999) The first case of H5N1 avian influenza infection in a human with complications of adult respiratory distress syndrome and Reye's syndrome. *J Paediatr Child Health* 35: 207-209.
31. Webster RG, Peiris M, Chen H, Guan Y (2006) H5N1 outbreaks and enzootic influenza. *Emerg Infect Dis* 12: 3-8.
32. Peiris JS, Yu WC, Leung CW, Cheung CY, Ng WF, et al. (2004) Re-emergence of fatal human influenza A subtype H5N1 disease. *Lancet* 363: 617-619.
33. World Health Organization (05 July, 2013) Cumulative number of confirmed human cases for avian influenza A(H5N1) reported to WHO, 2003–2013. http://www.who.int/influenza/human_animal_interface/EN_GIP_20130705CumulativeNumberH5N1cases_2.pdf.
34. MercoPress (2013) FAO urges readiness against possible major resurgence of H5N1 avian influenza. <http://en.mercopress.com/2011/08/31/fao-urges-readiness-against-possible-major-resurgence-of-h5n1-avian-influenza>.
35. Yang Y, Halloran ME, Sugimoto JD, Longini IM, Jr. (2007) Detecting human-to-human transmission of avian influenza A (H5N1). *Emerg Infect Dis* 13: 1348-1353.
36. Imai M, Watanabe T, Hatta M, Das SC, Ozawa M, et al. (2012) Experimental adaptation of an influenza H5 HA confers respiratory droplet transmission to a reassortant H5 HA/H1N1 virus in ferrets. *Nature* 486: 420-428.
37. Russell CA, Fonville JM, Brown AE, Burke DF, Smith DL, et al. (2012) The potential for respiratory droplet-transmissible A/H5N1 influenza virus to evolve in a mammalian host. *Science* 336: 1541-1547.
38. Gao R, Cao B, Hu Y, Feng Z, Wang D, et al. (2013) Human infection with a novel avian-origin influenza A (H7N9) virus. *N Engl J Med* 368: 1888-1897.

39. Wu Y, Gao GF (2013) Compiling of comprehensive data of human infections with novel influenza A (H7N9) virus. *Front Med*.
40. Van Ranst M, Lemey P (2013) Genesis of avian-origin H7N9 influenza A viruses. *Lancet* 381: 1883-1885.
41. Liu D, Shi W, Shi Y, Wang D, Xiao H, et al. (2013) Origin and diversity of novel avian influenza A H7N9 viruses causing human infection: phylogenetic, structural, and coalescent analyses. *Lancet* 381: 1926-1932.
42. Chen Y, Liang W, Yang S, Wu N, Gao H, et al. (2013) Human infections with the emerging avian influenza A H7N9 virus from wet market poultry: clinical analysis and characterisation of viral genome. *Lancet* 381: 1916-1925.
43. Kageyama T, Fujisaki S, Takashita E, Xu H, Yamada S, et al. (2013) Genetic analysis of novel avian A(H7N9) influenza viruses isolated from patients in China, February to April 2013. *Euro Surveill* 18: 20453.
44. Liu Q, Lu L, Sun Z, Chen GW, Wen Y, et al. (2013) Genomic signature and protein sequence analysis of a novel influenza A (H7N9) virus that causes an outbreak in humans in China. *Microbes Infect* 15: 432-439.
45. Qi X, Qian YH, Bao CJ, Guo XL, Cui LB, et al. (2013) Probable person to person transmission of novel avian influenza A (H7N9) virus in Eastern China, 2013: epidemiological investigation. *BMJ* 347: f4752.
46. Alexander DJ (2007) An overview of the epidemiology of avian influenza. *Vaccine* 25: 5637-5644.
47. Perez DR, Lim W, Seiler JP, Yi G, Peiris M, et al. (2003) Role of quail in the interspecies transmission of H9 influenza A viruses: molecular changes on HA that correspond to adaptation from ducks to chickens. *J Virol* 77: 3148-3156.
48. Dong G, Luo J, Zhang H, Wang C, Duan M, et al. (2011) Phylogenetic diversity and genotypical complexity of H9N2 influenza A viruses revealed by genomic sequence analysis. *PLoS One* 6: e17212.
49. Nicholson KG, Wood JM, Zambon M (2003) Influenza. *Lancet* 362: 1733-1745.
50. Alexander DJ (2000) A review of avian influenza in different bird species. *Vet Microbiol* 74: 3-13.

51. Alexander DJ (2008) Avian influenza - diagnosis. *Zoonoses Public Health* 55: 16-23.
52. Wiley DC, Skehel JJ (1987) The structure and function of the hemagglutinin membrane glycoprotein of influenza virus. *Annu Rev Biochem* 56: 365-394.
53. Tong S, Li Y, Rivaller P, Conrardy C, Castillo DA, et al. (2012) A distinct lineage of influenza A virus from bats. *Proc Natl Acad Sci U S A* 109: 4269-4274.
54. Fouchier RA, Munster V, Wallensten A, Bestebroer TM, Herfst S, et al. (2005) Characterization of a novel influenza A virus hemagglutinin subtype (H16) obtained from black-headed gulls. *J Virol* 79: 2814-2822.
55. Vareckova E, Mucha V, Kostolansky F HA2 glycopolypeptide of influenza A virus and antiviral immunity. *Acta Virol* 57: 247-256.
56. Du J, Cross TA, Zhou HX Recent progress in structure-based anti-influenza drug design. *Drug Discov Today* 17: 1111-1120.
57. Suarez DL Avian influenza: our current understanding. *Anim Health Res Rev* 11: 19-33.
58. Webster RG, Rott R (1987) Influenza virus A pathogenicity: the pivotal role of hemagglutinin. *Cell* 50: 665-666.
59. Ha Y, Stevens DJ, Skehel JJ, Wiley DC (2001) X-ray structures of H5 avian and H9 swine influenza virus hemagglutinins bound to avian and human receptor analogs. *Proc Natl Acad Sci U S A* 98: 11181-11186.
60. Stevens J, Blixt O, Tumpey TM, Taubenberger JK, Paulson JC, et al. (2006) Structure and receptor specificity of the hemagglutinin from an H5N1 influenza virus. *Science* 312: 404-410.
61. Yang H, Chen LM, Carney PJ, Donis RO, Stevens J Structures of receptor complexes of a North American H7N2 influenza hemagglutinin with a loop deletion in the receptor binding site. *PLoS Pathog* 6: e1001081.
62. Watowich SJ, Skehel JJ, Wiley DC (1994) Crystal structures of influenza virus hemagglutinin in complex with high-affinity receptor analogs. *Structure* 2: 719-731.
63. Weis W, Brown JH, Cusack S, Paulson JC, Skehel JJ, et al. (1988) Structure of the influenza virus haemagglutinin complexed with its receptor, sialic acid. *Nature* 333: 426-431.

64. Eisen MB, Sabesan S, Skehel JJ, Wiley DC (1997) Binding of the influenza A virus to cell-surface receptors: structures of five hemagglutinin-sialyloligosaccharide complexes determined by X-ray crystallography. *Virology* 232: 19-31.
65. Shinya K, Ebina M, Yamada S, Ono M, Kasai N, et al. (2006) Avian flu: influenza virus receptors in the human airway. *Nature* 440: 435-436.
66. Stevens J, Blixt O, Glaser L, Taubenberger JK, Palese P, et al. (2006) Glycan microarray analysis of the hemagglutinins from modern and pandemic influenza viruses reveals different receptor specificities. *J Mol Biol* 355: 1143-1155.
67. Rogers GN, D'Souza BL (1989) Receptor binding properties of human and animal H1 influenza virus isolates. *Virology* 173: 317-322.
68. Connor RJ, Kawaoka Y, Webster RG, Paulson JC (1994) Receptor specificity in human, avian, and equine H2 and H3 influenza virus isolates. *Virology* 205: 17-23.
69. Ito T, Couceiro JN, Kelm S, Baum LG, Krauss S, et al. (1998) Molecular basis for the generation in pigs of influenza A viruses with pandemic potential. *J Virol* 72: 7367-7373.
70. Soundararajan V, Tharakaraman K, Raman R, Raguram S, Shriver Z, et al. (2009) Extrapolating from sequence--the 2009 H1N1 'swine' influenza virus. *Nat Biotechnol* 27: 510-513.
71. Chen LM, Rivaller P, Hossain J, Carney P, Balish A, et al. Receptor specificity of subtype H1 influenza A viruses isolated from swine and humans in the United States. *Virology* 412: 401-410.
72. Matrosovich MN, Gambaryan AS, Teneberg S, Piskarev VE, Yamnikova SS, et al. (1997) Avian influenza A viruses differ from human viruses by recognition of sialyloligosaccharides and gangliosides and by a higher conservation of the HA receptor-binding site. *Virology* 233: 224-234.
73. Zhu X, Yu W, McBride R, Li Y, Chen LM, et al. (2013) Hemagglutinin homologue from H17N10 bat influenza virus exhibits divergent receptor-binding and pH-dependent fusion activities. *Proc Natl Acad Sci U S A* 110: 1458-1463.
74. Sun X, Shi Y, Lu X, He J, Gao F, et al. (2013) Bat-derived influenza hemagglutinin H17 does not bind canonical avian or human receptors and most likely uses a unique entry mechanism. *Cell Rep* 3: 769-778.

75. Srinivasan A, Viswanathan K, Raman R, Chandrasekaran A, Raguram S, et al. (2008) Quantitative biochemical rationale for differences in transmissibility of 1918 pandemic influenza A viruses. *Proc Natl Acad Sci U S A* 105: 2800-2805.
76. Medina RA, Rojas M, Tuin A, Huff S, Ferres M, et al. (2011) Development and characterization of a highly specific and sensitive SYBR green reverse transcriptase PCR assay for detection of the 2009 pandemic H1N1 influenza virus on the basis of sequence signatures. *J Clin Microbiol* 49: 335-344.
77. Wan H, Perez DR (2007) Amino acid 226 in the hemagglutinin of H9N2 influenza viruses determines cell tropism and replication in human airway epithelial cells. *J Virol* 81: 5181-5191.
78. Wan H, Sorrell EM, Song H, Hossain MJ, Ramirez-Nieto G, et al. (2008) Replication and transmission of H9N2 influenza viruses in ferrets: evaluation of pandemic potential. *PLoS One* 3: e2923.
79. Tharakaraman K, Jayaraman A, Raman R, Viswanathan K, Stebbins NW, et al. (2013) Glycan Receptor Binding of the Influenza A Virus H7N9 Hemagglutinin. *Cell* 153: 1486-1493.
80. Throsby M, van den Brink E, Jongeneelen M, Poon LL, Alard P, et al. (2008) Heterosubtypic neutralizing monoclonal antibodies cross-protective against H5N1 and H1N1 recovered from human IgM+ memory B cells. *PLoS One* 3: e3942.
81. Ekiert DC, Bhabha G, Elsliger MA, Friesen RH, Jongeneelen M, et al. (2009) Antibody recognition of a highly conserved influenza virus epitope. *Science* 324: 246-251.
82. Varghese JN, Colman PM (1991) Three-dimensional structure of the neuraminidase of influenza virus A/Tokyo/3/67 at 2.2 Å resolution. *J Mol Biol* 221: 473-486.
83. Webster RG, Laver WG (1967) Preparation and properties of antibody directed specifically against the neuraminidase of influenza virus. *J Immunol* 99: 49-55.
84. Matrosovich MN, Matrosovich TY, Gray T, Roberts NA, Klenk HD (2004) Neuraminidase is important for the initiation of influenza virus infection in human airway epithelium. *J Virol* 78: 12665-12667.

85. Baum LG, Paulson JC (1991) The N2 neuraminidase of human influenza virus has acquired a substrate specificity complementary to the hemagglutinin receptor specificity. *Virology* 180: 10-15.
86. Russell RJ, Haire LF, Stevens DJ, Collins PJ, Lin YP, et al. (2006) The structure of H5N1 avian influenza neuraminidase suggests new opportunities for drug design. *Nature* 443: 45-49.
87. Li Q, Sun X, Li Z, Liu Y, Vavricka CJ, et al. Structural and functional characterization of neuraminidase-like molecule N10 derived from bat influenza A virus. *Proc Natl Acad Sci U S A* 109: 18897-18902.
88. Zhu X, Yang H, Guo Z, Yu W, Carney PJ, et al. Crystal structures of two subtype N10 neuraminidase-like proteins from bat influenza A viruses reveal a diverged putative active site. *Proc Natl Acad Sci U S A* 109: 18903-18908.
89. Shtyrya YA, Mochalova LV, Bovin NV (2009) Influenza virus neuraminidase: structure and function. *Acta Naturae* 1: 26-32.
90. Colman PM, Tulip WR, Varghese JN, Tulloch PA, Baker AT, et al. (1989) Three-dimensional structures of influenza virus neuraminidase-antibody complexes. *Philos Trans R Soc Lond B Biol Sci* 323: 511-518.
91. Bossart-Whitaker P, Carson M, Babu YS, Smith CD, Laver WG, et al. (1993) Three-dimensional structure of influenza A N9 neuraminidase and its complex with the inhibitor 2-deoxy 2,3-dehydro-N-acetyl neuraminic acid. *J Mol Biol* 232: 1069-1083.
92. Hanessian S, Wang J, Montgomery D, Stoll V, Stewart KD, et al. (2002) Design, synthesis, and neuraminidase inhibitory activity of GS-4071 analogues that utilize a novel hydrophobic paradigm. *Bioorg Med Chem Lett* 12: 3425-3429.
93. Das K, Aramini JM, Ma LC, Krug RM, Arnold E (2010) Structures of influenza A proteins and insights into antiviral drug targets. *Nat Struct Mol Biol* 17: 530-538.
94. Takahashi T, Suzuki T, Hidari KI, Miyamoto D, Suzuki Y (2003) A molecular mechanism for the low-pH stability of sialidase activity of influenza A virus N2 neuraminidases. *FEBS Lett* 543: 71-75.
95. Hu Y, Lu S, Song Z, Wang W, Hao P, et al. (2013) Association between adverse clinical outcome in human disease caused by novel influenza A H7N9 virus and sustained viral shedding and emergence of antiviral resistance. *Lancet* 381: 2273-2279.

96. Sorrell EM, Song H, Pena L, Perez DR (2010) A 27-amino-acid deletion in the neuraminidase stalk supports replication of an avian H2N2 influenza A virus in the respiratory tract of chickens. *J Virol* 84: 11831-11840.
97. Obenauer JC, Denson J, Mehta PK, Su X, Mukatira S, et al. (2006) Large-scale sequence analysis of avian influenza isolates. *Science* 311: 1576-1580.
98. Hossain MJ, Hickman D, Perez DR (2008) Evidence of expanded host range and mammalian-associated genetic changes in a duck H9N2 influenza virus following adaptation in quail and chickens. *PLoS One* 3: e3170.
99. Zhou H, Yu Z, Hu Y, Tu J, Zou W, et al. (2009) The special neuraminidase stalk-motif responsible for increased virulence and pathogenesis of H5N1 influenza A virus. *PLoS One* 4: e6277.
100. Matrosovich M, Tuzikov A, Bovin N, Gambaryan A, Klimov A, et al. (2000) Early alterations of the receptor-binding properties of H1, H2, and H3 avian influenza virus hemagglutinins after their introduction into mammals. *J Virol* 74: 8502-8512.
101. Bao Y, Bolotov P, Dernovoy D, Kiryutin B, Zaslavsky L, et al. (2008) The influenza virus resource at the National Center for Biotechnology Information. *J Virol* 82: 596-601.
102. Wang Y, Dai Z, Cheng H, Liu Z, Pan Z, et al. (2013) Towards a better understanding of the novel avian-origin H7N9 influenza A virus in China. *Sci Rep* 3: 2318.
103. Wang CC, Chen JR, Tseng YC, Hsu CH, Hung YF, et al. (2009) Glycans on influenza hemagglutinin affect receptor binding and immune response. *Proc Natl Acad Sci U S A* 106: 18137-18142.
104. Matrosovich M, Zhou N, Kawaoka Y, Webster R (1999) The surface glycoproteins of H5 influenza viruses isolated from humans, chickens, and wild aquatic birds have distinguishable properties. *J Virol* 73: 1146-1155.
105. Martin K, Helenius A (1991) Nuclear transport of influenza virus ribonucleoproteins: the viral matrix protein (M1) promotes export and inhibits import. *Cell* 67: 117-130.
106. Gomez-Puertas P, Albo C, Perez-Pastrana E, Vivo A, Portela A (2000) Influenza virus matrix protein is the major driving force in virus budding. *J Virol* 74: 11538-11547.

107. Arzt S, Baudin F, Barge A, Timmins P, Burmeister WP, et al. (2001) Combined results from solution studies on intact influenza virus M1 protein and from a new crystal form of its N-terminal domain show that M1 is an elongated monomer. *Virology* 279: 439-446.
108. Hui EK, Barman S, Yang TY, Nayak DP (2003) Basic residues of the helix six domain of influenza virus M1 involved in nuclear translocation of M1 can be replaced by PTAP and YPDL late assembly domain motifs. *J Virol* 77: 7078-7092.
109. Liu T, Muller J, Ye Z (2002) Association of influenza virus matrix protein with ribonucleoproteins may control viral growth and morphology. *Virology* 304: 89-96.
110. Wang S, Zhao Z, Bi Y, Sun L, Liu X, et al. (2013) Tyrosine 132 phosphorylation of influenza A virus M1 protein is crucial for virus replication by controlling the nuclear import of M1. *J Virol* 87: 6182-6191.
111. Zhirnov OP, Klenk HD (1997) Histones as a target for influenza virus matrix protein M1. *Virology* 235: 302-310.
112. Boulo S, Akarsu H, Ruigrok RW, Baudin F (2007) Nuclear traffic of influenza virus proteins and ribonucleoprotein complexes. *Virus Res* 124: 12-21.
113. Cao S, Liu X, Yu M, Li J, Jia X, et al. (2012) A nuclear export signal in the matrix protein of Influenza A virus is required for efficient virus replication. *J Virol* 86: 4883-4891.
114. Bui M, Whittaker G, Helenius A (1996) Effect of M1 protein and low pH on nuclear transport of influenza virus ribonucleoproteins. *J Virol* 70: 8391-8401.
115. Das SC, Watanabe S, Hatta M, Noda T, Neumann G, et al. (2012) The highly conserved arginine residues at positions 76 through 78 of influenza A virus matrix protein M1 play an important role in viral replication by affecting the intracellular localization of M1. *J Virol* 86: 1522-1530.
116. Sharma M, Yi M, Dong H, Qin H, Peterson E, et al. Insight into the mechanism of the influenza A proton channel from a structure in a lipid bilayer. *Science* 330: 509-512.
117. Tang Y, Zaitseva F, Lamb RA, Pinto LH (2002) The gate of the influenza virus M2 proton channel is formed by a single tryptophan residue. *J Biol Chem* 277: 39880-39886.

118. Pinto LH, Dieckmann GR, Gandhi CS, Papworth CG, Braman J, et al. (1997) A functionally defined model for the M2 proton channel of influenza A virus suggests a mechanism for its ion selectivity. *Proc Natl Acad Sci U S A* 94: 11301-11306.
119. Schnell JR, Chou JJ (2008) Structure and mechanism of the M2 proton channel of influenza A virus. *Nature* 451: 591-595.
120. Yi M, Cross TA, Zhou HX (2008) A secondary gate as a mechanism for inhibition of the M2 proton channel by amantadine. *J Phys Chem B* 112: 7977-7979.
121. Stouffer AL, Acharya R, Salom D, Levine AS, Di Costanzo L, et al. (2008) Structural basis for the function and inhibition of an influenza virus proton channel. *Nature* 451: 596-599.
122. Hu J, Asbury T, Achuthan S, Li C, Bertram R, et al. (2007) Backbone structure of the amantadine-blocked trans-membrane domain M2 proton channel from Influenza A virus. *Biophys J* 92: 4335-4343.
123. Cady SD, Schmidt-Rohr K, Wang J, Soto CS, Degrado WF, et al. Structure of the amantadine binding site of influenza M2 proton channels in lipid bilayers. *Nature* 463: 689-692.
124. Stouffer AL, Ma C, Cristian L, Ohigashi Y, Lamb RA, et al. (2008) The interplay of functional tuning, drug resistance, and thermodynamic stability in the evolution of the M2 proton channel from the influenza A virus. *Structure* 16: 1067-1076.
125. Wang J, Wu Y, Ma C, Fiorin G, Pinto LH, et al. Structure and inhibition of the drug-resistant S31N mutant of the M2 ion channel of influenza A virus. *Proc Natl Acad Sci U S A* 110: 1315-1320.
126. Abed Y, Goyette N, Boivin G (2005) Generation and characterization of recombinant influenza A (H1N1) viruses harboring amantadine resistance mutations. *Antimicrob Agents Chemother* 49: 556-559.
127. Cheung CL, Rayner JM, Smith GJ, Wang P, Naipospos TS, et al. (2006) Distribution of amantadine-resistant H5N1 avian influenza variants in Asia. *J Infect Dis* 193: 1626-1629.
128. Pielak RM, Schnell JR, Chou JJ (2009) Mechanism of drug inhibition and drug resistance of influenza A M2 channel. *Proc Natl Acad Sci U S A* 106: 7379-7384.

129. Turrell L, Lyall JW, Tiley LS, Fodor E, Vreede FT (2013) The role and assembly mechanism of nucleoprotein in influenza A virus ribonucleoprotein complexes. *Nat Commun* 4: 1591.
130. Shen YF, Chen YH, Chu SY, Lin MI, Hsu HT, et al. (2011) E339...R416 salt bridge of nucleoprotein as a feasible target for influenza virus inhibitors. *Proc Natl Acad Sci U S A* 108: 16515-16520.
131. Neumann G, Castrucci MR, Kawaoka Y (1997) Nuclear import and export of influenza virus nucleoprotein. *J Virol* 71: 9690-9700.
132. Cros JF, Garcia-Sastre A, Palese P (2005) An unconventional NLS is critical for the nuclear import of the influenza A virus nucleoprotein and ribonucleoprotein. *Traffic* 6: 205-213.
133. Ketha KM, Atreya CD (2008) Application of bioinformatics-coupled experimental analysis reveals a new transport-competent nuclear localization signal in the nucleoprotein of influenza A virus strain. *BMC Cell Biol* 9: 22.
134. Dias A, Bouvier D, Crepin T, McCarthy AA, Hart DJ, et al. (2009) The cap-snatching endonuclease of influenza virus polymerase resides in the PA subunit. *Nature* 458: 914-918.
135. Obayashi E, Yoshida H, Kawai F, Shibayama N, Kawaguchi A, et al. (2008) The structural basis for an essential subunit interaction in influenza virus RNA polymerase. *Nature* 454: 1127-1131.
136. Yuan P, Bartlam M, Lou Z, Chen S, Zhou J, et al. (2009) Crystal structure of an avian influenza polymerase PA(N) reveals an endonuclease active site. *Nature* 458: 909-913.
137. He X, Zhou J, Bartlam M, Zhang R, Ma J, et al. (2008) Crystal structure of the polymerase PA(C)-PB1(N) complex from an avian influenza H5N1 virus. *Nature* 454: 1123-1126.
138. Crepin T, Dias A, Palencia A, Swale C, Cusack S, et al. Mutational and metal binding analysis of the endonuclease domain of the influenza virus polymerase PA subunit. *J Virol* 84: 9096-9104.
139. Shi L, Summers DF, Peng Q, Galarz JM (1995) Influenza A virus RNA polymerase subunit PB2 is the endonuclease which cleaves host cell mRNA and functions only as the trimeric enzyme. *Virology* 208: 38-47.

140. Sanz-Ezquerro JJ, de la Luna S, Ortin J, Nieto A (1995) Individual expression of influenza virus PA protein induces degradation of coexpressed proteins. *J Virol* 69: 2420-2426.
141. Flint SJ (2004) *Principles of Virology*.
142. Perez DR, Donis RO (2001) Functional analysis of PA binding by influenza A virus PB1: effects on polymerase activity and viral infectivity. *J Virol* 75: 8127-8136.
143. Huarte M, Falcon A, Nakaya Y, Ortin J, Garcia-Sastre A, et al. (2003) Threonine 157 of influenza virus PA polymerase subunit modulates RNA replication in infectious viruses. *J Virol* 77: 6007-6013.
144. Wanitchang A, Jengarn J, Jongkaewwattana A The N terminus of PA polymerase of swine-origin influenza virus H1N1 determines its compatibility with PB2 and PB1 subunits through a strain-specific amino acid serine 186. *Virus Res* 155: 325-333.
145. Kashiwagi T, Hara K, Nakazono Y, Hamada N, Watanabe H Artificial hybrids of influenza A virus RNA polymerase reveal PA subunit modulates its thermal sensitivity. *PLoS One* 5: e15140.
146. Chu C, Fan S, Li C, Macken C, Kim JH, et al. (2012) Functional analysis of conserved motifs in influenza virus PB1 protein. *PLoS One* 7: e36113.
147. Biswas SK, Nayak DP (1996) Influenza virus polymerase basic protein 1 interacts with influenza virus polymerase basic protein 2 at multiple sites. *J Virol* 70: 6716-6722.
148. Boivin S, Cusack S, Ruigrok RW, Hart DJ (2010) Influenza A virus polymerase: structural insights into replication and host adaptation mechanisms. *J Biol Chem* 285: 28411-28417.
149. Tarendeau F, Boudet J, Guilligay D, Mas PJ, Bougault CM, et al. (2007) Structure and nuclear import function of the C-terminal domain of influenza virus polymerase PB2 subunit. *Nat Struct Mol Biol* 14: 229-233.
150. Fontes MR, Teh T, Jans D, Brinkworth RI, Kobe B (2003) Structural basis for the specificity of bipartite nuclear localization sequence binding by importin- α . *J Biol Chem* 278: 27981-27987.
151. Ruigrok RW, Crepin T, Hart DJ, Cusack S (2010) Towards an atomic resolution understanding of the influenza virus replication machinery. *Curr Opin Struct Biol* 20: 104-113.

152. Kuzuhara T, Kise D, Yoshida H, Horita T, Murazaki Y, et al. (2009) Structural basis of the influenza A virus RNA polymerase PB2 RNA-binding domain containing the pathogenicity-determinant lysine 627 residue. *J Biol Chem* 284: 6855-6860.
153. Tarendeau F, Crepin T, Guilligay D, Ruigrok RW, Cusack S, et al. (2008) Host determinant residue lysine 627 lies on the surface of a discrete, folded domain of influenza virus polymerase PB2 subunit. *PLoS Pathog* 4: e1000136.
154. Hatta M, Gao P, Halfmann P, Kawaoka Y (2001) Molecular basis for high virulence of Hong Kong H5N1 influenza A viruses. *Science* 293: 1840-1842.
155. Hatta M, Hatta Y, Kim JH, Watanabe S, Shinya K, et al. (2007) Growth of H5N1 influenza A viruses in the upper respiratory tracts of mice. *PLoS Pathog* 3: 1374-1379.
156. de Jong MD, Hien TT (2006) Avian influenza A (H5N1). *J Clin Virol* 35: 2-13.
157. Gabriel G, Herwig A, Klenk HD (2008) Interaction of polymerase subunit PB2 and NP with importin alpha1 is a determinant of host range of influenza A virus. *PLoS Pathog* 4: e11.
158. Mehle A, Doudna JA (2009) Adaptive strategies of the influenza virus polymerase for replication in humans. *Proc Natl Acad Sci U S A* 106: 21312-21316.
159. Treanor JJ, Snyder MH, London WT, Murphy BR (1989) The B allele of the NS gene of avian influenza viruses, but not the A allele, attenuates a human influenza A virus for squirrel monkeys. *Virology* 171: 1-9.
160. Hale BG, Randall RE, Ortin J, Jackson D (2008) The multifunctional NS1 protein of influenza A viruses. *J Gen Virol* 89: 2359-2376.
161. Liu J, Lynch PA, Chien CY, Montelione GT, Krug RM, et al. (1997) Crystal structure of the unique RNA-binding domain of the influenza virus NS1 protein. *Nat Struct Biol* 4: 896-899.
162. Wang W, Riedel K, Lynch P, Chien CY, Montelione GT, et al. (1999) RNA binding by the novel helical domain of the influenza virus NS1 protein requires its dimer structure and a small number of specific basic amino acids. *RNA* 5: 195-205.

163. Bornholdt ZA, Prasad BV (2006) X-ray structure of influenza virus NS1 effector domain. *Nat Struct Mol Biol* 13: 559-560.
164. Bornholdt ZA, Prasad BV (2008) X-ray structure of NS1 from a highly pathogenic H5N1 influenza virus. *Nature* 456: 985-988.
165. Melen K, Kinnunen L, Fagerlund R, Ikonen N, Twu KY, et al. (2007) Nuclear and nucleolar targeting of influenza A virus NS1 protein: striking differences between different virus subtypes. *J Virol* 81: 5995-6006.
166. Han H, Cui ZQ, Wang W, Zhang ZP, Wei HP, et al. New regulatory mechanisms for the intracellular localization and trafficking of influenza A virus NS1 protein revealed by comparative analysis of A/PR/8/34 and A/Sydney/5/97. *J Gen Virol* 91: 2907-2917.
167. Li Y, Yamakita Y, Krug RM (1998) Regulation of a nuclear export signal by an adjacent inhibitory sequence: the effector domain of the influenza virus NS1 protein. *Proc Natl Acad Sci U S A* 95: 4864-4869.
168. Talon J, Horvath CM, Polley R, Basler CF, Muster T, et al. (2000) Activation of interferon regulatory factor 3 is inhibited by the influenza A virus NS1 protein. *J Virol* 74: 7989-7996.
169. Ludwig S, Wang X, Ehrhardt C, Zheng H, Donelan N, et al. (2002) The influenza A virus NS1 protein inhibits activation of Jun N-terminal kinase and AP-1 transcription factors. *J Virol* 76: 11166-11171.
170. Chen Z, Li Y, Krug RM (1999) Influenza A virus NS1 protein targets poly(A)-binding protein II of the cellular 3'-end processing machinery. *EMBO J* 18: 2273-2283.
171. Li Y, Chen ZY, Wang W, Baker CC, Krug RM (2001) The 3'-end-processing factor CPSF is required for the splicing of single-intron pre-mRNAs in vivo. *RNA* 7: 920-931.
172. Pichlmair A, Schulz O, Tan CP, Naslund TI, Liljestrom P, et al. (2006) RIG-I-mediated antiviral responses to single-stranded RNA bearing 5'-phosphates. *Science* 314: 997-1001.
173. Guo Z, Chen LM, Zeng H, Gomez JA, Plowden J, et al. (2007) NS1 protein of influenza A virus inhibits the function of intracytoplasmic pathogen sensor, RIG-I. *Am J Respir Cell Mol Biol* 36: 263-269.
174. Opitz B, Rejaibi A, Dauber B, Eckhard J, Vinzing M, et al. (2007) IFNbeta induction by influenza A virus is mediated by RIG-I which is regulated by the viral NS1 protein. *Cell Microbiol* 9: 930-938.

175. Gack MU, Albrecht RA, Urano T, Inn KS, Huang IC, et al. (2009) Influenza A virus NS1 targets the ubiquitin ligase TRIM25 to evade recognition by the host viral RNA sensor RIG-I. *Cell Host Microbe* 5: 439-449.
176. Imai H, Shinya K, Takano R, Kiso M, Muramoto Y, et al. The HA and NS genes of human H5N1 influenza A virus contribute to high virulence in ferrets. *PLoS Pathog* 6: e1001106.
177. Jia D, Rahbar R, Chan RW, Lee SM, Chan MC, et al. Influenza virus non-structural protein 1 (NS1) disrupts interferon signaling. *PLoS One* 5: e13927.
178. Zhao C, Hsiang TY, Kuo RL, Krug RM ISG15 conjugation system targets the viral NS1 protein in influenza A virus-infected cells. *Proc Natl Acad Sci U S A* 107: 2253-2258.
179. Toro H, Tang DC, Suarez DL, Sylte MJ, Pfeiffer J, et al. (2007) Protective avian influenza in ovo vaccination with non-replicating human adenovirus vector. *Vaccine* 25: 2886-2891.
180. Cooray S (2004) The pivotal role of phosphatidylinositol 3-kinase-Akt signal transduction in virus survival. *J Gen Virol* 85: 1065-1076.
181. Garcia-Sastre A, Egorov A, Matasov D, Brandt S, Levy DE, et al. (1998) Influenza A virus lacking the NS1 gene replicates in interferon-deficient systems. *Virology* 252: 324-330.
182. Krug RM, Yuan W, Noah DL, Latham AG (2003) Intracellular warfare between human influenza viruses and human cells: the roles of the viral NS1 protein. *Virology* 309: 181-189.
183. Cantley LC (2002) The phosphoinositide 3-kinase pathway. *Science* 296: 1655-1657.
184. Yu J, Zhang Y, McIlroy J, Rordorf-Nikolic T, Orr GA, et al. (1998) Regulation of the p85/p110 phosphatidylinositol 3'-kinase: stabilization and inhibition of the p110 α catalytic subunit by the p85 regulatory subunit. *Mol Cell Biol* 18: 1379-1387.
185. Eierhoff T, Hrincius ER, Rescher U, Ludwig S, Ehrhardt C (2010) The epidermal growth factor receptor (EGFR) promotes uptake of influenza A viruses (IAV) into host cells. *PLoS Pathog* 6: e1001099.
186. Eierhoff T, Hrincius ER, Rescher U, Ludwig S, Ehrhardt C The epidermal growth factor receptor (EGFR) promotes uptake of influenza A viruses (IAV) into host cells. *PLoS Pathog* 6: e1001099.

187. Hrinčius ER, Dierkes R, Anhlan D, Wixler V, Ludwig S, et al. Phosphatidylinositol-3-kinase (PI3K) is activated by influenza virus vRNA via the pathogen pattern receptor Rig-I to promote efficient type I interferon production. *Cell Microbiol* 13: 1907-1919.
188. Hale BG, Barclay WS, Randall RE, Russell RJ (2008) Structure of an avian influenza A virus NS1 protein effector domain. *Virology* 378: 1-5.
189. Li Y, Anderson DH, Liu Q, Zhou Y (2008) Mechanism of influenza A virus NS1 protein interaction with the p85beta, but not the p85alpha, subunit of phosphatidylinositol 3-kinase (PI3K) and up-regulation of PI3K activity. *J Biol Chem* 283: 23397-23409.
190. Matsuda M, Suizu F, Hirata N, Miyazaki T, Obuse C, et al. Characterization of the interaction of influenza virus NS1 with Akt. *Biochem Biophys Res Commun* 395: 312-317.
191. Enami K, Sato TA, Nakada S, Enami M (1994) Influenza virus NS1 protein stimulates translation of the M1 protein. *J Virol* 68: 1432-1437.
192. Min JY, Krug RM (2006) The primary function of RNA binding by the influenza A virus NS1 protein in infected cells: Inhibiting the 2'-5' oligo (A) synthetase/RNase L pathway. *Proc Natl Acad Sci U S A* 103: 7100-7105.
193. Li S, Min JY, Krug RM, Sen GC (2006) Binding of the influenza A virus NS1 protein to PKR mediates the inhibition of its activation by either PACT or double-stranded RNA. *Virology* 349: 13-21.
194. Soubies SM, Volmer C, Croville G, Loupias J, Peralta B, et al. Species-specific contribution of the four C-terminal amino acids of influenza A virus NS1 protein to virulence. *J Virol* 84: 6733-6747.
195. Liu H, Golebiewski L, Dow EC, Krug RM, Javier RT, et al. The ESEV PDZ-binding motif of the avian influenza A virus NS1 protein protects infected cells from apoptosis by directly targeting Scribble. *J Virol* 84: 11164-11174.
196. Zielecki F, Semmler I, Kalthoff D, Voss D, Mael S, et al. Virulence determinants of avian H5N1 influenza A virus in mammalian and avian hosts: role of the C-terminal ESEV motif in the viral NS1 protein. *J Virol* 84: 10708-10718.
197. Steidle S, Martinez-Sobrido L, Mordstein M, Lienenklaus S, Garcia-Sastre A, et al. Glycine 184 in nonstructural protein NS1 determines the

virulence of influenza A virus strain PR8 without affecting the host interferon response. *J Virol* 84: 12761-12770.

198. Wang Z, Robb NC, Lenz E, Wolff T, Fodor E, et al. NS reassortment of an H7-type highly pathogenic avian influenza virus affects its propagation by altering the regulation of viral RNA production and antiviral host response. *J Virol* 84: 11323-11335.
199. Keiner B, Maenz B, Wagner R, Cattoli G, Capua I, et al. Intracellular distribution of NS1 correlates with the infectivity and interferon antagonism of an avian influenza virus (H7N1). *J Virol* 84: 11858-11865.
200. Tu J, Guo J, Zhang A, Zhang W, Zhao Z, et al. Effects of the C-terminal truncation in NS1 protein of the 2009 pandemic H1N1 influenza virus on host gene expression. *PLoS One* 6: e26175.
201. Lamb DJ, Wagle JR, Tsai YH, Lee AL, Steinberger A, et al. (1982) Specificity and nature of the rapid steroid-stimulated increase in Sertoli cell nuclear RNA polymerase activity. *J Steroid Biochem* 16: 653-669.
202. Richardson JC, Akkina RK (1991) NS2 protein of influenza virus is found in purified virus and phosphorylated in infected cells. *Arch Virol* 116: 69-80.
203. Yasuda J, Nakada S, Kato A, Toyoda T, Ishihama A (1993) Molecular assembly of influenza virus: association of the NS2 protein with virion matrix. *Virology* 196: 249-255.
204. Akarsu H, Burmeister WP, Petosa C, Petit I, Muller CW, et al. (2003) Crystal structure of the M1 protein-binding domain of the influenza A virus nuclear export protein (NEP/NS2). *EMBO J* 22: 4646-4655.
205. Iwatsuki-Horimoto K, Horimoto T, Fujii Y, Kawaoka Y (2004) Generation of influenza A virus NS2 (NEP) mutants with an altered nuclear export signal sequence. *J Virol* 78: 10149-10155.
206. Akarsu H, Iwatsuki-Horimoto K, Noda T, Kawakami E, Katsura H, et al. Structure-based design of NS2 mutants for attenuated influenza A virus vaccines. *Virus Res* 155: 240-248.
207. Paterson D, Fodor E (2012) Emerging roles for the influenza A virus nuclear export protein (NEP). *PLoS Pathog* 8: e1003019.
208. Hutchinson EC, Denham EM, Thomas B, Trudgian DC, Hester SS, et al. (2012) Mapping the phosphoproteome of influenza A and B viruses by mass spectrometry. *PLoS Pathog* 8: e1002993.

209. Pal S, Santos A, Rosas JM, Ortiz-Guzman J, Rosas-Acosta G (2011) Influenza A virus interacts extensively with the cellular SUMOylation system during infection. *Virus Res* 158: 12-27.
210. Lakadamyali M, Rust MJ, Zhuang X (2004) Endocytosis of influenza viruses. *Microbes Infect* 6: 929-936.
211. Wharton SA, Belshe RB, Skehel JJ, Hay AJ (1994) Role of virion M2 protein in influenza virus uncoating: specific reduction in the rate of membrane fusion between virus and liposomes by amantadine. *J Gen Virol* 75 (Pt 4): 945-948.
212. Sasaki Y, Hagiwara K, Kakisaka M, Yamada K, Murakami T, et al. (2013) Importin alpha3/Qip1 is involved in multiplication of mutant influenza virus with alanine mutation at amino acid 9 independently of nuclear transport function. *PLoS One* 8: e55765.
213. Luo GX, Luytjes W, Enami M, Palese P (1991) The polyadenylation signal of influenza virus RNA involves a stretch of uridines followed by the RNA duplex of the panhandle structure. *J Virol* 65: 2861-2867.
214. Zhang S, Wang J, Wang Q, Toyoda T (2010) Internal initiation of influenza virus replication of viral RNA and complementary RNA in vitro. *J Biol Chem* 285: 41194-41201.
215. Gabriel G, Klingel K, Otte A, Thiele S, Hudjetz B, et al. (2011) Differential use of importin-alpha isoforms governs cell tropism and host adaptation of influenza virus. *Nat Commun* 2: 156.
216. Perez JT, Zlatev I, Aggarwal S, Subramanian S, Sachidanandam R, et al. (2012) A small-RNA enhancer of viral polymerase activity. *J Virol* 86: 13475-13485.
217. Lu Y, Qian XY, Krug RM (1994) The influenza virus NS1 protein: a novel inhibitor of pre-mRNA splicing. *Genes Dev* 8: 1817-1828.
218. Robb NC, Smith M, Vreede FT, Fodor E (2009) NS2/NEP protein regulates transcription and replication of the influenza virus RNA genome. *J Gen Virol* 90: 1398-1407.
219. Manz B, Brunotte L, Reuther P, Schwemmler M (2012) Adaptive mutations in NEP compensate for defective H5N1 RNA replication in cultured human cells. *Nat Commun* 3: 802.
220. Paterson D, Fodor E Emerging roles for the influenza A virus nuclear export protein (NEP). *PLoS Pathog* 8: e1003019.

221. Elton D, Simpson-Holley M, Archer K, Medcalf L, Hallam R, et al. (2001) Interaction of the influenza virus nucleoprotein with the cellular CRM1-mediated nuclear export pathway. *J Virol* 75: 408-419.
222. Alamares-Sapuay JG, Martinez-Gil L, Stertz S, Miller MS, Shaw ML, et al. (2013) Serum- and glucocorticoid-regulated kinase 1 is required for nuclear export of the ribonucleoprotein of influenza A virus. *J Virol* 87: 6020-6026.
223. Wu Y, Guo Z, Wu H, Wang X, Yang L, et al. (2012) SUMOylation represses Nanog expression via modulating transcription factors Oct4 and Sox2. *PLoS One* 7: e39606.
224. Hirayama E, Atagi H, Hiraki A, Kim J (2004) Heat shock protein 70 is related to thermal inhibition of nuclear export of the influenza virus ribonucleoprotein complex. *J Virol* 78: 1263-1270.
225. Watanabe T, Watanabe S, Kawaoka Y (2010) Cellular networks involved in the influenza virus life cycle. *Cell Host Microbe* 7: 427-439.
226. Rossman JS, Jing X, Leser GP, Lamb RA (2010) Influenza virus M2 protein mediates ESCRT-independent membrane scission. *Cell* 142: 902-913.
227. Hutchinson EC, von Kirchbach JC, Gog JR, Digard P Genome packaging in influenza A virus. *J Gen Virol* 91: 313-328.
228. Chou YY, Vafabakhsh R, Doganay S, Gao Q, Ha T, et al. (2012) One influenza virus particle packages eight unique viral RNAs as shown by FISH analysis. *Proc Natl Acad Sci U S A* 109: 9101-9106.
229. Liang Y, Hong Y, Parslow TG (2005) cis-Acting packaging signals in the influenza virus PB1, PB2, and PA genomic RNA segments. *J Virol* 79: 10348-10355.
230. Watanabe T, Watanabe S, Noda T, Fujii Y, Kawaoka Y (2003) Exploitation of nucleic acid packaging signals to generate a novel influenza virus-based vector stably expressing two foreign genes. *J Virol* 77: 10575-10583.
231. Fujii Y, Goto H, Watanabe T, Yoshida T, Kawaoka Y (2003) Selective incorporation of influenza virus RNA segments into virions. *Proc Natl Acad Sci U S A* 100: 2002-2007.
232. Gorai T, Goto H, Noda T, Watanabe T, Kozuka-Hata H, et al. (2012) F1Fo-ATPase, F-type proton-translocating ATPase, at the plasma membrane is critical for efficient influenza virus budding. *Proc Natl Acad Sci U S A* 109: 4615-4620.

233. Soubies SM, Volmer C, Croville G, Loupiau J, Peralta B, et al. (2010) Species-specific contribution of the four C-terminal amino acids of influenza A virus NS1 protein to virulence. *J Virol* 84: 6733-6747.
234. Nemeroff ME, Barabino SM, Li Y, Keller W, Krug RM (1998) Influenza virus NS1 protein interacts with the cellular 30 kDa subunit of CPSF and inhibits 3'end formation of cellular pre-mRNAs. *Mol Cell* 1: 991-1000.
235. Kainov DE, Muller KH, Theisen LL, Anastasina M, Kaloinen M, et al. (2011) Differential effects of NS1 proteins of human pandemic H1N1/2009, avian highly pathogenic H5N1, and low pathogenic H5N2 influenza A viruses on cellular pre-mRNA polyadenylation and mRNA translation. *J Biol Chem* 286: 7239-7247.
236. Tu J, Guo J, Zhang A, Zhang W, Zhao Z, et al. (2011) Effects of the C-terminal truncation in NS1 protein of the 2009 pandemic H1N1 influenza virus on host gene expression. *PLoS One* 6: e26175.
237. Hayman A, Comely S, Lackenby A, Murphy S, McCauley J, et al. (2006) Variation in the ability of human influenza A viruses to induce and inhibit the IFN-beta pathway. *Virology* 347: 52-64.
238. Ayllon J, Hale BG, Garcia-Sastre A (2012) Strain-specific contribution of NS1-activated phosphoinositide 3-kinase signaling to influenza A virus replication and virulence. *J Virol* 86: 5366-5370.
239. Seo SH, Hoffmann E, Webster RG (2002) Lethal H5N1 influenza viruses escape host anti-viral cytokine responses. *Nat Med* 8: 950-954.
240. Davenport FM (1962) Current knowledge of influenza vaccine. *JAMA* 182: 11-13.
241. Francis T, Jr., Salk JE, Brace WM (1946) The protective effect of vaccination against epidemic influenza B. *J Am Med Assoc* 131: 275-278.
242. Wolf YI, Viboud C, Holmes EC, Koonin EV, Lipman DJ (2006) Long intervals of stasis punctuated by bursts of positive selection in the seasonal evolution of influenza A virus. *Biol Direct* 1: 34.
243. Fiore AE, Bridges CB, Cox NJ (2009) Seasonal influenza vaccines. *Curr Top Microbiol Immunol* 333: 43-82.
244. Novartis (2012) Novartis receives FDA approval for Flucelvax®, the first cell-culture vaccine in US to help protect against seasonal influenza.

245. Pollack A (2013) Rapid Produced Flu Vaccine Wins F.D.A. Approval. The New York Times.
246. Jin H, Zhou H, Liu H, Chan W, Adhikary L, et al. (2005) Two residues in the hemagglutinin of A/Fujian/411/02-like influenza viruses are responsible for antigenic drift from A/Panama/2007/99. *Virology* 336: 113-119.
247. Pada S, Tambyah PA (2011) Overview/reflections on the 2009 H1N1 pandemic. *Microbes Infect* 13: 470-478.
248. Parrish CR, Kawaoka Y (2005) The origins of new pandemic viruses: the acquisition of new host ranges by canine parvovirus and influenza A viruses. *Annu Rev Microbiol* 59: 553-586.
249. Peiris JS, de Jong MD, Guan Y (2007) Avian influenza virus (H5N1): a threat to human health. *Clin Microbiol Rev* 20: 243-267.
250. Webster RG, Govorkova EA (2006) H5N1 influenza--continuing evolution and spread. *N Engl J Med* 355: 2174-2177.
251. Parry J H7N9 avian flu infects humans for the first time. *BMJ* 346: f2151.
252. Gao R, Cao B, Hu Y, Feng Z, Wang D, et al. Human infection with a novel avian-origin influenza A (H7N9) virus. *N Engl J Med* 368: 1888-1897.
253. Swayne DE, Kapczynski D (2008) Strategies and challenges for eliciting immunity against avian influenza virus in birds. *Immunol Rev* 225: 314-331.
254. Song H, Nieto GR, Perez DR (2007) A new generation of modified live-attenuated avian influenza viruses using a two-strategy combination as potential vaccine candidates. *J Virol* 81: 9238-9248.
255. Hghihghi HR, Read LR, Mohammadi H, Pei Y, Ursprung C, et al. (2010) Characterization of host responses against a recombinant fowlpox virus-vectored vaccine expressing the hemagglutinin antigen of an avian influenza virus. *Clin Vaccine Immunol* 17: 454-463.
256. Lambert LC, Fauci AS Influenza vaccines for the future. *N Engl J Med* 363: 2036-2044.
257. Kang SM, Song JM, Compans RW Novel vaccines against influenza viruses. *Virus Res* 162: 31-38.

258. Jonges M, Liu WM, van der Vries E, Jacobi R, Pronk I, et al. (2010) Influenza virus inactivation for studies of antigenicity and phenotypic neuraminidase inhibitor resistance profiling. *J Clin Microbiol* 48: 928-940.
259. The US Food and Drug Administration (2007) April 17, 2007 Approval Letter - Influenza Virus Vaccine, H5N1. <http://www.fda.gov/BiologicsBloodVaccines/Vaccines/ApprovedProducts/ucm112838.htm>.
260. The US Food and Drug Administration (2007) H5N1 Influenza Virus Vaccine, A/Vietnam/1203/2004 (Clade 1) 90 mcg/ml http://www.fda.gov/ohrms/dockets/ac/07/briefing/2007-4282b1_01.pdf.
261. McKenna M (2007) THE PANDEMIC VACCINE PUZZLE - Part 3: H5N1 poses major immunologic challenges. <http://www.cidrap.umn.edu/news-perspective/2007/10/pandemic-vaccine-puzzle-part-3-h5n1-poses-major-immunologic-challenges>.
262. Robertson JS, Nicolson C, Harvey R, Johnson R, Major D, et al. The development of vaccine viruses against pandemic A(H1N1) influenza. *Vaccine* 29: 1836-1843.
263. Neumann G, Kawaoka Y (2001) Reverse genetics of influenza virus. *Virology* 287: 243-250.
264. Muszkat M, Friedman G, Schein MH, Naveh P, Greenbaum E, et al. (2000) Local SIgA response following administration of a novel intranasal inactivated influenza virus vaccine in community residing elderly. *Vaccine* 18: 1696-1699.
265. Boyce TG, Hsu HH, Sannella EC, Coleman-Dockery SD, Baylis E, et al. (2000) Safety and immunogenicity of adjuvanted and unadjuvanted subunit influenza vaccines administered intranasally to healthy adults. *Vaccine* 19: 217-226.
266. Ambrozaitis A, Groth N, Bugarini R, Sparacio V, Podda A, et al. (2009) A novel mammalian cell-culture technique for consistent production of a well-tolerated and immunogenic trivalent subunit influenza vaccine. *Vaccine* 27: 6022-6029.
267. bsargent (2012) A First – Cell Culture Based Seasonal Influenza Vaccine Approved by the FDA. <http://cellculturedish.com/2012/12/a-first-cell-culture-based-seasonal-influenza-vaccine-approved-by-the-fda/>.

268. Qiao C, Tian G, Jiang Y, Li Y, Shi J, et al. (2006) Vaccines developed for H5 highly pathogenic avian influenza in China. *Ann N Y Acad Sci* 1081: 182-192.
269. Marangon S, Cecchinato M, Capua I (2008) Use of vaccination in avian influenza control and eradication. *Zoonoses Public Health* 55: 65-72.
270. Swayne DE, Beck JR, Perdue ML, Beard CW (2001) Efficacy of vaccines in chickens against highly pathogenic Hong Kong H5N1 avian influenza. *Avian Dis* 45: 355-365.
271. Swayne DE, Beck JR, Kinney N (2000) Failure of a recombinant fowl poxvirus vaccine containing an avian influenza hemagglutinin gene to provide consistent protection against influenza in chickens preimmunized with a fowl pox vaccine. *Avian Dis* 44: 132-137.
272. Wareing MD, Tannock GA (2001) Live attenuated vaccines against influenza; an historical review. *Vaccine* 19: 3320-3330.
273. Belshe RB, Gruber WC, Mendelman PM, Cho I, Reisinger K, et al. (2000) Efficacy of vaccination with live attenuated, cold-adapted, trivalent, intranasal influenza virus vaccine against a variant (A/Sydney) not contained in the vaccine. *J Pediatr* 136: 168-175.
274. Forrest BD, Pride MW, Dunning AJ, Capeding MR, Chotpitayasunondh T, et al. (2008) Correlation of cellular immune responses with protection against culture-confirmed influenza virus in young children. *Clin Vaccine Immunol* 15: 1042-1053.
275. Maassab HF, Bryant ML (1999) The development of live attenuated cold-adapted influenza virus vaccine for humans. *Rev Med Virol* 9: 237-244.
276. Jin H, Zhou H, Lu B, Kemble G (2004) Imparting temperature sensitivity and attenuation in ferrets to A/Puerto Rico/8/34 influenza virus by transferring the genetic signature for temperature sensitivity from cold-adapted A/Ann Arbor/6/60. *J Virol* 78: 995-998.
277. Belshe RB, Ambrose CS, Yi T (2008) Safety and efficacy of live attenuated influenza vaccine in children 2-7 years of age. *Vaccine* 26 Suppl 4: D10-16.
278. Belshe RB, Edwards KM, Vesikari T, Black SV, Walker RE, et al. (2007) Live attenuated versus inactivated influenza vaccine in infants and young children. *N Engl J Med* 356: 685-696.

279. Ambrose CS, Luke C, Coelingh K (2008) Current status of live attenuated influenza vaccine in the United States for seasonal and pandemic influenza. *Influenza Other Respi Viruses* 2: 193-202.
280. Park MS, Steel J, Garcia-Sastre A, Swayne D, Palese P (2006) Engineered viral vaccine constructs with dual specificity: avian influenza and Newcastle disease. *Proc Natl Acad Sci U S A* 103: 8203-8208.
281. Zhirnov OP, Klenk HD (2009) Alterations in caspase cleavage motifs of NP and M2 proteins attenuate virulence of a highly pathogenic avian influenza virus. *Virology* 394: 57-63.
282. Talon J, Salvatore M, O'Neill RE, Nakaya Y, Zheng H, et al. (2000) Influenza A and B viruses expressing altered NS1 proteins: A vaccine approach. *Proc Natl Acad Sci U S A* 97: 4309-4314.
283. Jin H, Lu B, Zhou H, Ma C, Zhao J, et al. (2003) Multiple amino acid residues confer temperature sensitivity to human influenza virus vaccine strains (FluMist) derived from cold-adapted A/Ann Arbor/6/60. *Virology* 306: 18-24.
284. Steel J, Lowen AC, Pena L, Angel M, Solorzano A, et al. (2009) Live attenuated influenza viruses containing NS1 truncations as vaccine candidates against H5N1 highly pathogenic avian influenza. *J Virol* 83: 1742-1753.
285. Hickman D, Hossain MJ, Song H, Araya Y, Solorzano A, et al. (2008) An avian live attenuated master backbone for potential use in epidemic and pandemic influenza vaccines. *J Gen Virol* 89: 2682-2690.
286. Hoelscher MA, Garg S, Bangari DS, Belser JA, Lu X, et al. (2006) Development of adenoviral-vector-based pandemic influenza vaccine against antigenically distinct human H5N1 strains in mice. *Lancet* 367: 475-481.
287. Schwartz JA, Buonocore L, Suguitan AL, Jr., Silaghi A, Kobasa D, et al. Potent vesicular stomatitis virus-based avian influenza vaccines provide long-term sterilizing immunity against heterologous challenge. *J Virol* 84: 4611-4618.
288. DiNapoli JM, Nayak B, Yang L, Finneyfrock BW, Cook A, et al. Newcastle disease virus-vectored vaccines expressing the hemagglutinin or neuraminidase protein of H5N1 highly pathogenic avian influenza virus protect against virus challenge in monkeys. *J Virol* 84: 1489-1503.

289. Van Kampen KR, Shi Z, Gao P, Zhang J, Foster KW, et al. (2005) Safety and immunogenicity of adenovirus-vectored nasal and epicutaneous influenza vaccines in humans. *Vaccine* 23: 1029-1036.
290. Taylor J, Weinberg R, Kawaoka Y, Webster RG, Paoletti E (1988) Protective immunity against avian influenza induced by a fowlpox virus recombinant. *Vaccine* 6: 504-508.
291. Veits J, Wiesner D, Fuchs W, Hoffmann B, Granzow H, et al. (2006) Newcastle disease virus expressing H5 hemagglutinin gene protects chickens against Newcastle disease and avian influenza. *Proc Natl Acad Sci U S A* 103: 8197-8202.
292. Chambers TM, Kawaoka Y, Webster RG (1988) Protection of chickens from lethal influenza infection by vaccinia-expressed hemagglutinin. *Virology* 167: 414-421.
293. Tang M, Harp JA, Wesley RD (2002) Recombinant adenovirus encoding the HA gene from swine H3N2 influenza virus partially protects mice from challenge with heterologous virus: A/HK/1/68 (H3N2). *Arch Virol* 147: 2125-2141.
294. Maeda Y, Hatta M, Takada A, Watanabe T, Goto H, et al. (2005) Live bivalent vaccine for parainfluenza and influenza virus infections. *J Virol* 79: 6674-6679.
295. Vicente T, Roldao A, Peixoto C, Carrondo MJ, Alves PM Large-scale production and purification of VLP-based vaccines. *J Invertebr Pathol* 107 Suppl: S42-48.
296. Lee DH, Bae SW, Park JK, Kwon JH, Yuk SS, et al. (2013) Virus-like particle vaccine protects against H3N2 canine influenza virus in dog. *Vaccine* 31: 3268-3273.
297. Tretyakova I, Pearce MB, Florese R, Tumpey TM, Pushko P (2013) Intranasal vaccination with H5, H7 and H9 hemagglutinins co-localized in a virus-like particle protects ferrets from multiple avian influenza viruses. *Virology* 442: 67-73.
298. Cox MM, Hollister JR (2009) FluBlok, a next generation influenza vaccine manufactured in insect cells. *Biologicals* 37: 182-189.
299. Cox MM, Patriarca PA, Treanor J (2008) FluBlok, a recombinant hemagglutinin influenza vaccine. *Influenza Other Respi Viruses* 2: 211-219.

300. Song JM, Wang BZ, Park KM, Van Rooijen N, Quan FS, et al. Influenza virus-like particles containing M2 induce broadly cross protective immunity. *PLoS One* 6: e14538.
301. Chun S, Li C, Van Domselaar G, Wang J, Farnsworth A, et al. (2008) Universal antibodies and their applications to the quantitative determination of virtually all subtypes of the influenza A viral hemagglutinins. *Vaccine* 26: 6068-6076.
302. Ekiert DC, Friesen RH, Bhabha G, Kwaks T, Jongeneelen M, et al. A highly conserved neutralizing epitope on group 2 influenza A viruses. *Science* 333: 843-850.
303. Corti D, Voss J, Gamblin SJ, Codoni G, Macagno A, et al. A neutralizing antibody selected from plasma cells that binds to group 1 and group 2 influenza A hemagglutinins. *Science* 333: 850-856.
304. Sui J, Hwang WC, Perez S, Wei G, Aird D, et al. (2009) Structural and functional bases for broad-spectrum neutralization of avian and human influenza A viruses. *Nat Struct Mol Biol* 16: 265-273.
305. Donnelly JJ, Friedman A, Martinez D, Montgomery DL, Shiver JW, et al. (1995) Preclinical efficacy of a prototype DNA vaccine: enhanced protection against antigenic drift in influenza virus. *Nat Med* 1: 583-587.
306. Ljungberg K, Wahren B, Almqvist J, Hinkula J, Linde A, et al. (2000) Effective construction of DNA vaccines against variable influenza genes by homologous recombination. *Virology* 268: 244-250.
307. Drape RJ, Macklin MD, Barr LJ, Jones S, Haynes JR, et al. (2006) Epidermal DNA vaccine for influenza is immunogenic in humans. *Vaccine* 24: 4475-4481.
308. Jones S, Evans K, McElwaine-Johnn H, Sharpe M, Oxford J, et al. (2009) DNA vaccination protects against an influenza challenge in a double-blind randomised placebo-controlled phase 1b clinical trial. *Vaccine* 27: 2506-2512.
309. Suarez DL, Schultz-Cherry S (2000) The effect of eukaryotic expression vectors and adjuvants on DNA vaccines in chickens using an avian influenza model. *Avian Dis* 44: 861-868.
310. Swayne DE (2004) Application of new vaccine technologies for the control of transboundary diseases. *Dev Biol (Basel)* 119: 219-228.

311. Suarez DL, Schultz-Cherry S (2000) Immunology of avian influenza virus: a review. *Dev Comp Immunol* 24: 269-283.
312. Schmolke M, Garcia-Sastre A Evasion of innate and adaptive immune responses by influenza A virus. *Cell Microbiol* 12: 873-880.
313. Blasius AL, Beutler B Intracellular toll-like receptors. *Immunity* 32: 305-315.
314. Kawai T, Akira S (2007) Antiviral signaling through pattern recognition receptors. *J Biochem* 141: 137-145.
315. Panne D (2008) The enhanceosome. *Curr Opin Struct Biol* 18: 236-242.
316. Kim TK, Maniatis T (1997) The mechanism of transcriptional synergy of an in vitro assembled interferon-beta enhanceosome. *Mol Cell* 1: 119-129.
317. Barchet W, Krug A, Cella M, Newby C, Fischer JA, et al. (2005) Dendritic cells respond to influenza virus through TLR7- and PKR-independent pathways. *Eur J Immunol* 35: 236-242.
318. Randall RE, Goodbourn S (2008) Interferons and viruses: an interplay between induction, signalling, antiviral responses and virus countermeasures. *The Journal of general virology* 89: 1-47.
319. Garcia MA, Gil J, Ventoso I, Guerra S, Domingo E, et al. (2006) Impact of protein kinase PKR in cell biology: from antiviral to antiproliferative action. *Microbiol Mol Biol Rev* 70: 1032-1060.
320. Silverman RH (2007) Viral encounters with 2',5'-oligoadenylate synthetase and RNase L during the interferon antiviral response. *J Virol* 81: 12720-12729.
321. Lenschow DJ, Lai C, Frias-Staheli N, Giannakopoulos NV, Lutz A, et al. (2007) IFN-stimulated gene 15 functions as a critical antiviral molecule against influenza, herpes, and Sindbis viruses. *Proc Natl Acad Sci U S A* 104: 1371-1376.
322. van de Sandt CE, Kreijtz JH, Rimmelzwaan GF (2012) Evasion of influenza A viruses from innate and adaptive immune responses. *Viruses* 4: 1438-1476.
323. Young LJ, Wilson NS, Schnorrer P, Mount A, Lundie RJ, et al. (2007) Dendritic cell preactivation impairs MHC class II presentation of vaccines and endogenous viral antigens. *Proc Natl Acad Sci U S A* 104: 17753-17758.

324. Yu X, Tsibane T, McGraw PA, House FS, Keefer CJ, et al. (2008) Neutralizing antibodies derived from the B cells of 1918 influenza pandemic survivors. *Nature* 455: 532-536.
325. Nayak B, Kumar S, DiNapoli JM, Paldurai A, Perez DR, et al. Contributions of the avian influenza virus HA, NA, and M2 surface proteins to the induction of neutralizing antibodies and protective immunity. *J Virol* 84: 2408-2420.
326. Hashimoto G, Wright PF, Karzon DT (1983) Antibody-dependent cell-mediated cytotoxicity against influenza virus-infected cells. *J Infect Dis* 148: 785-794.
327. El Bakkouri K, Descamps F, De Filette M, Smet A, Festjens E, et al. (2011) Universal vaccine based on ectodomain of matrix protein 2 of influenza A: Fc receptors and alveolar macrophages mediate protection. *J Immunol* 186: 1022-1031.
328. Armstrong SJ, Dimmock NJ (1992) Neutralization of influenza virus by low concentrations of hemagglutinin-specific polymeric immunoglobulin A inhibits viral fusion activity, but activation of the ribonucleoprotein is also inhibited. *J Virol* 66: 3823-3832.
329. Min JY, Li S, Sen GC, Krug RM (2007) A site on the influenza A virus NS1 protein mediates both inhibition of PKR activation and temporal regulation of viral RNA synthesis. *Virology* 363: 236-243.
330. Ehrhardt C, Wolff T, Pleschka S, Planz O, Beermann W, et al. (2007) Influenza A virus NS1 protein activates the PI3K/Akt pathway to mediate antiapoptotic signaling responses. *J Virol* 81: 3058-3067.
331. Lam WY, Tang JW, Yeung AC, Chiu LC, Sung JJ, et al. (2008) Avian influenza virus A/HK/483/97(H5N1) NS1 protein induces apoptosis in human airway epithelial cells. *J Virol* 82: 2741-2751.
332. Stasakova J, Ferko B, Kittel C, Sereinig S, Romanova J, et al. (2005) Influenza A mutant viruses with altered NS1 protein function provoke caspase-1 activation in primary human macrophages, resulting in fast apoptosis and release of high levels of interleukins 1beta and 18. *J Gen Virol* 86: 185-195.
333. Gao S, Song L, Li J, Zhang Z, Peng H, et al. (2012) Influenza A virus-encoded NS1 virulence factor protein inhibits innate immune response by targeting IKK. *Cell Microbiol* 14: 1849-1866.

334. Hale BG, Steel J, Medina RA, Manicassamy B, Ye J, et al. (2010) Inefficient control of host gene expression by the 2009 pandemic H1N1 influenza A virus NS1 protein. *J Virol* 84: 6909-6922.
335. Berkhoff EG, Geelhoed-Mieras MM, Fouchier RA, Osterhaus AD, Rimmelzwaan GF (2007) Assessment of the extent of variation in influenza A virus cytotoxic T-lymphocyte epitopes by using virus-specific CD8+ T-cell clones. *J Gen Virol* 88: 530-535.
336. Price GE, Ou R, Jiang H, Huang L, Moskophidis D (2000) Viral escape by selection of cytotoxic T cell-resistant variants in influenza A virus pneumonia. *J Exp Med* 191: 1853-1867.
337. Steel J, Burmakina SV, Thomas C, Spackman E, Garcia-Sastre A, et al. (2008) A combination in-ovo vaccine for avian influenza virus and Newcastle disease virus. *Vaccine* 26: 522-531.
338. Tan J, Cooke J, Clarke N, Tannock GA (2007) Molecular evaluation of responses to vaccination and challenge by Marek's disease viruses. *Avian Pathol* 36: 351-359.
339. Sharma JM (1987) Delayed replication of Marek's disease virus following in ovo inoculation during late stages of embryonal development. *Avian Dis* 31: 570-576.
340. Ricks CA, Avakian A, Bryan T, Gildersleeve R, Haddad E, et al. (1999) In ovo vaccination technology. *Adv Vet Med* 41: 495-515.
341. Williams CJ, Zedek AS Comparative field evaluations of in ovo applied technology. *Poult Sci* 89: 189-193.
342. Webby RJ, Perez DR, Coleman JS, Guan Y, Knight JH, et al. (2004) Responsiveness to a pandemic alert: use of reverse genetics for rapid development of influenza vaccines. *Lancet* 363: 1099-1103.
343. Kido H, Okumura Y, Takahashi E, Pan HY, Wang S, et al. (2008) Host envelope glycoprotein processing proteases are indispensable for entry into human cells by seasonal and highly pathogenic avian influenza viruses. *J Mol Genet Med* 3: 167-175.
344. Lee CW, Lee YJ, Senne DA, Suarez DL (2006) Pathogenic potential of North American H7N2 avian influenza virus: a mutagenesis study using reverse genetics. *Virology* 353: 388-395.
345. Lee CW, Saif YM (2009) Avian influenza virus. *Comp Immunol Microbiol Infect Dis* 32: 301-310.

346. Negash T, al-Garib SO, Gruys E (2004) Comparison of in ovo and post-hatch vaccination with particular reference to infectious bursal disease. A review. *Vet Q* 26: 76-87.
347. Chen Z, Wang W, Zhou H, Suguitan AL, Jr., Shambaugh C, et al. Generation of live attenuated novel influenza virus A/California/7/09 (H1N1) vaccines with high yield in embryonated chicken eggs. *J Virol* 84: 44-51.
348. Hatta Y, Hatta M, Bilsel P, Neumann G, Kawaoka Y An M2 cytoplasmic tail mutant as a live attenuated influenza vaccine against pandemic (H1N1) 2009 influenza virus. *Vaccine* 29: 2308-2312.
349. Zhou B, Li Y, Speer SD, Subba A, Lin X, et al. Engineering temperature sensitive live attenuated influenza vaccines from emerging viruses. *Vaccine* 30: 3691-3702.
350. Ye J, Sorrell EM, Cai Y, Shao H, Xu K, et al. Variations in the hemagglutinin of the 2009 H1N1 pandemic virus: potential for strains with altered virulence phenotype? *PLoS Pathog* 6: e1001145.
351. Pena L, Vincent AL, Ye J, Ciacci-Zanella JR, Angel M, et al. Modifications in the polymerase genes of a swine-like triple-reassortant influenza virus to generate live attenuated vaccines against 2009 pandemic H1N1 viruses. *J Virol* 85: 456-469.
352. Livak KJ, Schmittgen TD (2001) Analysis of relative gene expression data using real-time quantitative PCR and the 2(-Delta Delta C(T)) Method. *Methods* 25: 402-408.
353. Nicolson C, Harvey R, Johnson R, Guilfoyle K, Engelhardt OG, et al. An additional oligosaccharide moiety in the HA of a pandemic influenza H1N1 candidate vaccine virus confers increased antigen yield in eggs. *Vaccine* 30: 745-751.
354. Mochalova L, Gambaryan A, Romanova J, Tuzikov A, Chinarev A, et al. (2003) Receptor-binding properties of modern human influenza viruses primarily isolated in Vero and MDCK cells and chicken embryonated eggs. *Virology* 313: 473-480.
355. Medeiros R, Escriou N, Naffakh N, Manuguerra JC, van der Werf S (2001) Hemagglutinin residues of recent human A(H3N2) influenza viruses that contribute to the inability to agglutinate chicken erythrocytes. *Virology* 289: 74-85.

356. Lu B, Zhou H, Chan W, Kemble G, Jin H (2006) Single amino acid substitutions in the hemagglutinin of influenza A/Singapore/21/04 (H3N2) increase virus growth in embryonated chicken eggs. *Vaccine* 24: 6691-6693.
357. Lu B, Zhou H, Ye D, Kemble G, Jin H (2005) Improvement of influenza A/Fujian/411/02 (H3N2) virus growth in embryonated chicken eggs by balancing the hemagglutinin and neuraminidase activities, using reverse genetics. *J Virol* 79: 6763-6771.
358. Eidenschenk C, Crozat K, Krebs P, Arens R, Popkin D, et al. Flt3 permits survival during infection by rendering dendritic cells competent to activate NK cells. *Proc Natl Acad Sci U S A* 107: 9759-9764.
359. Gambaryan AS, Robertson JS, Matrosovich MN (1999) Effects of egg-adaptation on the receptor-binding properties of human influenza A and B viruses. *Virology* 258: 232-239.
360. Kawakami E, Watanabe T, Fujii K, Goto H, Watanabe S, et al. Strand-specific real-time RT-PCR for distinguishing influenza vRNA, cRNA, and mRNA. *J Virol Methods* 173: 1-6.
361. Kuchipudi SV, Tellabati M, Nelli RK, White GA, Perez BB, et al. 18S rRNA is a reliable normalisation gene for real time PCR based on influenza virus infected cells. *Virol J* 9: 230.
362. Thontiravong A, Kitikoon P, Wannaratana S, Tantilertcharoen R, Tuanudom R, et al. Quail as a potential mixing vessel for the generation of new reassortant influenza A viruses. *Vet Microbiol* 160: 305-313.
363. Kimble B, Nieto GR, Perez DR Characterization of influenza virus sialic acid receptors in minor poultry species. *Virol J* 7: 365.
364. Liu M, He S, Walker D, Zhou N, Perez DR, et al. (2003) The influenza virus gene pool in a poultry market in South central china. *Virology* 305: 267-275.
365. Melen K, Tynell J, Fagerlund R, Roussel P, Hernandez-Verdun D, et al. Influenza A H3N2 subtype virus NS1 protein targets into the nucleus and binds primarily via its C-terminal NLS2/NoLS to nucleolin and fibrillarlin. *Virol J* 9: 167.
366. Falcon AM, Fortes P, Marion RM, Beloso A, Ortin J (1999) Interaction of influenza virus NS1 protein and the human homologue of Staufin in vivo and in vitro. *Nucleic Acids Res* 27: 2241-2247.

367. Schultz-Cherry S, Dybdahl-Sissoko N, Neumann G, Kawaoka Y, Hinshaw VS (2001) Influenza virus ns1 protein induces apoptosis in cultured cells. *J Virol* 75: 7875-7881.
368. Lozano R, Naghavi M, Foreman K, Lim S, Shibuya K, et al. (2012) Global and regional mortality from 235 causes of death for 20 age groups in 1990 and 2010: a systematic analysis for the Global Burden of Disease Study 2010. *Lancet* 380: 2095-2128.
369. Solorzano A, Ye J, Perez DR (2010) Alternative live-attenuated influenza vaccines based on modifications in the polymerase genes protect against epidemic and pandemic flu. *J Virol* 84: 4587-4596.
370. Qian XY, Alonso-Caplen F, Krug RM (1994) Two functional domains of the influenza virus NS1 protein are required for regulation of nuclear export of mRNA. *J Virol* 68: 2433-2441.
371. Greenspan D, Palese P, Krystal M (1988) Two nuclear location signals in the influenza virus NS1 nonstructural protein. *J Virol* 62: 3020-3026.